FLUID FLOW AT SMALL REYNOLDS NUMBER:

Numerical Applications

Tayfour El-Bashir

Department of Mathematics and Statistics, College of Science
Sultan Qaboos University P.O. Box 36, Al-Khod 123
Sultanate of Oman

HIKARI LTD

HIKARI LTD

Hikari Ltd is a publisher of international mathematical journals and books.
www.m-hikari.com

Tayfour El-Bashir, FLUID FLOW AT SMALL REYNOLDS NUMBER: Numerical Applications, First published 2006.

No part of this publication may be reproduced, stored in a retrieval system, or transmitted, in any form or by any means, without the prior permisson of the publisher Hikari Ltd.

Typeset using LaTeX.

Mathematics Subject Classification: 65N38, 74S20, 68Q85

Keywords: Slow flow, cylinder, rotlet, boundary element method

Published by Hikari Ltd

PREFACE

This book is concerned with the numerical solution of the Navier-Stokes equations for some steady, two-dimensional, incompressible viscous fluid flow problems at small and moderate values of the Reynolds number.

The first problem relates to a two-dimensional, incompressible flow both with and without a line rotlet at various small values of the Reynolds number. A circular cylinder of radius a is rotated with a constant angular velocity ω_0 in the presence of a uniform stream of magnitude U. Two techniques are introduced, one in order to avoid the difficulties in satisfying the boundary conditions at large distances from the cylinder, the other to achieve convergence of the solution at zero Reynolds number. Transformations are applied to both the coordinate system and the stream function.

The second problem considers the solution of the biharmonic equation for the slow viscous flow generated by a line rotlet in the presence of a circular cylinder. On identifying the coefficients of some of the terms in the asymptotic expansion of the stream function, in terms of the force components and the torque on the body, and using an integral constraint, the Boundary Element Method provides a closed system of equations. Excellent agreement is obtained between the numerical results and the analytical expressions and some new results relating to forces and torques on the cylinder are presented.

In the third problem the solution of the biharmonic equation, which represents the Stokes flow created by two rotating circular cylinder in which the force system acting on the two cylinders is in a state of overall equilibrium is examined. In this situation the total force and the total torque are both assumed to be zero and the Boundary Element Method, together with the relationships between the forces and the torque on the combined system and the coefficients in the asymptotic expansion for the stream function, is applied.

The final problem relates to a line rotlet outside an elliptical cylinder and the solution shows that it is possible to generate a flow at infinity which corresponds to that of rigid body rotation. This contrary to the situation for a line rotlet outside a circular cylinder, where the fluid flow at infinity corresponds to that of a uniform stream which is the direction perpendicular to the line joining the rotlet to the center of the cylinder.

Tayfour El-Bashir
Sultan Qaboos University

August, 2006

Contents

Chapter 1

INTRODUCTION

1.1 The Navier-Stokes Equations

One of the simplest steady, two-dimensional fluid flow problems is that of a infinite, stationary, viscous fluid, which is disturbed by a circular cylinder of radius a moving with a uniform velocity U through it. When the fluid is incompressible and Newtonian then the governing equations are the continuity equation and the Navier-Stokes equations, which in dimensionless form, are expressible as

$$\underline{\nabla^*} \,.\, \underline{u^*} = 0, \tag{1.1.1}$$

$$\frac{D\underline{u}^*}{Dt^*} = \frac{\partial \underline{u}^*}{\partial t^*} + (\underline{u}^*.\underline{\nabla}^*)\underline{u}^* = -\underline{\nabla}^* \underline{p}^* + \frac{1}{Re}\underline{\nabla}^{*2}\underline{u}, \tag{1.1.2}$$

where (*) denotes the dimensionless form of the physical quantity, t^* the time, $\underline{u}^*$ the fluid velocity vector, $\underline{p}^*$ the pressure and $Re = aU/\nu$, with ν the coefficient of kinematic viscosity, is the Reynolds number. For simplicity the (*)' s will be omitted throughout the remainder of this Chapter. When one is concerned with situations where the fluid is extremely viscous, namely ν large, or the motion of the body is very slow, so $U << 1$, then the Reynolds number is very small and the inertia terms on the left hand side of equation (1.1.2) can be neglected. Although a similar conclusion applies for small values of a one must ensure that this value is not reduced to a level where the continuum model is no longer applicable.

When the equations of motion are simplified by the omission of the inertia terms, i. e. $Re << 1$, and the motion is two-dimensional then the introduction of the stream function, so that the continuity equation (1.1.1) is identically satisfied, by

$$u = \frac{\partial \psi}{\partial y} \; and \; v = -\frac{\partial \psi}{\partial x}, \tag{1.1.3}$$

together with the removal of the pressure by taking the curl of equation (1.1.2), results in the biharmonic equation

$$\nabla^4 \psi = O. \tag{1.1.4}$$

It is the solution of this equation that the majority of this book is related to. When the initial problem of a circular cylinder moving through a fluid is considered and the Reynolds number parameter Re is assumed small then no solution of equation (1.1.4) is possible. This phenomenon is usually referred to as the "Stokes Paradox" .

1.2 Stokes Paradox

The cause of the Stokes paradox in a two-dimensional flow is that no solution of the simplified equations can be found for which the fluid velocity satisfies both the boundary conditions on the body and at infinity, since the solution, which satisfies all the boundary conditions on the obstacle is unbounded at infinity. However, the fluid velocity is found to be logarithmically infinite, see Stokes (1851), thus tends to infinity as the logarithm of the distance from the cylinder, i.e. it increases slowly with this distance, and so it should give a fairly good approximation to the fluid motion at small and moderate distances from the cylinder. In mathematical terms the solution of the Stokes equation, which for the non-dimensional stream function, ψ, is expressible as

$$\psi = A \sin(\theta)[(\frac{r}{a}) \ln(\frac{r}{a}) - \frac{1}{2}(\frac{r}{a}) + \frac{1}{2}(\frac{a}{r})], \tag{1.2.1}$$

though valid near the cylinder, does not form a uniformly valid approximation to the Navier-Stokes equations far from the cylinder.

Briefly, the difficulty arises since any body moving with a constant speed through a viscous fluid experiences some resistance, and, see Tomotika and Imai (1938), by considering the momentum flux across a large surface, which

surrounds the body one can show that the magnitude of the disturbance to the uniform fluid velocity cannot fall to zero more rapidly than the inverse square of the distance from the body. This results in a singularity at infinity in the perturbation solution for non-zero Reynolds number, where the convection terms at large distances from the body are of the same order of magnitude as the viscous forces. Hence, the Stokes's solution fails to provide a uniform valid approximation to the fluid flow. Only if the disturbance decays exponentially is it possible for the convection terms to continue to be neglected in the outer flow region.

It should be noted that for the fluid flow past an sphere the Stokes equation provides a uniform approximation to the total velocity distribution. This, at first, appears 'contrary to the situation for a cylinder where, as discussed above, the solution is unbounded as r becomes infinitely large. This uniformly valid approximation to the fluid velocity enables properties of the flow, such as the lift, drag and moment on the sphere, to be determined by the uniformly valid approximations. The Stokes solution does not break down until the distance from the body is such that the velocity approaches that of the uniform stream. Here, the flaw in the solution arises because of the fluid velocity derivatives at large distances being in error and it is these derivatives in the neglected inertia terms that are required to obtain the second approximation to the fluid flow.

It is necessary to establish a uniformly valid approximation to the neglected inertia terms in the Navier-Stokes equation so one can determine the second approximation to the solution even in the region close to the body. This requires the introduction of an expansion procedure, similar to that described by Whitehead (1889), in powers of the Reynolds number Re, where the neglected inertia terms are reintroduced into the equations of motion. Although producing the correct differential equation for the flow in the region not far from the body this approach fails to produce a solution, which satisfies the condition at infinity, even in the case when the body corresponds to a sphere.

Unlike the Stokes solution of steady uniform fluid flow past a sphere there is no uniform approximation for the case of flow past a two-dimensional cylinder since the solution is unbounded. In particular it is found from equation 1.2.1 that terms like $rln(r)sin(\theta)$ give rise to a non-uniformly valid expression, which initially appears to make the solution completely unsatisfactory. It is seen that the neglected inertia terms should be included when $Re(rln(r))$ is 0(1) and for

values of r of this magnitude the classical Stokes solution will be invalid. This suggests that close to the cylinder the Stokes approximation is a reasonable representation to the fluid flow, but fails to provide the uniform approximation to the total velocity distribution.

However, it is possible to rewrite the approximation in such a manner such that the severity of the non-uniformity appears to be somewhat decreased and leads one to obtain a uniform stream in that region where the Stokes equation ceases to be valid and this suggests that the uniform stream condition has been attained prior to the break down of the approximation. This idea was the basis of the work by Oseen (1910), where for both the sphere and the cylinder a uniform approximation to the disturbance of the stream is possible by taking the inertia terms into account when they are comparable in magnitude to the viscous terms, namely where the flow is nearly a uniform stream, and neglecting them close to the body. Oseen (1910) proposed that the inertia terms should be retained in the far field, where the fluid velocity is approximately equal to U, since in that region the assumptions underlying the Stokes equation are not valid at sufficiently large distances from the cylinder no matter how small Re may be. These inertia terms are of 0(Re) near to the cylinder, where it is permissible to neglect them altogether, and so one finds that in three-dimensional fluid flow past an obstacle both the Stokes and Oseen equations yield the same terms, which are of 0(1), and differ only in the terms of O(Re). However, it was not until Kaplun and Lagerstrom (1957) and Proudman and Pearson (1957) that the whole process was placed on a rigorous mathematical foundation using the ideas of matched asymptotic expansions and the technique extended to higher order approximations for both the two and three-dimensional cases.

As the perturbation theory arising for small non-zero Reynolds numbers is singular, both the above sets of authors developed a technique for overcoming this difficulty when expanding in terms of the small Reynolds number parameter. Essentially this considers separate local expansions for the regions close to, and far from, the body, usually referred to as the (inner) Stokes and (outer) Oseen expansions, respectively. The two sets of differential equations resulting from substituting the above expansions into the Navier-Stokes equations have only one set of physical boundary conditions applicable to each expansion, namely no slip at the body for the Stokes expansion and the uniform stream condition for the Oseen expansion. In order to establish a unique solution it is

necessary to introduce a matching procedure by which the outer solution provides an outer boundary condition for the inner solution and the inner solution provides an inner boundary condition on the outer solution. This technique of matched asymptotic expansions allows for the determination of the alternatively successive terms in the two expansions, as well as the form of the local expansions for the two regions. Consequently, the solution of the biharmonic equation for two-dimensional, slow streaming flows in an unbounded fluid may be interpreted as an inner solution of the Navier-Stokes equations. This solution will be valid within some finite distance from the body, but requires an outer solution in order to satisfy the uniform stream condition at infinity, so explaining how the Stokes Paradox can be overcome.

1.3 Work by Jeffery (1922)

An additional paradox caused by local effects was that discovered by Jeffery (1922) when two cylinders of equal radii in an unbounded fluid are rotating with equal speeds, but in opposite senses about parallel axes. Jeffery (1922) established the presence of a uniform stream at infinity in the direction perpendicular to the line joining the centers of the two cylinders. Al though his result was known to be in error due to it being impossible to establish within any finite time no explanation was presented, yet the author must have been aware of the earlier work by Oseen (1910). It was probably this paradoxical situation, which caused Jeffery to restrict his solution to that one particular case, even though he had formulated the problem for two cylinders with different radii and different angular speeds. This paradox was extended to the general case by Smith (1991). He found that the above situation uniform flow was present only when the combined angular momentum of the two cylinders was zero, in all other cases, instead of the far field corresponding to a uniform stream, a rigid body rotation occurred.

One striking feature of Jeffery's and Smith's solutions was that they restricted their stream function expansion to that corresponding to a finite number of terms in the Fourier Series describing the solution, which although satisfying the boundary conditions failed to produce any other physical situation except that in which the combined system of the two cylinders was in a state of overall equilibrium, namely zero total force and zero total moment. As Smith (1991)

was aware that he was constructing only an inner solution he was able to match, unfortunately erroneously, with a complete solution of the Navier-Stokes equations for the outer flow field.

However, it should be stressed that in Watson (1995) the solutions to this problem and that of a rotlet outside a circular cylinder have been fully developed using an inner and outer matching technique. The results in the far field of the outer solution always correspond to a Jet behavior along one of the axes. Whilst by allowing the complete Fourier Series to represent his solution, Watson established that the inner condition on the outer solution always represented a force, so removing the above restriction concerning the equilibrium conditions on the combined system.

1.4 Work by Dorrepaal, O'Nei11 and Ranger (1984)

Another example of a paradoxical situation arising from a local affect was presented by Dorrepaal, O'Nei11 and Ranger (1983) when a rotlet, or stokeslet, is placed in front of a circular cylinder. However, these authors established that both Jeffrey's and their problem are well-posed Stokes flow problems provided there is a uniform stream at infinity having an appropriate direction and magnitude. Whereas the parameters involved in Jeffery's case are the radii and the angular velocities of the cylinders and the distance separating the two cylinders. In the case of the rotlet it is the position and strength of the rotlet as well as the radius of the cylinder. Avudainayagam and Jothiram (1987) extended this work to show that with a particular singularity present in the flow field outside a circular cylinder then for a suitably chosen rotational flow at infinity, in addition to a uniform stream, the problem is also well-posed.

1.5 Existence of Possible Paradoxical Flows

A rotating cylinder produces a somewhat specialized flow in the case of three-dimensional, slow viscous flow since there is no motion in the direction parallel to the axis of rotation. This restriction of the flow to planes perpendicular to the axis allows a stream function to be introduced, which in turn simplifies the equations of motion and enables an analytical solution to be obtained. It was

to avoid this constraint that Smith (1990) investigated the Jeffrey paradox in the case of a rotlet by considering it as the limit of the three-dimensional Stokes flow where the length h of the rotlet tends to infinity. It was shown that the two-dimensional situation could be established only as the $O[(ln(h)^{-l}]$ terms become negligible. Since this represents a very slow decay rate as h increases it makes the usefulness of the two-dimensional results questionable.

This research further investigates the formulation of Smith (1991) of a sink, and a source-sink combination, in the presence of a circular cylinder. In the case of the sink alone the Jeffrey paradox is again present with a uniform stream at infinity. However, in the source-sink situation the results are more complex, with the positions of the singularities being crucial to the established flow pattern. For example, with the source and sink equidistant from the cylinder, but on directly opposite sides of the cylinder, all the fluid passing into the sink comes from infinity and all that departing from the source moves to infinity. Whereas, with the sink and source at angles $\theta = \alpha$ and $\theta = \pi - \alpha$, (where θ is the polar angle in cylindrical coordinates measured from the x-axis with the origin at the center of the cylinder), respectively, where $0 < \alpha < \pi/2$, but at the equal distances from the center of the cylinder, then two possibilities exist depending upon whether the line joining the source and sink intersects the cylinder. When the intersection condition exists then a total blockage in the flow from the source to the sink occurs, but once this restriction is removed some of the fluid leaving the source can move directly to the sink without departing to infinity.

The question being asked by Smith (1990) was whether these two-dimensional flows formed locally, yet producing paradoxical behavior, represent the limit of other flows as might be expected. Firstly, the above geometrical situations were considered, but with the flow constrained within a circular cylinder, whose radius tends to infinity. Secondly, an unbounded three-dimensional flow of a finite line singularity outside a circular cylinder, with the length of the line singularity tending to infinity is examined. Finally, the limit, as time approaches infinity, of the impulsively started two-dimensional situation in an unbounded domain is considered, namely its approach to steady state. As in his earlier conclusion regarding the limit of the three-dimensional Jeffrey problem produced the two-dimensional situation only when $O[(ln(h))^{-l}]$ terms are negligible. Smith (1990) established that a similar result applies to all the above limiting cases. The two-dimensional solution being established but with an error, which is $O[(ln(k))^{-l}]$,

where k represents the various different parameters, which tend to infinity. The overall conclusion drawn from the analysis is that locally generated unbounded flows are not attainable.

1.6 The Outline

Whether or not it is possible to set up many of these steady, two-dimensional paradoxical situations will be left open at present and an investigation undertaken as to how such problems can be tackled numerically. Throughout this book it will be assumed that the paradoxical behavior occurs due to some form of singularity or object outside a circular cylinder in an unbounded fluid, and is not that arising from the classical problem of simply the flow of a uniform stream past a circular cylinder.

Before providing a description of the topics within each Chapter it is proposed to outline the fundamental ideas over-riding much of this material, and whilst reference here initially will be to the case of a rotlet outside a cylinder it could just as easily have been related to the material within Chapters 5 or 6, that is the cases of two rotating cylinders or that of a rotlet outside an ellipse. From the analytical solution of the biharmonic equation for either a sink, source or rotlet outside a circular cylinder in an unbounded fluid it is known that a uniform stream of a prescribed magnitude and direction is generated at infinity. The direction and magnitude of the stream being dependent upon the strength and position of the singularity. Hence, a given singularity outside a circular cylinder in a uniform stream of the appropriate magnitude and direction constitutes a well posed Stokes problem.

The question is how to determine numerically the magnitude and direction of this uniform stream, which in reality is the outer boundary condition. Even if one accepts the direction of the uniform stream from the analytical solution then there is still its magnitude to determine in order to generate the known analytical solution to this Stokes problem. Whilst obtaining an analytical solution does not require a definite outer boundary condition to be prescribed, the situation in the numerical approach is far more complex. Even if the exact value from the analytical solution is used then due to the discrepancy between the finite-difference representation of the biharmonic equation and the biharmonic equation itself there is no certainty of convergence. Yet, at the same time one

would not expect it necessary to have to introduce any additional information from the analytical solution to obtain the numerical solution.

If this is not the case then it should be possible to leave the conditions at infinity arbitrary and perform some kind of iterative scheme, which will lead to convergence and the required answer. The problem is to decide on the physical quantity, or quantities, that must be given some prescribed value to start the iteration process. The quantities that most obviously come to mind are the lift, drag and moment acting on the circular cylinder. If this is so then what are the values that these various quantities should possess? An alternative way of prescribing the problem may be, "for a singularity of a certain strength and at a given distance from a circular cylinder, what is the form of the solution at infinity, which produces a prescribed lift, drag and moment on the cylinder"?

In any problem where the biharmonic equation represents the fluid motion then it can be shown that the lift, drag and the moment on surfaces of fluid are invariants whenever it is possible to deform one surface into another without either passing outside the fluid domain or through any singularity of the flow, for example, a rotlet. However, accommodating the extra contribution arising from moving the surface through a singularity is a relatively easy matter, hence, it is possible to express the lift, drag and moment on an obstacle using that on the surface of fluid at infinity. Applying the asymptotic form of the Fourier Series for the stream function

$$\psi = F_o(r) + \sum_{n=1}^{\infty}(F_n(r)sin(n\theta) + G_n(r)cos(n\theta)) \tag{1.6.1}$$

where

$$F_0(r) = A_0(r^2\ln(r) - r^2) + B_0r^2 + C_0\ln(r) + D_0, \tag{1.6.2}$$

$$F_1(r) = FA_1r^3 + FB_1r\ln(r) + FC_1r + FD_1r^{-1}, \tag{1.6.3}$$

$$G_1(r) = GA_1r^3 + GB_1r\ln(r) + GC_1r + GD_1r^{-1}, \tag{1.6.4}$$

at large values of r enables the lift, drag and moment on the obstacle to be expressed as multiples of the constants GB_1, FB_1 and C_0, respectively. Hence a feature of fluid flows around obstacles governed by the biharmonic equation, whether generated locally or at infinity, is that the force and moment on the

obstacle can be established as directly equivalent to that on any surface of fluid, which contains the obstacle, provided that this surface encloses no singularities of the flow field. However, if singularities are present within the surface, then the relationship between the force and moment on the body and that on the surface of fluid enclosing these singularities must be modified to account for the extra contributions to the force and moment acting at the various singularities. This enables the force and moment on an obstacle in an unbounded flow to be determined from the contribution on the surface at infinity, which surrounds the obstacle.

As mentioned above if the appropriate conditions are imposed at infinity then the fluid flow produced by a singularity outside a circular cylinder in an unbounded fluid can be shown to produce a well-posed problem. However, it is possible to introduce to such a situation any arbitrary rotational flow, namely $\psi = A(r^2 - 2\ln(r) + 1)$, which satisfies the no-slip condition on the cylinder and produces a circulation around any closed contour enclosing the cylinder. By this means an arbitrary moment has been added to the cylinder.

In chapter 2 we investigate the fluid flow generated by rotating a circular cylinder within a uniform stream of viscous fluid in the presence of a rotlet at non-zero Reynolds numbers. The fluid flow created by a circular cylinder, which is in steady motion, or has been started from rest, has long been of interest, both experimentally and theoretically, see for example Imai (1951), Kawaguti (1953), Moore (1957), Smith (1979,1985), Fornberg (1980,1985), and Badr and Dennis (1985).

There are three basic parameters to be considered in this type of problem; the Reynolds number, now defined as $Re = 2aU/\nu$, where ν is the coefficient of kinematic viscosity of the fluid, U the unperturbed main stream speed (in the positive x direction), a the radius of the cylinder; the rotational parameter $\alpha = a\omega_0/U$, which is a dimensionless measure of the speed of rotation, where ω_0 is the angular velocity of the rotating cylinder; and the non-dimensional strength of the rotlet $\beta = \Gamma/Ua$, where Γ the strength of the rotlet. When $\beta = 0$ and $\alpha = 0$ the motion is symmetrical about the line parallel to the direction of the stream through the center of the cylinder and this situation has previously received a considerable amount of attention, e.g. Dennis and Chang (1970) and Fornberg (1980,1985) who both provide a comprehensive list of references. The problem of the flow past a rotating cylinder is of fundamental interest for several

reasons, e.g. in boundary-layer control on aerofoil, see for example Tennant et al. (1976) and the lift force experienced by the cylinder is an example of the Magnus affect, which can be used for lift enhancement, see for example Sayers (1979).

Although there are numerous computations in existence of two-dimensional flows, both steady and unsteady, about various shapes of cylinders in an unbounded fluid, very little theoretical and numerical work has been reported on either the steady or unsteady flow past a rotating circular cylinder. The earliest numerical solutions of the Navier-Stokes equations at non-zero values of α were given by Thoman and Szewczyk (1966) who obtained numerical results for Reynolds numbers in the range $1 \leq Re \leq 10^6$ and rotational parameters $1 \leq \alpha \leq 6$ and they compared their findings with the experimental results of Swanson (1956) and Prandtl and Tietjens (1937). Lyul'ka (1977) studied the problem for Reynolds numbers, Re = 0, 2, 10, 20 and values of the rotational parameter in the range of $0 \leq \alpha \leq 5$. The problem was formulated in terms of the stream function ψ and the vorticity ω and the time-dependent form of the governing equations were solved until the steady-state solution was obtained. The main objective of Lyul'ka's work was to study the formation of the lift and this was actually done by investigating the variation of the lift and drag coefficients on the cylinder. His results suggest that the lift coefficient C_L increases steadily as the rotational parameter α increases for all of the values of the Reynolds numbers considered. In contrast the drag coefficient C_D decreases for Re = 2 and increases for Re = 10, 15 and 20 as the value of α increases. Similar work was performed by Shkadova (1982) who extended the numerical solutions to Re = 80. He found that the lift coefficient C_L increases almost linearly as α varies from 0 to 2 for the flows that can be regarded as steady, i.e. when $Re < 60$. The calculated results of Shkadova (1982) for C_L were found to be in good agreement with those obtained by Lyul'ka (1977).

A few numerical calculations have been performed for the case of steady flow past a rotating circular cylinder by employing the steady-state Navier-Stokes equations. Ta Phuoc Loc (1915) obtained results for Re = 5 and 20 by solving the Navier-Stokes equations numerically within a finite region of space, which surrounds the cylinder subject to boundary conditions on the perimeter of the domain, which he states are consistent with the external flow. Results for the steady-state fluid flow were obtained together with values of C_L and

C_D at small values of α. However, it was found that even in the symmetrical flow situation his results for the drag coefficient were substantially larger than the more accurate results obtained by Fornberg (1980,1985). This may be due to the use of a computational region, which is too small and the form of the approximation of the outer boundary conditions.

In obtaining numerical solutions for the problem under investigation difficulties arise in the determination of the boundary conditions at large distances. This problem has been discussed in detail by several authors, see for example Dennis (1918)and Fornberg (1980). Even in the symmetrical flow situation, Fornberg (1980) realized the importance of using the most appropriate form of the boundary conditions to be applied at large distances from the circular cylinder. He considered four possible infinity boundary conditions and performed a detailed comparison on the different results. Fornberg (1980,1985) has obtained numerical solutions up to a Reynolds number of 600 using a technique for dealing with the boundary conditions at large distances and an iterative scheme, which is based on Newton's method, which minimizes the numerical difficulties previously encountered around and beyond Re = 100.

Dennis (1978) investigated the steady, asymmetrical flow past an elliptical cylinder using the method of series truncation to solve the Navier-Stokes equations with the Oseen approximation throughout the flow. He found that for asymmetrical flows, by considering the asymptotic nature of the decay of vorticity at large distances, it is not sufficient merely that the vorticity vanishes far from the cylinder but it must decay rapidly enough. This was achieved by a suitable adjustment of the leading term in the asymptotic expansion for the vorticity. This problem does not arise in the case of symmetrical flows because the leading the asymptotic term in expansion for the vorticity is identically zero. It is clear that in the case of asymmetrical flows it is more difficult to obtain the most appropriate form of the boundary conditions, which are to be applied at large distances from the cylinder.

In the present work a numerical technique has been introduced in order to avoid the difficulties in satisfying the boundary conditions at large distances from the cylinder. Transformations applied to both the coordinate system and to the stream function. To avoid numerical errors introduced by approximating the location of the outer boundary condition, exact boundary conditions at infinity were obtained and used in the calculations.

The numerical solution was then extended to the two-dimensional flow of an infinite viscous fluid generated by a rotating circular cylinder in the presence of a line rotlet. The aim of the work is to show that the presence of a rotlet in a uniform stream at non-zero Reynolds number allows an otherwise singular problem to become well-posed as the Reynolds number approaches zero. Initially the strength of the rotlet was set to zero and the problem was solved with Re = 5 and 20. This solution was then used as an initial estimate when a rotlet of small strength was introduced to the flow.

In Chapter 3 the problem originally discussed by Dorrepaal, O'Neill and Ranger (1984) namely that of a rotlet of non-dimensional unit strength placed at a non-dimensional distance c, where $c > 1$, from a cylinder whose radius a has been used as the non-dimensional investigated by an alternative length scale is approach using Fourier Series. This method is a more routine and a less sophisticated approach than that mentioned by Dorrepaal, O'Neill and Ranger (1984) and it enables information from a surface of fluid at infinity, which encloses the cylinder to predict the values of the force and moment on the object. Also in this Chapter the forces and moment on the cylinder were obtained using two different techniques, namely

(i) by using the stress acting on a surface element to represent the components of the force (F_x, F_y) and the moment M acting on a volume of fluid surrounded by the surface S,

(ii) by using the separation of variables solution of the biharmonic equation.

Relations between the forces and moments acting on different surfaces were found analytically and no difference in the value of the force components was found between surfaces containing the cylinder and those which in addition contain the rotlet. In the case of the moment on any surface GS_{CR} (see Figure 3.4.1) of fluid containing both the cylinder and the rotlet, this value is equal to the sum of the moment on any surface CS_c of fluid containing only the cylinder plus the contribution from the moment on the rotlet. The affect of these physical quantities on the solution was intended as a bench mark against which the numerical solution in Chapter 4 is compared.

In Chapter 4 the basic formulation of the Boundary Element Method (BEM) for the solution of the biharmonic equation is described. The constant Boundary Element approximation has been used to solve the biharmonic equation for the problem of flow generated by a rotlet outside a circular cylinder. This

particular numerical method was chosen because the technique presented in Chapter 2 fails to accommodate the situation when the force and moment on the cylinder are non-zero. In addition this method is capable of varying the components of force and moment on the cylinder. In applying this method to the problem of a uniform flow past a rotating circular cylinder in the presence of a rotlet it is necessary to divide the stream function into two separate parts, one part containing the terms, which tend to zero at infinity, whilst the other part contains the remainder of the terms, which are bounded and unbounded at infinity. Relating the coefficients of some of the terms in the asymptotic expansion of the stream function to the force components and the torque on the circular cylinder, together with the imposition of an integral constraint, gives a closed system of equations and produces results in excellent agreement with the analytical solution provided by Dorrepall, O'Neill and Ranger (1984). Numerical solutions were found for several problems, namely,

(a) the uniform stream at infinity and with no force and no moment on the cylinder,

(b) unbounded fluid flow at infinity, which corresponds to a stokeslet at the origin (in this situation one has a specified non-dimensional force and no moment),

(c) unbounded flow at infinity, which is a combination of a uniform stream and a rotational far field flow (where one has a prescribed non-dimensional moment and no force),

(d) a combination of unbounded flows at infinity due to a stokes let at the origin together with a rotating far field flow (in this situation we have the general situation where both the force and the moment being specified).

Chapter 5 deals with the rotation of two circular cylinders of different radii, which rotate at different angular velocities in a viscous fluid in which the fluid flow is governed by the biharmonic equation. This Stokes flow is solved using information from the far flow field of the inner region in the form of the coefficients of the stream function, which are related to values of the lift, drag and moment generated by the two bodies and the BEM approach. Successful application of the BEM technique in this situation of two cylinders of different radii will enable it to be applied with confidence to other multiple body problems for which no analytical solution is possible. In such problems the cross-sections of the bodies can differ, even within a particular problem, and the number of such

bodies present will be limited only by the computing restriction related to the number of required elements on the bodies.

However, in order to apply the BEM it is necessary for the stream function under consideration to tend to zero at infinity. This can be achieved in the standard manner, namely by redefining the stream function to be its asymptotic value at large distances, plus a perturbation stream function, and the BEM then applied to the perturbation stream function. This means that only those terms, which form a non-zero contribution to the stream function at infinity will occur in the governing equations with their values being those on the cylindrical boundaries. Since it is known, from the analytical solution, that terms $O(r^2)$ may be present at infinity, the non-zero stream function part must include all the solutions of the biharmonic equation up to this order whose magnitude are greater or equal to $O(1)$. This requires the presence of the terms in r^2, $r\sin(\theta)\ln(r)$, $r\cos(\theta)\ln(r)$, $r\sin(\theta)$, $r\cos(\theta)$, $\ln(r)$, $\sin(2\theta)$ and $\cos(2\theta)$ and a constant term. Perturbing the stream function about its asymptotic form at infinity will introduce into the equations to be solved the nine coefficients associated with each of the above terms. A further unknown in the problem is the difference between the stream function values on the two cylinders and this increases the overall number of unknowns in the problem to ten. Thus the same numbers of conditions are required to be found in order for the numbers of unknowns in the equations to match the numbers of equations present. As the forces and torque on the cylinders are related to the various coefficients in the above terms in the asymptotic form of the stream function at large distances, it is proposed to utilize this information to provide some of the extra conditions required. The other conditions, which are required to close the system are found from the single valuedness of the pressure and by choosing three points inside one cylinder and two points inside the other cylinder. The problem was solved for three cases, namely,

(a) two circular cylinders of equal radius, which rotate with equal but opposite angular velocities about their parallel axes,

(b) the situation where the cylinders have different angular velocities, but the combined angular momentum of the two cylinders is zero,
i.e. $\omega_1 {r_1}^2 = \omega_2 {r_2}^2$

(c) the general case when $\omega_1 {r_1}^2$ is not equal to $\omega_2 {r_2}^2$, which produces a rotational flow at infinity.

In Chapter 6 the fluid motion in an unbounded viscous fluid, which is generated by a rotlet placed outside an elliptical cylinder has been solved numerically using the BEM. The analytical solution for this problem was obtained by Smith (1994). This problem is similar to the problem discussed in chapter 4 but with a more complicated body shape. Hence, the basic BEM formulation is the same as that described in chapter 4 but the discretization is different due to the complexity of the evaluation of the force, moment and integral condition on the boundary. The results obtained are found to be in excellent agreement with the analytical solution given by Smith (1994) and confirm the situation of the flow at infinity corresponding to that of a rigid body rotation, except for one particular placement of the rotlet when the flow at large distances reduces to that of a uniform stream.

In Chapter 7 the significant points of the preceding Chapters are discussed and the areas in which further work should be performed are highlighted.

Chapter 2

ROTATING CIRCULAR CYLINDER AND A ROTLET

2.1 Introduction

A study has been made of the flow generated by rotating a circular cylinder within a uniform stream of viscous fluid in the presence of a line rotlet. With the origin of the coordinates coinciding with the center of the cylinder, then the polar coordinate system (r, ϑ) has the boundary of the cylinder at $r = a$ and the position of the rotlet at $(c^*, 3\pi/2)$, as shown in Figure 2.1.1. There are four basic parameters that occur in this problem, namely, the Reynolds number, defined as $Re = 2aU/\nu$, the rotational parameter $\alpha = a\omega_0/U$, the non dimensional length $c = c^*/a$ and the non dimensional strength of the rotlet $\beta = \Gamma/Ua$, where ν is the coefficient of kinematic viscosity of the fluid, U the unperturbed main stream speed, (the stream at infinity is assumed to flow parallel to the x-axis in the positive x direction), $\omega_0$the angular velocity of the cylinder and Γ the strength of the rotlet.

At zero Reynolds number the governing equation is the biharmonic equation. In the absence of a rotlet no solution of this equation, which satisfies both the boundary conditions on the cylinder and at infinity, is possible. This arises since

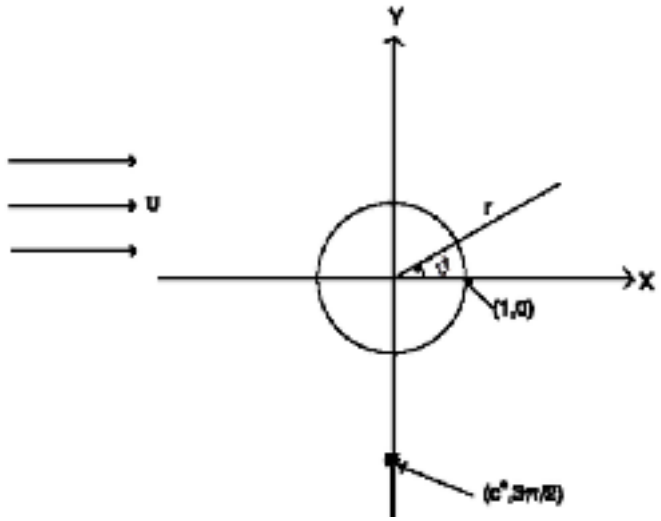

Figure 2.1.1: Diagram illustrating The geometry of the elliptical cylinder and the position of the rotlet.

it is necessary to maintain in the solution a term of the form $r\ln(r)\sin(\vartheta)$ in order for both the velocity components on the rotating cylinder to be satisfied. However, although a solution retaining such a term is obviously valid at points not too far away from the cylinder such a solution deteriorates as one moves further away. As such this solution fails to satisfy the boundary condition at infinity, with the exact multiple of the unwanted term at infinity remaining undetermined. This unknown constant can be established by treating the solution of the problem as the first approximation to the inner flow past the circular cylinder as the Reynolds number tends to the zero. Then matching with the solution as obtained from the outer region where the first approximation to the Navier Stokes equations are the Oseen equations. Full details regarding these expansions and matching procedure can be found in Proudman and Pearson (1957). Basically what this means is that uniform flow past a circular cylinder is not a well-posed Stokes problem. In fact at zero Reynolds number the problem is singular.

However, the introduction of a rotlet into the flow field at any given distance c^*along the negative y-axis, but with a strength specified as $\Gamma = Uc^*$, in other

words with the parameter $\beta = c$, allows a solution to be obtained. analytical solutions to this problem have been obtained by Dorrepaal, O'Neill and Ranger (1984). Their work examines the flows generated in a fluid by the introduction of a line singularity, such as a stokeslet or rotlet, in the presence of a circular cylinder and shows that a phenomenon analogous to the Stokes paradox exists in that flows with a uniform stream far from the cylinder may be produced. As a consequence, the uniform streaming flow past a circular cylinder, when a line stokeslet or rotlet of certain strength is present, is a well-posed problem in Stokes flow.

The solution by Dorrepaal et al. (1984) employed an image type approach, plus a clever and simplistic deduction, which enabled the result to be constructed devoid of most of the analysis. However, the present work has established the same solution by using a Fourier Series approach and has confirmed this numerically by the application of a modification to the Boundary Element Method. The latter appears to provide an approach for the solution of the biharmonic equation, which requires only the position of the singularity, plus the physical values of the drag, lift and the moment on the circular cylinder to be known. In addition it seems capable of being extended to accommodate the presence of several different bodies as well as allowing more complex shapes for which an analytical solution is impossible. It is intended to show that the presence of a rotlet in a uniform flow at non-zero Reynolds number allows an otherwise singular problem to become well-posed as the Reynolds number becomes zero.

The main aim of this chapter is to solve numerically the Navier-Stokes equations for steady, two-dimensional, incompressible viscous fluid flow past a rotating circular cylinder of radius a in the presence of a rotlet of strength Γ, which is located at the point $(r, \vartheta) = (c^*, 3\pi/2), c^* >$ a. At large distance from the cylinder it is assumed that there is a uniform flow of speed U, which is parallel to negative x-axis. Initially the strength of the rotlet is set to zero and the problem solved with Reynolds numbers 5 and 20. The results are in very good agreement with those obtained by Tang (1990). Using this as an initial estimate of the solution when a line singularity is present an iterative technique is developed in order to solve the problem when a rotlet, at $(c^*, 3\pi/2)$, of small strength is introduced into the flow. As the drag, lift and moment on the circular cylinder are the most important physical quantities, as well as being easy to measure experimentally, Tang (1990), then in this work particular attention

has been paid to these quantities.

2.2 Basic Equations and the Boundary Conditions

The origin of the coordinate system is fixed at the center of the circular cylinder of radius a and the positive x-axis taken in the same direction as that of the uniform flow at large distances from the cylinder. Polar coordinates (r, ϑ) are chosen such that $\vartheta = 0$ coincides with the positive x-axis,

$$x = rcos(\vartheta) \; and \; y = rsin(\vartheta). \tag{2.2.1}$$

A line rotlet of strength Γ is located at the point $r = c^*, \vartheta = 3\pi/2$, where $c^* >$ a. The steady flow of an incompressible fluid in a fixed two-dimensional Cartesian frame of reference can be described by the equations,

$$(\underline{u}.\underline{\nabla})\underline{u} = -\frac{1}{\rho}\underline{\nabla}p + \nu\underline{\nabla}^2\underline{u} \tag{2.2.2}$$

$$\underline{\nabla}.\underline{u} = 0 \tag{2.2.3}$$

where $\underline{u}, \rho, p$ and ν are the velocity, density, pressure and the kinematic viscosity of the fluid, respectively.

Applying the curl operator to equation (2.2.2) produces

$$(\underline{u}.\underline{\nabla})\underline{\omega} = \nu\nabla^2\underline{\omega} \tag{2.2.4}$$

where $\underline{\omega} = \underline{\nabla}X\underline{u}$.

In two-dimensional motion the polar resolute of $\underline{u}$ can be expressed in terms of the stream function Ψ by

$$v_r = \frac{1}{r}\frac{\partial\Psi}{\partial\vartheta}, \;\; v_\vartheta = -\frac{\partial\Psi}{\partial r} \tag{2.2.5}$$

where $v_r$and $v_\vartheta$are the velocity components in the r and ϑ directions, respectively. By introducing the dimensionless variables

$$\underline{x}' = \underline{x}/a, \underline{u}' = \underline{u}/U, \Psi' = \Psi/U a \; and \; \underline{\omega}' = \underline{\omega} a/U, \tag{2.2.6}$$

then the governing equations in non-dimensional form become

$$\nabla^2 \omega' = -\frac{Re}{2} \frac{\partial(\psi', \omega')}{\partial(x', y')} \tag{2.2.7}$$

$$\nabla^2 \Psi' = -\omega' \tag{2.2.8}$$

where ω' and Ψ' are the non-dimensional scalar vorticity and stream function, respectively. For convenience the $'s$ will from now on be removed. It is required to solve equations (2.2.7) and (2.2.8) subject to the no-slip conditions imposed by the circular cylinder, namely

$$\Psi = 0, \frac{\partial \psi}{\partial r} = -\alpha \; on \; r = 1, 0 \leq \vartheta < 2\pi \tag{2.2.9}$$

and the boundary conditions at large distances from the cylinder

$$\frac{\partial \psi}{\partial r} \rightarrow -\sin(\vartheta), \frac{1}{r} \frac{\partial \psi}{\partial \vartheta} \rightarrow \cos(\vartheta) \; as \; r \rightarrow \infty, 0 \leq \vartheta < 2\pi \tag{2.2.10}$$

In the presence of a line rotlet the stream function behaves as

$$\Psi \approx -\beta \ln R_1 \; as \; R_1 \rightarrow 0 \tag{2.2.11}$$

where R_1measures the distance from the rotlet and is thus given by

$$R_1 = (r^2 + c^2 + 2rc \sin(\vartheta))^{1/2}, \tag{2.2.12}$$

where $(c, 3\pi/2)$ is the position of the rotlet.

In the above definition of the stream function the signs appearing in the expressions in (2.2.5) are the opposite to those given by Dorrepaal et al. (1984) but follow those adopted by Tang (1990) since it is a comparison with their results at non zero Reynolds number that is to be undertaken.

For numerical convenience the perturbation stream function ψ is introduced as

$$\psi = \Psi - y - \beta V, \tag{2.2.13}$$

where $V = \ln(r^2 + c^2 + 2\text{rcsin}(\vartheta))^{1/2}$with $c = c^*/a$ and $\beta = \Gamma/(Ua)$ being two non-dimensional parameters. Expansion (2.2.13) has been taken so that $\psi \to 0$ as $r \to \infty$. If the parameter $\beta = 0$ then the problem reduces to that solved by Tang (1990). However, with the Reynolds number equal to zero and the parameter $\beta = c$ then the situation is that studied by Dorrepaal et al. (1984) except that the geometry in the present case corresponds to a rotation through $\pi/2$ of their flow pattern. Hence, their stream is flowing along the negative y-axis with their rotlet at $(c^*, 0)$, whereas in the present geometry the stream flows along the negative x-axis with the rotlet at $(c^*, 3\pi/2)$.

Using expression (2.2.13) in equations (2.2.7) and (2.2.8) gives

$$\begin{aligned}
&\frac{\partial^2\omega}{\partial r^2} + \frac{1}{r}\frac{\partial\omega}{\partial r} + \frac{1}{r^2}\frac{\partial^2\omega}{\partial\vartheta^2} = -\frac{Re}{2r}\left(\frac{\partial\psi}{\partial r}\frac{\partial\omega}{\partial\vartheta} - \frac{\partial\psi}{\partial\vartheta}\frac{\partial\omega}{\partial r}\right)\\
&- \frac{Re}{2r}\left[\frac{\partial\omega}{\partial\vartheta}\left(sin(\vartheta) + \beta\frac{r + csin(\vartheta)}{r^2 + c^2 + 2rcsin(\vartheta)}\right]\right.\\
&+ \frac{Re}{2r}\left[\frac{\partial\omega}{\partial r}\left(rcos(\vartheta) + \beta\frac{rccos(\vartheta)}{r^2 + c^2 + 2rcsin(\vartheta)}\right]\right.
\end{aligned} \tag{2.2.14}$$

$$\frac{\partial^2\psi}{\partial r^2} + \frac{1}{r}\frac{\partial\psi}{\partial r} + \frac{1}{r^2}\frac{\partial^2\psi}{\partial\vartheta^2} = -\omega \tag{2.2.15}$$

respectively.

The boundary conditions (2.2.9) and (2.2.10) are then expressed in the form

$$\psi = -\sin(\vartheta) - \beta\ln(1 + c^2 + 2csin(\vartheta))^{1/2} \; on \; r = 1, 0 < \vartheta < 2\pi \tag{2.2.16}$$

$$\frac{\partial\psi}{\partial r} = -\alpha - \sin(\vartheta) - \beta\left(\frac{1 + c\sin(\vartheta)}{1 + c^2 + 2c\sin(\vartheta)}\right) \; on \; r = 1, 0 < \vartheta < 2\pi, \tag{2.2.17}$$

$$\frac{\partial\psi}{\partial r} = \frac{1}{r}\frac{\partial\psi}{\partial\vartheta} \to 0, \; as \; r \to \infty, 0 \le \vartheta < 2\pi. \tag{2.2.18}$$

Filon (1926) showed that in the absence of any rotlet the asymptotic form for the dimensional stream function at large distances from the cylinder and outside the wake region is given by

$$\psi \approx rsin(\vartheta) + \frac{C_L \ln(r/a)}{2\pi} + \frac{C_D(\vartheta - \pi)}{2\pi},\ as\ r \to \infty, 0 < \vartheta < 2\pi, \qquad (2.2.19)$$

where $C_L = L/(\rho U^2 a)$ and $C_D = D/(\rho U^2 a), L$ and D being the lift and drag on the cylinder . Imai (1951) found higher-order terms in this stream function expansion and showed how the coefficients related to the moment on the cylinder. In the case of zero Reynolds number no solution of the equation $\nabla^4 \Psi = 0$ is possible, which matches the free stream condition at infinity and satisfies the boundary condition on $r = 1$. The solution, which satisfies the no slip condition on the cylinder and tends to infinity most slowly as $r \to \infty$ is

$$\Psi \approx Asin(\vartheta)[rln(r) - r/2 + 1/(2r)], \qquad (2.2.20)$$

which has been obtained by discarding the term involving r^3. The non-dimensional drag is directly related to the coefficient A, via the expression $4\pi A$, but the solution suffers from the defect that it does not determine the value of the constant A. The neglected inertial terms are of the order $((A)^2 \ln(r))/r^2$whilst the viscous forces are of the order $A/(Rer^3)$ and these terms are of comparable order when $ARe(r \ln(r))/a \simeq \mathbf{0}(1)$. Hence, the Stokes solution should not be expected to be valid beyond a value given by this expression. That is why the Stokes solution may be an adequate representation of the fluid flow relatively close to the cylinder but cannot represent a uniform approximation to the total velocity distribution. However, it is possible to write the Stokes solution in the form

$$\Psi = A[(-rln(f(Re)) + rln(rf(Re))) - r/2 + 1/(2r)]\sin(\vartheta), \qquad (2.2.21)$$

where $f(Re)$ is an arbitrary function of Re . For $f(Re) << 1$ and $rf(Re)$ of order unity, the dominant term is $-A(\ln(f(Re))\text{rsin}(\vartheta)$. If this is to represent the external flow, namely a uniform stream Ursin(ϑ), then one must set $A = -1/\ln(f(Re))$. By substituting this value of A and $r = 1/f(Re)$ into $ARe(r \ln(r))/a$, one obtains

$$Re/f(Re) \simeq \mathbf{0}(1). \tag{2.2.22}$$

So for $f(Re) = Re$ the Stokes solution leads to a uniform stream of order unity in that region where the Stokes equation ceases to be valid . This suggests that for small Reynolds number the external uniform stream condition is reached before the Stokes approximation breaks down, so the Stokes flow represents the solution in the inner region near the cylinder but the outer flow requires the introduction of an Oseen variable and the procedure involves the matching of the inner and outer expansions. This matching process leads to the obvious linkage between the coefficients of the terms in Oseen's expansion in the outer region, closely related to Filon's expansion, with those from the in the inner region. Hence, the appropriate value of A can be obtained, as already indicated from the solution in the outer region. Any similar term in a Stokes expansion, such as a $\mathrm{Brln}(r)\cos(\vartheta)$ term in the stream function expansion, has its coefficient similarly related to the lift. Solutions of the Stokes equation represented by the form $f(r)\sin(\vartheta)$ or $g(r)\sin(\vartheta)$ fail to produce any moment contribution, but it can easily be seen that the solution of $\nabla^4\Psi = 0$, which has a non-zero moment arises from the $\ln(r/a)$ term. Using these results, it is possible from the Stokes expansion far from the cylinder to establish both the force and the moment on the cylinder. The Stokes solution produced by Dorrepaal, O'Neill and Ranger (1984) is able to immediately produce the drag, lift and moment on the circular cylinder from its expansion at large distances from the cylinder; although the contribution from the singularity at the rotlet must first be removed from the coefficient of the $\ln(r/a)$ term before it represents the moment on the cylinder.

Since the stream function and vorticity equations are both elliptical in nature we should supply one condition for each of the variables rather than use directly conditions (2.2.16), (2.2.17) and (2.2.18). It has been reported by Fornberg (1980,1985)and Tang (1990) that the choice of the boundary condition for the vorticity, ω, is not as sensitive as that for the stream function, ψ, and many authors have paid particular attention to the boundary condition for ψ at large distances from the cylinder.

In this work we use the technique described by Tang (1990) in order to avoid having to enforce the boundary condition (2.2.19) at large distances from the cylinder. We therefore introduce the transformation

$$\xi = \frac{1}{r}, \eta = \frac{2\vartheta}{\pi} \tag{2.2.23}$$

and

$$f(r, \vartheta) = \psi(r, \vartheta)/r, \tag{2.2.24}$$

namely

$$f(\xi, \eta) = \xi\psi(\xi, \eta) \tag{2.2.25}$$

Thus, we have $f = 0$ on $\xi = 0$(i.e. at $r = \infty$) and this requires no approximation to be made for ψ at large distances from the cylinder.

With the transformation (2.2.23) then the solution domain ($1 \leq r < \infty, 0 \leq \vartheta < 2\pi$) is transformed into a finite rectangular region in the (ξ, η) plane ($0 \leq \xi < 1, 0 \leq \eta < 4$), see figure (2.2.1). Substituting expressions (2.2.23) and (2.2.24) into the governing equations (2.2.14) and (2.2.15) one obtains

(2.2.26)

$$\xi^3 \frac{\partial^2 f}{\partial \xi^2} - \xi^2 \frac{\partial f}{\partial \xi} + \frac{4\xi}{\pi^2} \frac{\partial^2 f}{\partial \eta^2} + \xi f = -\omega \tag{2.2.27}$$

and the boundary conditions (2.2.10) and (2.2.11) now become

$$\begin{aligned} f &= -\sin(\pi\eta/2) - \beta \ln(1 + c^2 + ^{1/2} 2csin(\pi\eta/2)) \\ &= f_B on r = 1, 0 \leq \eta < 4, \end{aligned} \tag{2.2.28}$$

$$\begin{aligned} \frac{\partial f}{\partial \xi} &= \alpha + sin(\pi\eta/2) + \beta(\frac{1 + csin(\pi\eta/2)}{1 + c^2 + 2csin(\pi\eta/2)}) \\ &= f'_B \ on \ r = 1, 0 \leq \eta < 4, \end{aligned} \tag{2.2.29}$$

$$f = 0, \omega = 0, \ on \ \xi = 0, 0 \leq \eta < 4. \tag{2.2.30}$$

Further, since the solution is periodic in η we also require that

$$f(\xi, 4) = f(\xi, 0), \omega(\xi, 4) = \omega(\xi, 0), \ for \ 0 \leq \xi \leq 1, \tag{2.2.31}$$

which along with all the other boundary conditions are indicated in figure 2.2.1.

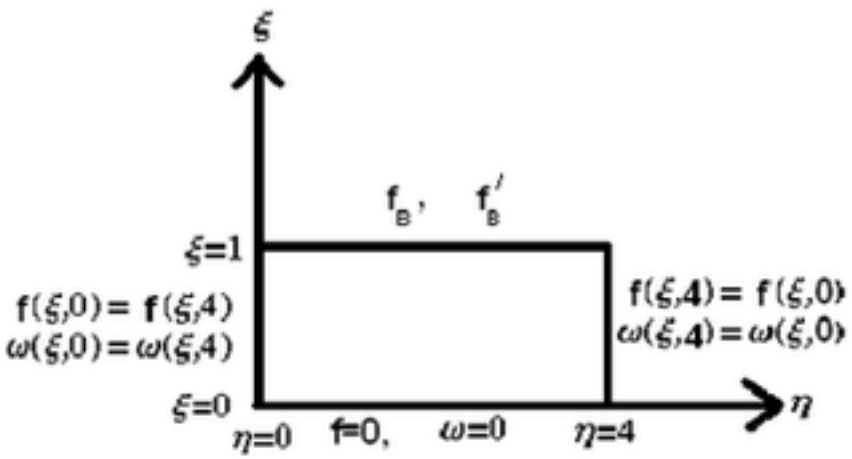

Figure 2.2.1: The geometry of the solution domain.

2.3 The Solution Technique

In order to obtain numerical solutions of the equations (2.2.26) and (2.2.27) subject to the boundary conditions (2.2.28), (2.2.29), (2.2.30) and (2.2.31) the region of integration $0 \leq \xi \leq 1, 0 \leq \eta < 4$ is covered by a rectangular mesh system of size h and k in the η and ξ directions, respectively, and a modified finite-difference approximation to the differential equations (2.2.26) and (2.2.27) is employed. If the standard central-difference approximation is employed, then it is not always possible to obtain a convergent solution especially at moderate and large values of the Reynolds number. A number of schemes have been introduced with the object of improving the efficiency of the convergence of such schemes, e.g. upwind and downwind differencing as discussed by Greenspan (1968), Gosman et al. (1969), Runchal, Spalding and Wolfshtein (1969), etc.. These improved efficiencies arise from the fact that the difference equations are associated with matrices, which are diagonally dominant and thus amenable to iterative methods of solution. However, these schemes suffer from a deficiency in that they are only of first-order accurate since forward or backward differences are employed to approximate first derivatives rather than the more accurate

second-order central-difference formula. The formulation in which all derivatives are approximated by central differences is of second-order accuracy but the matrix associated with the difference equations may not be diagonally dominant. The iterative procedures may be slowly convergent or even divergent when this method is applied .

There are also finite-difference schemes, which are of second-order accuracy and for which the associated matrices are always diagonally dominant. These methods rely upon rather specialized forms of local approximations and yield difference equations, which involve the exponential function. These schemes were first introduced by Allen and Southwell (1955) in approximating the equation governing the vorticity during the course of finding numerical solutions for the steady two-dimensional flow past a circular cylinder. Dennis and Hudson (1978) showed that by a suitable adaptation of an alternative to the Allen and Southwell method suggested by Dennis (1960), an approximation of second-order accuracy, yielding difference equations with an associated matrix, which is diagonally dominant, can be obtained. These difference equations do not involve the exponential function and can be looked upon as a rather more complicated version of the central-difference formulation. The Dennis and Hudson method contains more terms in the finite-difference equations than the usual central-difference approximation but the presence of these extra terms is very important for the associated matrix to be diagonally dominant. Numerous authors have performed several numerical experiments, which confirm that the method by Dennis and Hudson succeeds where the standard central-difference formulation fails, see Dennis (1960), Price, Varga and Warren, Nallasamy and Krishna Prasad (1977) and Dennis and Hudson (1978). Thus, in this book a modified version of the finite-difference approximation as described by Hudson and Dennis, has been used.

It is found most convenient to set up a mesh system such that the mesh size in both the ξ and η directions are $k = h = 1/N$, where N is a preassigned positive integer. In view of the periodic conditions (2.2.31), an extra line of computation $\eta = 4 + h$ for $0 \leq \xi \leq 1$ is introduced. Then we have $(N + 1)x(M + 1)$ mesh points, where $M = 4N + 1$, the mesh points $(\xi_i, \eta_i)(0 \leq i \leq N, 0 \leq j \leq M)$ are (ih, jh). If subscripts 0,1,2,3 and 4 denote quantities at the grid points $(\xi_0, \eta_0), (\xi_0, \eta_0 - h), (\xi_0 + h, \eta_0), (\xi_0, \eta_0 + h)$ and $(\xi_0 - h, \eta_0)$, respectively, then on using the Dennis and Hudson scheme, equations (2.2.26) and (2.2.27) may

be written in the form

$$\begin{aligned}(\frac{{\beta^*}^2}{2}+\frac{2}{\pi^2{\xi_0}^2}-\frac{h^2}{4{\xi_0}^2})f_0 = (\frac{1}{\pi^2{\xi_0}^2})f_1+(\frac{{\beta^*}^2}{4}-\frac{\beta^* h}{8\xi_0})f_2+(\frac{1}{\pi^2{\xi_0}^2})f_3 \\ +(\frac{\beta^*}{4}+\frac{\beta^* h}{8\xi_0})f_4+(\frac{h^2}{4{\xi_0}^3})\omega_0\end{aligned} \tag{2.3.1}$$

$$\begin{aligned}&(\frac{{\beta^*}^2}{2}+\frac{2}{\pi^2{\xi_0}^2})\omega_0 = (\frac{1}{\pi^2\xi_0}-a(\xi_0,\eta_0)-D(\xi_0,\eta_0))\omega_1 \\ &+(\frac{{\beta^*}^2}{4}+b(\xi_0,\eta_0)+E(\xi_0,\eta_0))\omega_2+(\frac{1}{\pi^2\xi_0}+a(\xi_0,\eta_0)+D(\xi_0,\eta_0))\omega_3 \\ &+(\frac{\beta^*}{4}-b(\xi_0,\eta_0)-E(\xi_0,\eta_0))\omega_4\end{aligned} \tag{2.3.2}$$

with $\beta^* = \frac{h}{k}$

$$a(\xi_0,\eta_0) = \frac{Reh}{8\pi{\xi_0}^2}(v_0+\frac{f_0}{\xi_0}+\frac{1}{\xi_0}\sin(\vartheta)) \tag{2.3.3}$$

$$b(\xi_0,\eta_0) = \beta(\frac{Reh}{8\pi{\xi_0}^2}u_0+\frac{h}{8\xi_0}+\frac{Reh}{16\xi_0}\cos(\vartheta)) \tag{2.3.4}$$

$$D(\xi_0,\eta_0) = -\frac{\beta Reh}{8\pi{\xi_0}^2}(\frac{1+c\xi_0\sin(\vartheta)}{1+c^2{\xi_0}^2+2c\xi_0\sin(\vartheta)}) \tag{2.3.5}$$

$$E(\xi_0,\eta_0) = -\frac{\beta Reh}{16}(\frac{c\cos(\vartheta)}{1+c^2{\xi_0}^2+2c\xi_0\sin(\vartheta)}) \tag{2.3.6}$$

where (u_0, v_0) are defined as

$$u_0 = \frac{\partial f(\xi_0,\eta_0)}{\partial\eta}, v_0 = \frac{\partial f(\xi_0,\eta_0)}{\partial\xi} \tag{2.3.7}$$

The standard central-difference approximations may be obtained by setting the extra terms $D(\xi_0,\eta_0), E(\xi_0,\eta_0)$ to be zero.

We now briefly outline how the boundary conditions (2.2.28)-(2.2.30) can be implemented. The boundary condition for the vorticity on $\xi = 1$ can be found by using Taylor expansion for f and ω and inserting in equation (2.2.27) to get second-order accurate finite differences.

boundary conditions for ω :

$$\begin{aligned} &\text{on } \xi = 0,\ 0 \le \eta < 4 :\ i = 0,\ 0 \le j < M;\ \omega_{0j} = 0; \\ &\text{on } \xi = 1,\ 0 \le \eta < 4 :\ i = N,\ 0 \le j < M;\ \omega_{0j} = \omega_{nj}; \end{aligned} \tag{2.3.8}$$

$$\begin{aligned} \omega_{nj} = [(1 - \frac{h^2}{2} - \frac{h^3}{6})f_{nj} - f_{(n-1)j} - \frac{h^2}{6}\omega_{(n-1)j} \\ - h(1 - \frac{h^2}{2} - \frac{h^3}{6})f'_{nj} + \frac{4h^3}{6\pi^2}(g_{2j} - (1 + \frac{3}{h})g_{1j})]/(\frac{h^2}{3}(1 + h)) \end{aligned} \tag{2.3.9}$$

with

$$f'_{nj} = \alpha - \frac{\beta(1 + csin(\frac{\pi}{2}\eta_j))}{1 + c^2 + 2csin(\frac{\pi}{2}\eta_j)} + \frac{\beta}{2}\ln(1 + c^2 + 2csin(\frac{\pi}{2}\eta_j)) \tag{2.3.10}$$

$$g_{ij} = \frac{\pi^2}{4}sin(\frac{\pi}{2}\eta_j) - \frac{\beta\pi^2}{4}\frac{(csin(\frac{\pi}{2}\eta_j(1 + c^2) + 2c^2)}{(1 + c^2 + 2csin(\frac{\pi}{2}\eta_j))^2} \tag{2.3.11}$$

$$g_{2j} = -\frac{\beta\pi^2 c(3c + c^3 + (1 + 3c^2)sin(\frac{\pi}{2}\eta_j) - 2c^3 cos^2(\frac{\pi}{2}\eta_j))}{2(1 + c^2 + 2csin(\frac{\pi}{2}\eta_j))^3} \tag{2.3.12}$$

$$\text{on } \eta = 4 + h,\ 0 \le \xi \le 1 :\ 0 \le i \le N,\ j = M;\ \omega_{im} = \omega_{i1}; \tag{2.3.13}$$

$$\text{on } \eta = 0,\ 0 \le \xi \le 1 :\ 0 \le i \le N,\ j = 0;\ \omega_{i0} = \omega_{\mathrm{im}-1}; \tag{2.3.14}$$

boundary conditions for f:

$$\begin{aligned} &\text{on } \xi = 0,\ 0 \le \eta < 4 :\ 0 \le j < M, i = 0;\ f_{0j} = 0; \\ &\text{on } \xi = 1,\ 0 \le \eta < 4 :\ 0 \le j < M, i = N; \end{aligned} \tag{2.3.15}$$

$$f_{nj} = -\sin(\frac{\pi}{2}\eta_j) + \frac{\beta}{2}\ln(1 + c^2 + 2csin(\frac{\pi}{2}\eta_j)) \tag{2.3.16}$$

$$\text{on } \eta = 4 + h, 0 \le \xi \le 1 : 0 \le i \le N, j = M; f_{\mathrm{im}} = f_{i1}; \tag{2.3.17}$$

$$\text{on } \eta = 0, 0 \le \xi \le 1 : 0 \le i \le N, j = 0; f_{i0} = f_{\mathrm{im}-1}; \tag{2.3.18}$$

The resulting finite-difference equations (2.3.1) and (2.3.2), subject to the boundary conditions (2.3.8)-(2.3.18), were solved iteratively in a similar way to that described by Tang (1990).

¿From equation (2.2.6) the non-dimensional speed of the uniform stream at large distance from the cylinder is unity, whereas the non-dimensional strength of the rotlet at the position $(c, 3\pi/2)$, namely β, is variable. In order to compare the results with Dorrepaal et al. (1984) the value of c is fixed at the magnitude used in their calculations, namely $c = 3$.

Since the force components (drag and lift) and the moment are very sensitive to the method of solution, particular attention has been given to these quantities. If F_x and F_y are the dimensional drag and lift on the cylinder, then

$$F_x = \int_0^{2\pi} (\sigma_{rr}\cos(\vartheta) - \sigma_{r\vartheta}\sin(\vartheta))_{r=1}\ r d\vartheta \tag{2.3.19}$$

$$F_y = -\int_0^{2\pi} (\sigma_{\vartheta r}\cos(\vartheta) + \sigma_{rr}\sin(\vartheta))_{r=1}\ r d\vartheta \tag{2.3.20}$$

Introducing the constitutive relations

$$\sigma_{rr} = -p + 2\mu\frac{\partial V_r}{\partial r}, \tag{2.3.21}$$

$$\sigma_{r\vartheta} = \sigma_{\vartheta r} = \mu(r\frac{\partial}{\partial r}(\frac{V_\vartheta}{r}) + \frac{1}{r}\frac{\partial V_r}{\partial \vartheta}), \tag{2.3.22}$$

$$\sigma_{\vartheta\vartheta} = -p + 2\mu(\frac{1}{r}\frac{\partial V_\vartheta}{\partial \vartheta} + \frac{V_r}{r}), \tag{2.3.23}$$

into expressions (2.3.19) and (2.3.20) results in

$$F_x = \int_0^{2\pi} r[\frac{\partial p}{\partial \vartheta} - 2\mu\frac{1}{r}\frac{\partial}{\partial r}(\frac{\partial^2\Psi}{\partial\vartheta^2} + \Psi) + \mu\nabla^2\Psi]\sin(\vartheta)d\vartheta, \tag{2.3.24}$$

$$F_y = -\int_0^{2\pi} r[\frac{\partial p}{\partial \vartheta} - 2\mu\frac{1}{r}\frac{\partial}{\partial r}(\frac{\partial^2\Psi}{\partial\vartheta^2} + \Psi) + \mu\nabla^2\Psi]\cos(\vartheta)d\vartheta, \tag{2.3.25}$$

Using the ϑ component of the Navier Stokes equations, namely

$$\frac{1}{r}(\frac{\partial p}{\partial \vartheta}) = -\mu \frac{\partial \nabla^2 \Psi}{\partial r} \tag{2.3.26}$$

and substituting $\nabla^2 \Psi = -\omega$, which is equation (2.2.8) but in its dimensional form, the equations (2.3.24) and (2.3.25) can be written in the form

$$F_x = \mu \int_0^{2\pi} r[r\frac{\partial \omega}{\partial \vartheta} - \omega - \frac{2}{r}\frac{\partial}{\partial r}(\frac{\partial^2 \Psi}{\partial \vartheta^2} + \Psi)] \sin(\vartheta) d\vartheta, \tag{2.3.27}$$

$$F_y = -\mu \int_0^{2\pi} r[r\frac{\partial \omega}{\partial \vartheta} - \omega - \frac{2}{r}\frac{\partial}{\partial r}(\frac{\partial^2 \Psi}{\partial \vartheta^2} + \Psi)] \cos(\vartheta) d\vartheta, \tag{2.3.28}$$

The above expressions are still dimensional, but defining the

lift and the drag coefficients by

$$C_D = F_x/(\rho U^2 a) \text{ and } C_L = F_y/(\rho U^2 a) \tag{2.3.29}$$

enables $C_D$and $C_L$to be written as

$$C_D = \frac{2}{Re} \int_0^{2\pi} r[r\frac{\partial \omega}{\partial \vartheta} - \omega - \frac{2}{r}\frac{\partial}{\partial r}(\frac{\partial^2 \Psi}{\partial \vartheta^2} + \Psi)] \sin(\vartheta) d\vartheta, \tag{2.3.30}$$

$$C_L = -\frac{2}{Re} \int_0^{2\pi} r[r\frac{\partial \omega}{\partial \vartheta} - \omega - \frac{2}{r}\frac{\partial}{\partial r}(\frac{\partial^2 \Psi}{\partial \vartheta^2} + \Psi)] \cos(\vartheta) d\vartheta, \tag{2.3.31}$$

where r, Ψ and ω are all non-dimensional.

In terms of the independent variables ζ and ϑ, C_D and C_L become

$$C_D = \frac{2}{Re} \int_0^{2\pi} [-\frac{\partial \xi}{\partial \vartheta} - \omega - 2\frac{\partial}{\partial \xi}(\frac{\partial^2 \Psi}{\partial \vartheta^2} + \Psi)] \sin(\vartheta) d\vartheta, \tag{2.3.32}$$

$$C_L = -\frac{2}{Re} \int_0^{2\pi} [-\frac{\partial \omega}{\partial \vartheta} - \omega - 2\frac{\partial}{\partial \xi}(\frac{\partial^2 \Psi}{\partial \vartheta^2} + \Psi)] \cos(\vartheta) d\vartheta, \tag{2.3.33}$$

When the boundary conditions on the cylinder are introduced expressions (2.3.32) and (2.3.33) reduce to those given by Tang (1990), except for a reversal of the sign in C_L and the omission of a factor 2 in the definition of both C_L and C_D.

The moment on the cylinder

$$M = \int_0^{2\pi} r\sigma_{r\vartheta} r d\vartheta \tag{2.3.34}$$

becomes, in dimensional form, on substituting the appropriate constitutive equation

$$M = -\mu \int_0^{2\pi} r^2 [\frac{\partial^2 \psi}{\partial r^2} - \frac{1}{r}\frac{\partial \psi}{\partial r} - \frac{1}{r^2}\frac{\partial^2 \Psi}{\partial \vartheta^2}]\ d\vartheta. \tag{2.3.35}$$

Introducing the moment coefficient defined by

$$C_M = M/(\rho U^2 a^2) \tag{2.3.36}$$

results in the non dimensional expression

$$C_M = \frac{2}{Re}\int_0^{2\pi} r^2 [\omega + \frac{2}{r}\frac{\partial \psi}{\partial r} + \frac{2}{r^2}\frac{\partial^2 \Psi}{\partial \vartheta^2}]\ d\vartheta. \tag{2.3.37}$$

In terms of the independent variables ξ and ϑ the moment coefficient becomes

$$C_M = \frac{2}{Re}\int_0^{2\pi} [\omega - 2\frac{\partial \psi}{\partial \xi} + 2\frac{\partial^2 \Psi}{\partial \vartheta^2}]\ d\vartheta, \tag{2.3.38}$$

and the boundary conditions on the cylinder reduce this expression to

$$C_M = \frac{2}{Re}\int_0^{2\pi} [\omega - 2\omega_0]\ d\vartheta. \tag{2.3.39}$$

Formulas (2.3.32), (2.3.33) and (2.3.39) are evaluated using Simpson's rule. Due to the need to evaluate the drag, lift and moment when $Re = 0$ we will work with the non-dimensional quantities $\mathrm{ReC}_D/2$, $\mathrm{ReC}_L/2$ and $\mathrm{ReC}_M/2$ from now on, namely $F_x/(\mu U), F_y/(\mu U)$ and $M/(\mu U a)$. However, when the Reynolds number vanishes, that is the independence of the mainstream at infinity from the strength of the rotlet is no longer valid, then when discussing an iterative scheme in the following results section it is necessary to redefine the above three quantities as $(F_x a)/(\mu\Gamma), (F_y a)/(\mu\Gamma)$ and $M/(\mu\Gamma)$.

2.4 Results

Before we undertake a detailed discussion of the results it is important to stress from Dorrepaal et al. (1984), and from our own investigation, that at $Re = 0$ it is impossible to obtain a solution for an arbitrary value of the parameter β, which is contrary to what occurs at non zero Reynolds numbers. In the $Re = 0$ situation there is only one unique value of β, which will produce the uniform stream at infinity, and the difficulty numerically is to achieve some mechanism, which will enable the numerical method to converge to this quantity. Since Stokes flow with a uniform flow at infinity means that the body must be free of any force one can develop an iterative numerical scheme based upon this fact to enable the unique value of β and the corresponding flow solution to be determined. Exactly how this is achieved will be discussed in detail later within this section. In order to compare the results obtained by the present numerical method with those obtained previously, the values of the Reynolds number $Re = 5$ and $Re = 20$, together with the absence of any rotlet ($\beta = 0$) and with the rotational parameter $\alpha = 0, 0.5, 1$ and 2, were initially investigated. Solutions are obtained for the mesh sizes $h = 1/10, 1/15, 1/20$ and $1/40$. In Tang (1990), at both the above Reynolds numbers, repeated extrapolation of results derived from h^2extrapolation of the results from $h = 1/10, 1/15, 1/20$ and $1/40$ produced only a 0.1% change in the coefficients of the lift and the drag when compared with the values derived directly from using $h = 1/40$. As a consequence it is proposed not to implement extrapolation but instead to utilize a small value of h, namely $h = 1/40$. Values of $Re/2$ times the coefficients of the lift, drag and moment are presented in table (2.4.1). The lift and drag coefficients are in good agreement with those produced by Tang (1990).

At this stage, having established that the numerical procedure is producing the correct results for $Re \neq 0$ and $\alpha \neq 0$, then the condition $\beta = 0$ is relaxed. However, since the interest is in whether the problem is well posed as the Reynolds number tends to zero, it is proposed to set α to be zero in the remainder of the calculations to be presented in this chapter. Although such a restriction can easily be removed if required.

It has already been established analytically by Dorrepaal et al. (1984) that at $Re = 0a$ solution in which there is a uniform stream of unit non-dimensional strength flowing parallel to the positive y-axis is possible provided that the

TABLE (2.4.1)
The variation of $Re/2$ times the coefficients of lift, drag
and moment with α for $Re = 5$ and 20.
Re = 5 Re = 20

α	$ReC_L/2$	$ReC_D/2$	$ReC_M/2$	$ReC_L/2$	$ReC_D/2$	$ReC_M/2$
0.0	0.000	19.716	0.000	0.000	39.861	0.000
0.5	6.939	19.565	0.616	25.635	39.430	2.354
1.0	14.176	19.226	1.197	52.289	38.465	4.426
2.0	29.122	17.514	2.246	114.275	32.515	7.026

rotlet is placed at the non-dimensional position $(c, 0)$, where the non-dimensional strength of the rotlet is β =c. In the present situation the stream is flowing parallel to the positive x-axis and therefore the position of the rotlet has to be $(c, 3\pi/2)$ in order to produce a solution. The question is whether the solutions at $Re \neq 0$ for a range of values of β, namely varying non-dimensional strengths of the rotlet, can be used to predict the unique analytical value of this parameter, which produces the solution at $Re = 0$. The results of the solution by Dorrepaal et al. (1984) show that there is no force or moment on the cylinder. Hence, in the numerical solution it is possible that the value of β will tend to its correct value for $Re = 0$ if one considers the values of the parameter β at which the quantities such as the force or moment on the cylinder are zero as the Reynolds number tends to zero. To investigate this possibility values of ReC_D, $\mathrm{ReC}_L$and $\mathrm{ReC}_M$are calculated as functions of the parameter β for $0 \leq \beta \leq 3.5$ at $Re = 5, 3$ and 1 with $h = 1/10, 1/20$ and $1/40$.

Figures 2.4.1, 2.4.2 and 2.4.3 show the variation of ReC_D, $\mathrm{ReC}_L$and ReC_Mas a function of the strength of the rotlet, β, for $Re = 5, 3$ and 1, respectively, when using mesh sizes $10 \times 40, 20 \times 80$ and 40×160. It is observed from figures 2.4.2 and 2.4.3 that the variations of the lift and moment as a function of β are very non-linear. However, the drag, see figure 2.4.1, appears to behave almost linearly with respect to β, over the range $0 \leq \beta \leq 3.5$ for all the values of Re considered. Further, all the three values of Re considered in this book, predict that zero drag appears to occur close to the value of $\beta(= c) = 3$. It has already been established by Dorrepaal et al. (1984) that only for a stream whose direction and

magnitude are related to the position and strength of the rotlet will a solution be possible when $Re = 0$. In this case only for the specific value of $\beta = c$ will the problem be well posed and produce a solution for which the values for the drag, lift and moment on the cylinder are all zero. For all other values of β one will have the force and moment dependent on this parameter. It has been shown elsewhere that when $Re = 0$ non-zero values of the drag and lift implies that there are terms of the type $\mathrm{rln}(r)\sin(\vartheta)$ and $\mathrm{rln}(r)\cos(\vartheta)$ at large values of r. Similarly non zero values of the moment requires $a\ln(r)$ term. Obviously the presence of such terms violates the boundary condition that $f = 0$ as $r \to \infty$, and it is only when all such terms are absent that one will achieve the required solution. This is why at $Re = 0$ it is impossible to obtain a convergent solution for an arbitrary value of β, unlike the situation at $Re \neq 0$.

However, for $Re = 0$ one can think of the lift, drag and moment as functions of β and only when these quantities acquire the value of zero will β achieve its required value, namely $\beta = c$, and produce a convergent solution. Hence, the technique adopted was that of a Newton Raphson iteration on $C_D(\beta)$. The choice of C_D, rather than $C_L$or $C_M$being based upon the linearity of this expression with respect to β, compared with the rather complex behavior of the latter two quantities when considered as functions of this variable. The governing partial differential in finite-difference form, namely equations (2.3.1) and (2.3.2), were solved for two values of β, say $\beta_1$and β_2, the number of iterations being terminated after a prescribed number since due to the boundary condition posed at $\xi = 0$ convergent solutions are impossible. The resulting two non-zero values of $C_D(\beta_1)$ and $C_D(\beta_2)$ are the values used in the Newton Raphson method in order to establish a new value of β, say β_3, at which $C_D(\beta_3)$ is estimated to be zero. Resolving for this new value of β, and using $C_D(\beta_3)$ together with $C_D(\beta_1)$, or $C_D(\beta_2)$, whichever is closest to zero, to produce from the Newton Raphson solution a new value of β. The whole process is continued until the value of $C_D(\beta_3)$ reaches zero to within the required tolerance need to state what this is. The value of β automatically results in the correct values of $C_L$and C_M. The whole iterative procedure could equally well have been applied to setting either the values of $C_L(\beta)$ or $C_M(\beta)$ to zero. The resulting value of β achieved by this process was $3.0004, 3.0005$ and 3.0010 for the mesh sizes $40 \times 160, 20 \times 80$ and 10×40 respectively, compared with the exact analytical value of 3. The streamline and vorticity patterns produced from the numerical computation and

shown in figures 2.4.4 (a) and 2.4.5 (a) are identical with those obtained from the analytical solution.

Figure 2.4.4 show the streamline pattern obtain for $\beta = 3$ and $Re = 0, 1, 3$ and 5 for fine mesh size 40×160. In this figure the affect of changing Reynolds number it appear to be slight, but if we compare this figure by figure 2.4.8 the affect of Reynolds number become more clear. The region include the rotlet causes the separating streamline to close nearer the body.

Figure 2.4.5 show the vorticity pattern for $\beta = 3$ and $Re = 0, 1, 3$ and 5 for 40×160. The affect of changing Reynolds number not clear, since Reynolds number is very small and the strength of the rotlet is very strong.

Figure 2.4.6 show the streamline pattern for $\beta = 1.5$ and $Re = 1, 3$ and 5. The region include the rotlet becomes shorter but it appear to be unaffected by the small change in the Reynolds number.

Figure 2.4.7 show the vorticity pattern for $\beta = 1.5$ and $Re = 1, 3$ and 5. We note a slight movement of the line for equal vorticity. The vorticity in this outer area is almost constant and the point wise change is much smaller than the movement would seem to suggest.

Figure 2.4.8 shows the affect of the strength of the rotlet and how the result it tends to result obtained by Tang (1984). Figure 2.4.8 (f) is identical with the figure obtained by Tang (1990).

2.5 Conclusion

Numerical solutions of the full, steady, two-dimensional Navier-Stokes equations have been obtained for the fluid flow past a circular cylinder for Reynolds numbers $Re = 1, 3, 5$ and 20 and rotational parameter $0 \leq \alpha \leq 2$ when a rotlet of any given strength is placed at various positions outside the cylinder. Although numerical solutions can be found for any value of the Reynolds number greater than zero it is well known that when the Reynolds number is zero that a solution only exists provided there is a relationship between the strength of the rotlet and its location. Further, when the Reynolds number is zero the analytical solutions are such that the drag, lift and moment are all identically zero. Therefore in this chapter we have concentrated on obtaining numerical results with the drag, lift and moment zero and developed a technique for extrapolating the results obtained at small values of the Reynolds number to predict the solution for zero

Reynolds number. Using this technique it is found that the numerical results are in excellent agreement with all the available theoretical results. We conclude that the technique developed in this chapter may be used with confidence to predict solutions for flows at zero Reynolds numbers for situations where there are no analytical solutions.

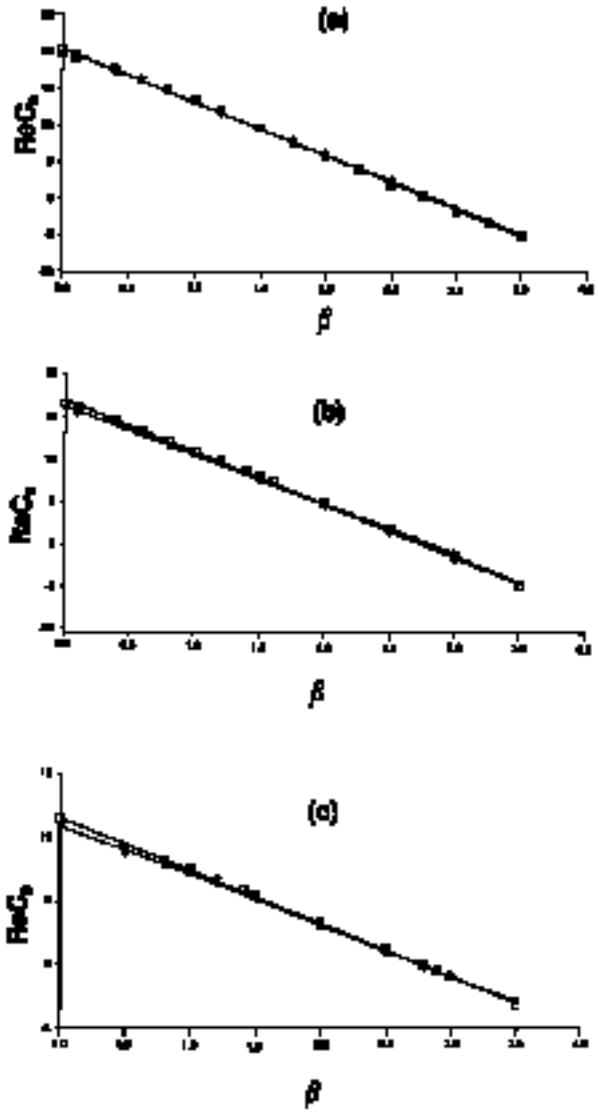

Figure 2.4.1: The variation of R_eC_D as a function of β.
$\diamond\diamond\diamond$ 10×40, $+++20 \times 80$, $***$ 40×160
$(a)Re = 5$ $(b)Re = 3$, and $(c)Re = 1$.

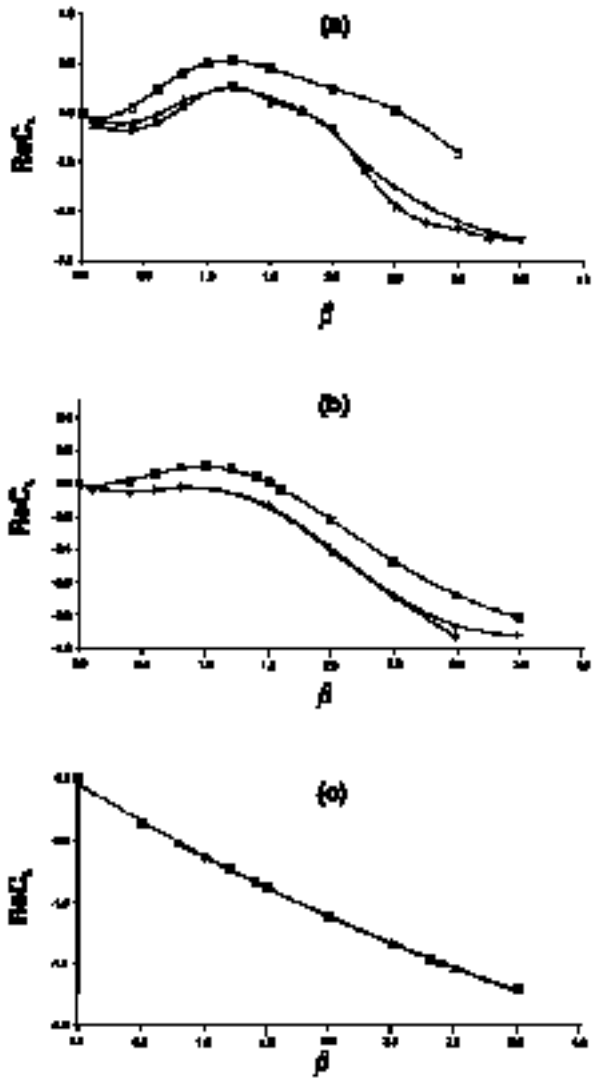

Figure 2.4.2: The variation of $R_e C_L$ as a function of β.
$\diamond\diamond\diamond$ 10×40, $+++20 \times 80$, $***$ 40×160
$(a) Re = 5$ $(b) Re = 3$, and $(c) Re = 1$.

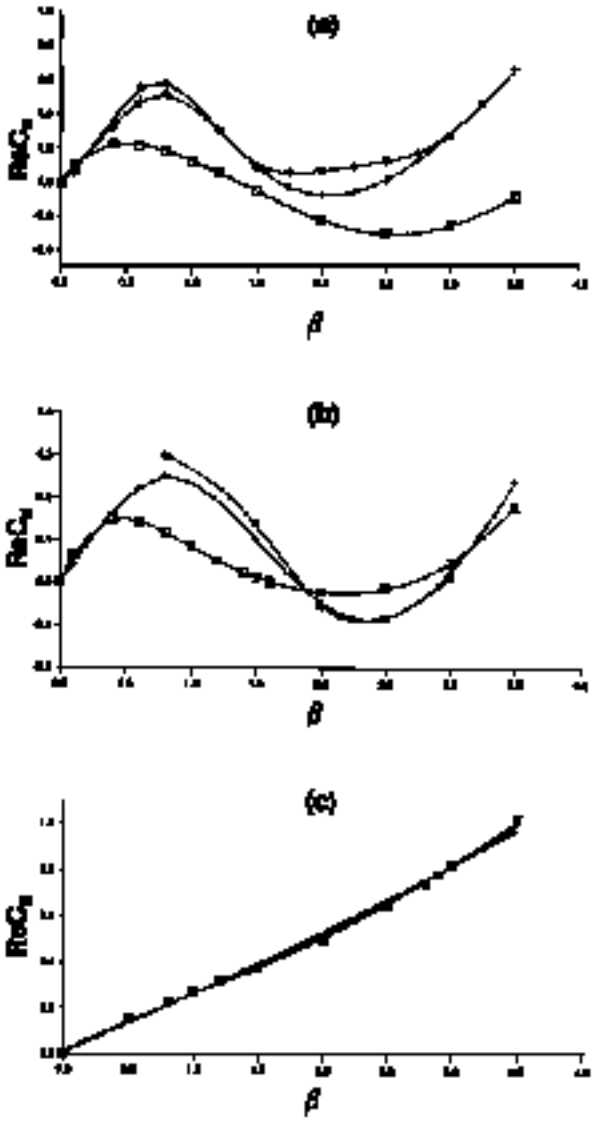

Figure 2.4.3: The variation of R_eC_M as a function of β.
$\diamond\diamond\diamond$ 10×40, $+++20 \times 80$, $***$ 40×160
$(a)Re = 5$ $(b)Re = 3$, and $(c)Re = 1$.

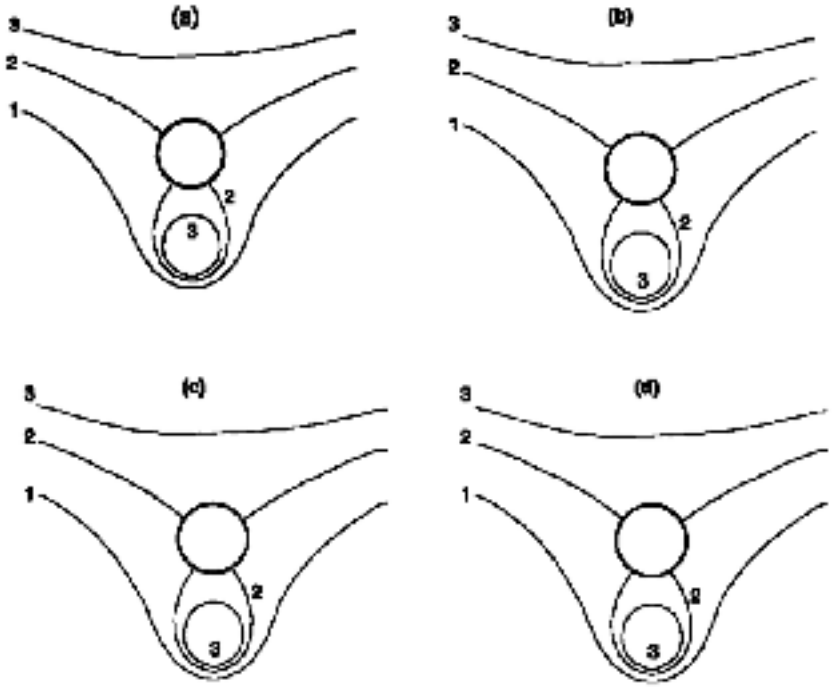

Figure 2.4.4: The numerically obtained streamlines, Ψ, for $\beta = 3$ with a mesh size 40×160. The streamlines labeled 1, 2 and 3 correspond to $\Psi = -1, 0$ and 0.7, respectively.
$(a) Re = 0, \quad (b) Re = 1, \quad (c) Re = 3, \quad and \quad (d) Re = 5.$

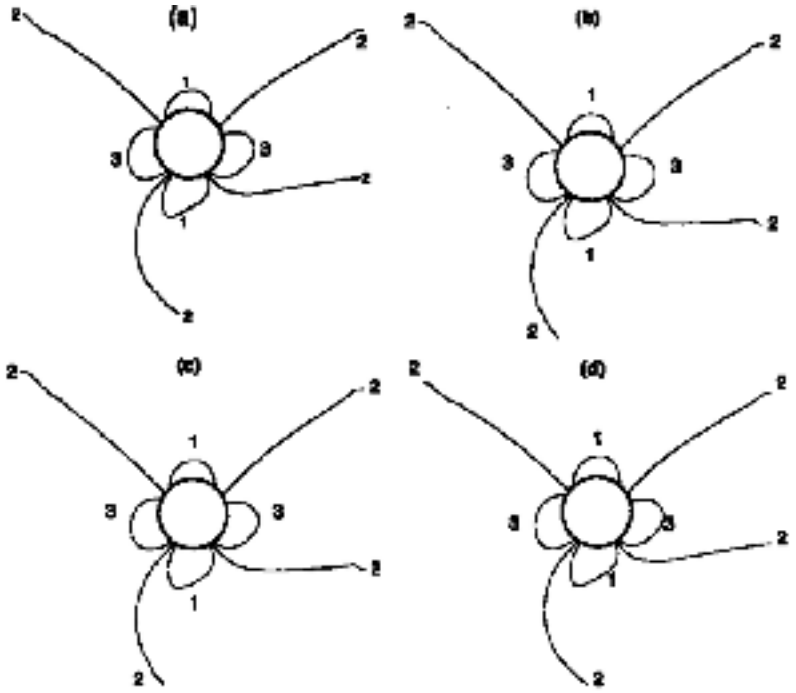

Figure 2.4.5: The numerically obtained vorticity , ω, for $\beta = 3$ with a mesh size 40×160. The vorticity lines labeled 1, 2 and 3 correspond to $\omega = -0.4, 0$ and 0.4, respectively. labeled 1, 2 and 3 correspond to $\omega = -0.4, 0$ and 0.4, respectively.
$(a) Re = 0, \quad (b) Re = 1, \quad (c) Re = 3, \quad \text{and} \quad (d) Re = 5.$

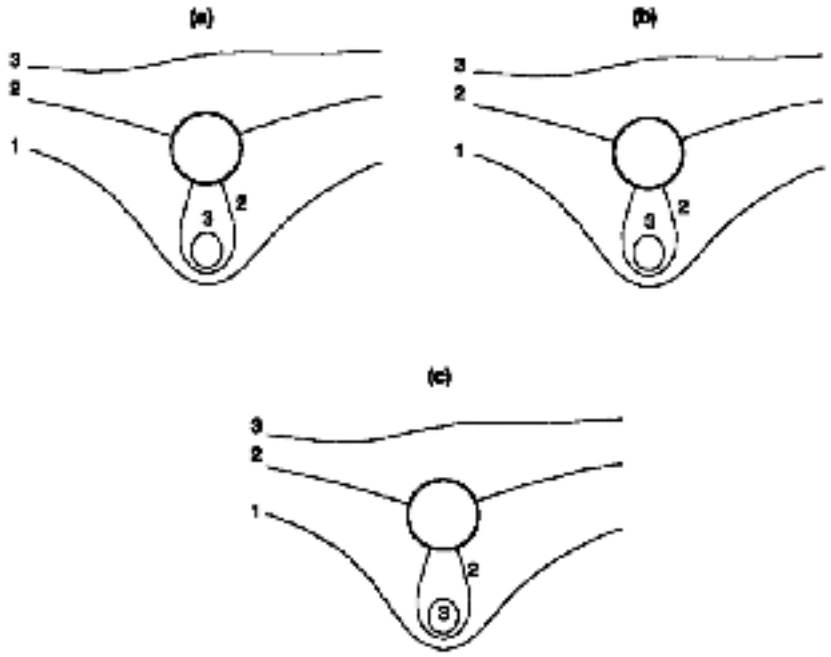

Figure 2.4.6: The numerically obtained streamlines, Ψ, for $\beta = 1.5$ with a mesh size 40×160. The streamlines labeled 1, 2 and 3 correspond to $\Psi = -1, 0$ and 0.7, respectively.
$(a) Re = 1, \quad (b) Re = 3, \quad \text{and} \quad (c) Re = 5.$

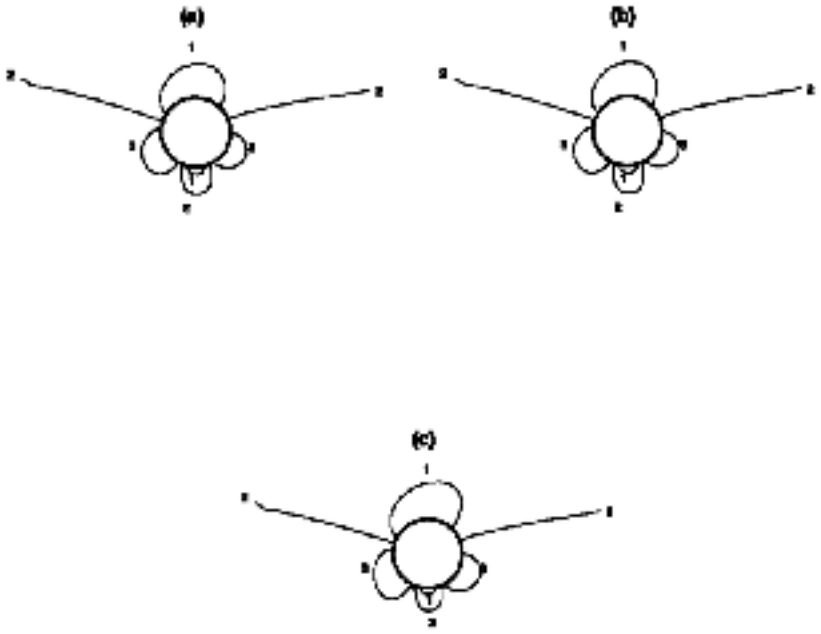

Figure 2.4.7: The numerically obtained vorticity, ω, for $\beta = 1.5$ with a mesh size 40×160. The vorticity lines labeled 1, 2 and 3 correspond to $\omega = -0.4, 0$ and 0.4, respectively.
$(a) Re = 1, \quad (b) Re = 3, \quad \text{and} \quad (c) Re = 5.$

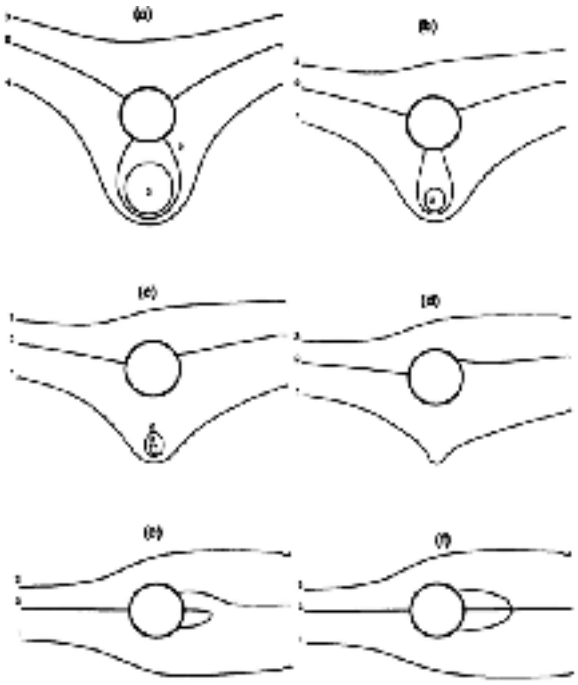

Figure 2.4.8: The numerically obtained streamlines, Ψ, for $Re = 20$ with a mesh size 40×160. The streamlines labeled 1, 2 and 3 correspond to $\Psi = -1, 0$ and 0.7, respectively.
$(a)\beta = 3, \quad (b)\beta = 1.5, \quad (c)\beta = 1, \quad (d)\beta = 0.5, \quad (e)\beta = 0.1, \quad \text{and} \quad (f)\beta = 0.$

Chapter 3

ANALYTICAL SOLUTION

3.1 Solution Using Fourier Series

In this section the problem originally discussed by Dorrepaal, O'Neill and Ranger (1984), namely that of a rotlet of non dimensional unit strength placed at a non dimensional distance c, where $c > 1$, from a cylinder whose radius a has been used as the non-dimensional length scale is investigated by an alternative approach. With the origin of the coordinates coinciding with the center of the cylinder, then the non-dimensional polar coordinate system (r, ϑ), where

$$x = r\cos\vartheta \text{ and } y = r\sin\vartheta, \tag{3.1.1}$$

has the boundary of the cylinder at $r = 1$ and the position of the rotlet at $(c, 0)$, as shown in Figure 3.1.1. Since the equations to be considered are those arising for two dimensional Stokes flow, then the elimination of the pressure terms from these equations, together with the introduction of a non dimensional stream function ψ, results in the biharmonic equation being the governing equation.

In the present approach it is required to solve the biharmonic equation

$$\nabla^4\psi = 0 \tag{3.1.2}$$

for the stream function $\psi(r, \vartheta)$, where $r \geq 1$ and $\nabla^2$is the standard Laplacian operator. The no slip and no normal flow boundary conditions imposed by the circular cylinder are

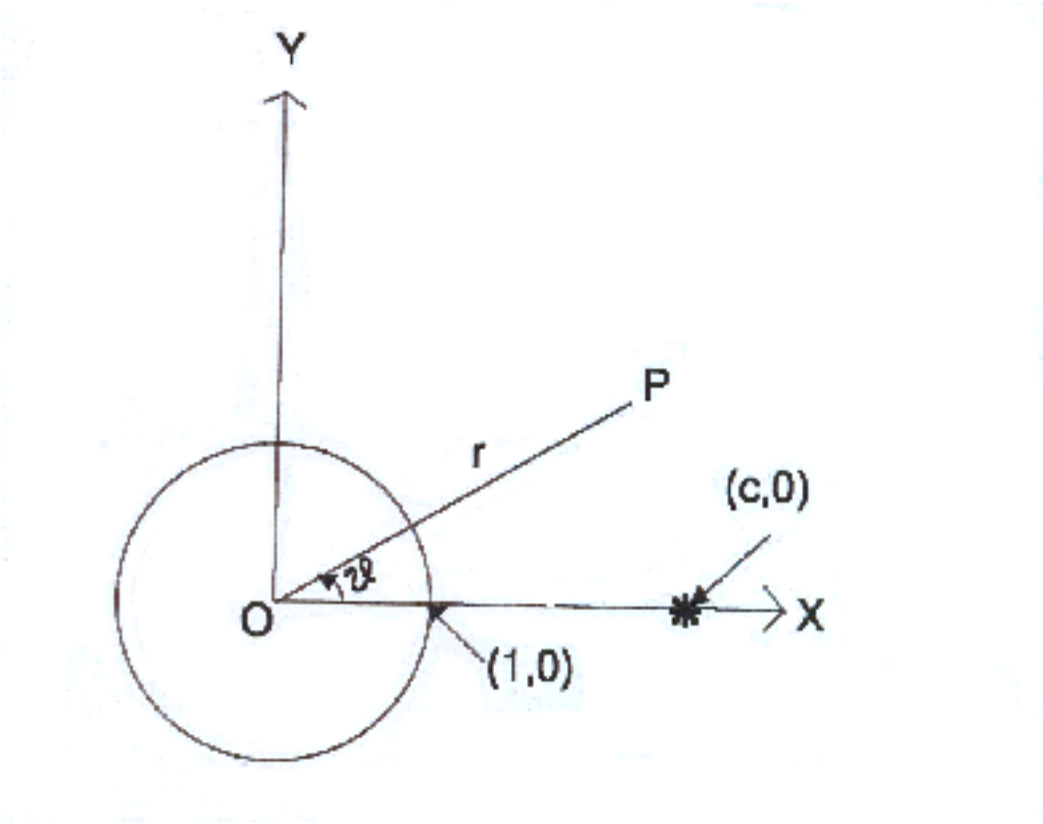

Figure 3.1.1: Position of circular cylinder and rotlet.

$$\psi = \frac{\partial \psi}{\partial r} = 0, \qquad \text{on } r = 1. \tag{3.1.3}$$

At present there appears no obvious condition to impose at infinity on the flow developed locally by a rotlet placed outside a cylinder. However, without any restrictions whatsoever then there are an infinite number of possibilities. As such if one is to allow for the locally generated flows at infinity to be present, then it appears realistic to assume that the flow which is established there is that with the slowest possible growth rate. This would seem plausible due to such a solution requiring the least amount of energy.

Before embarking on the present approach a few words relating to the solution by Dorrepaal, O'Niell and Ranger (1984) ought to be included due to its relatively clever and simplistic nature. The knowledge that the solution of the

biharmonic equation can be expressed as the sum of two solutions of Laplace's equation, namely

$$\psi = \phi_1 + (r^2 - 1)\phi_2, \tag{3.1.4}$$

where $\phi_1$and $\phi_2$are harmonic functions, enabled the function $\phi_1$to be taken as the potential solution for the flow due to a rotlet or stokelet outside a circular cylinder. This means that the function $\phi_1$satisfies the constant stream function condition on the boundary due to being formed from the singularity itself and the two images inside the cylinder at the image point and the origin. The choice of $(r^2 - 1)$ multiplying the harmonic function $\phi_2$results in the stream function maintaining its constant value on the boundary of the cylinder. Hence, the only requirement still outstanding in order to determine the complete solution is that on the boundary of the cylinder the normal derivative of $(r^2 - 1)\phi_2$is the negative of the normal derivative of ϕ_1. This usage of $(r^2 - 1)$, instead of the usual r^2, results in the above reducing to the necessity of find an harmonic function $\phi_2$whose value on $r = 1$ is half the known normal derivative of $\phi_1$there. It is this neat argument that enables the construction of the solution

$$\psi = \ln(R_1) - \ln(R_2 c) + \ln(r) + \frac{(r^2 - 1)(rc\cos\vartheta - 1)}{R_2^2 c^2}, \tag{3.1.5}$$

from what appears at first glance to be void of any analysis, where R_1 and R_2 are the distances from the rotlet and the image rotlet in the cylinder, and are given by

$$R_1 = (r^2 + c^2 - 2rccos\vartheta)^{1/2} \tag{3.1.6}$$

and

$$R_2 = (r^2 + \frac{1}{c^2} - 2\frac{r}{c}\cos\vartheta)^{1/2} \tag{3.1.7}$$

respectively. The present method is a more routine and less sophisticated approach than that mentioned above, however it follows a similar method but without the clever insight. Initially the value of ψ is expressed as

$$\psi = \psi_1 + \psi_2, \tag{3.1.8}$$

where ψ_1 is the stream function corresponding to a single rotlet at $(c, 0)$ and $\psi_2$is the change caused to this flow due to the presence of the cylinder and is free of any singularities in the region $r > 1$. The expression for ψ_1

$$\psi_1 = \frac{1}{2}\ln(r^2 + c^2 - 2rccos\vartheta) \tag{3.1.9}$$

is obviously an even function in ϑ and following Oberhettinger (1973) can be expressed as a Fourier Series representation, namely

$$\ln(c) - \sum_{n=1}^{\infty} \frac{r^n}{nc^n}\cos(n\vartheta) \qquad 1 \leq r \leq c. \tag{3.1.10}$$

The restriction on the domain of r is due to the series being convergent only for $r \leq$ c. Using the result that the general solution of

$$\nabla^4\psi_2 = 0, \tag{3.1.11}$$

can be written as $\psi_2 = \phi_1 + r^2\phi_2$, where ϕ_1 and ϕ_2 are harmonic functions, enables ψ_2 to be expressed as

$$\begin{aligned}\psi_2 = c_0 &+ \sum_{n=1}^{\infty}(b_n\sin(n\vartheta) + c_n\cos(n\vartheta))/r^n \\ &+ r^2 d_0 + \sum_{n=1}^{\infty}(a_n\sin(n\vartheta) + d_n\cos(n\vartheta))/r^{(n-2)}.\end{aligned} \tag{3.1.12}$$

Obviously, the lowest positive power of r in the choice of ϕ_1 and $\phi_2$is taken subject to being able to find a ψ which satisfies the boundary conditions on $r = 1$, and hence produces the solution with the slowest possible growth as $r \to \infty$. Applying the boundary conditions given by expressions (3.1.3) results in

$$\begin{aligned}&c_0 = -\ln c, \qquad d_0 = 0 \\ &a_1 = b_1 = c_1 = 0, \qquad d_1 = \frac{1}{2} \\ &a_n = b_n = 0, \qquad c_n = \frac{1}{c^n}(\frac{1}{n} - 1), \qquad d_n = \frac{1}{c^n}, \qquad n \geq 1.\end{aligned} \tag{3.1.13}$$

The series in expression (3.1.12) can now be summed to produce the result obtained by Dorrepaal, O'Neill and Ranger (1984), namely expression (3.1.5). Using the relationship between the vorticity ω and the stream function ψ,

$$\omega = \nabla^2 \psi \tag{3.1.14}$$

establishes the vorticity as

$$\omega = \frac{4}{c}[\frac{r\cos\vartheta}{R_2^2} - \frac{2r(rc\cos\vartheta - 1)(rc - \cos\vartheta)}{R_2^4 c^2} + \frac{(rc\cos\vartheta - 1)}{cR_2^2}]. \tag{3.1.15}$$

As the biharmonic equation and the boundary conditions are linear then the modification of the problem to accommodate the circular cylinder rotating with a non-dimensional clockwise angular velocity α, instead of being at rest, can easily be achieved by the addition of the term $\alpha \ln(r)$ to expression (3.1.5). This is possible since $\ln(r)$ is a solution of the biharmonic equation and satisfies the boundary conditions

$$v_r = -\frac{1}{r}\frac{\partial \psi}{\partial \vartheta} = 0 \text{ and } v_\vartheta = \frac{\partial \psi}{\partial r} = \alpha \text{ on } r = 1. \tag{3.1.16}$$

Hence, the stream function becomes

$$\psi = \ln(R_1) - \ln(R_2 c) + \ln(r) + \frac{(r^2 - 1)(rc\cos\vartheta - 1)}{R_2^2 c^2} + \alpha \ln(r), \tag{3.1.17}$$

whilst the vorticity remains unchanged.

3.2 Forces and Moment on the Cylinder

The components of force (F_x, F_y) and the moment M acting on a volume of fluid V surrounded by the surface S can be expressed as

$$F_x = \int_S (\sigma_{xx} n_x + \sigma_{xy} n_y) dS, \tag{3.2.1}$$

$$F_y = \int_S (\sigma_{yx} n_x + \sigma_{yy} n_y) dS, \tag{3.2.2}$$

$$M = \int_S x(\sigma_{yx}n_x + \sigma_{yy}n_y) - y(\sigma_{xx}n_x + \sigma_{xy}n_y)dS, \tag{3.2.3}$$

respectively, where $= (n_x, n_y)$ is the normal vector on the surface

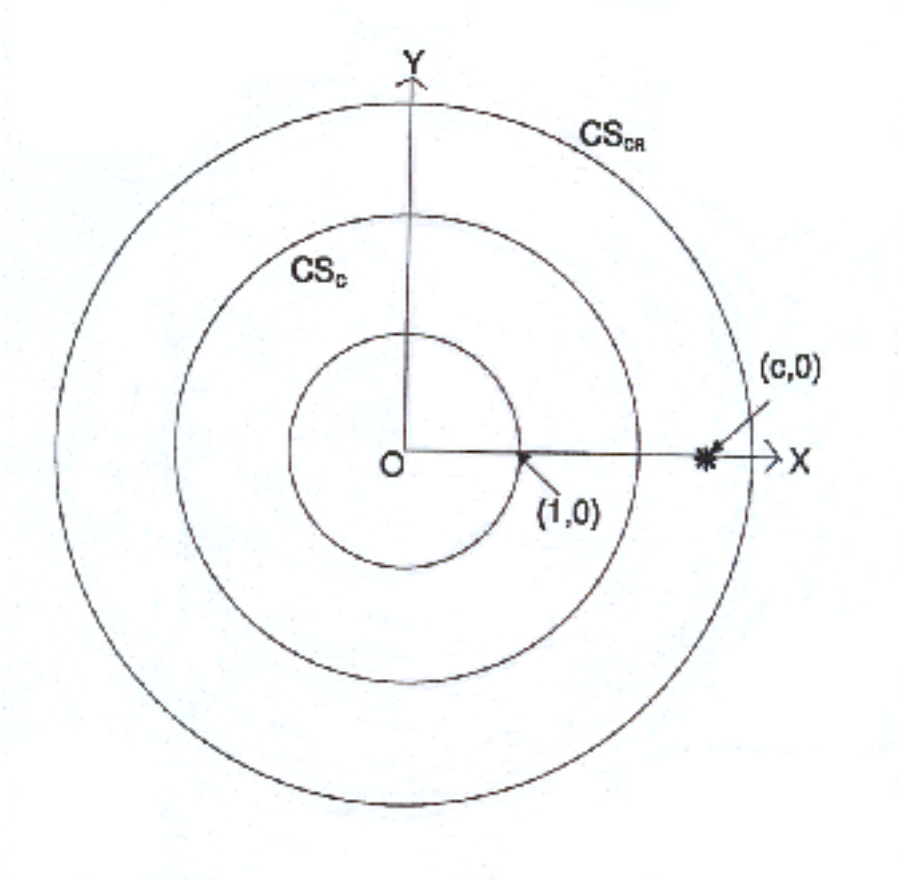

Figure 3.2.1: Concentric surfaces with center O. $CS_C$and CS_{CR}represent concentric surfaces enclosing the circular cylinder and both the circular cylinder and the rotlet respectively.

S. The quantity σ_{ij}denotes the stress acting in the direction on a surface element whose normal is in the direction. The reason for initially using the cartesian stress tensor rather than the cylindrical polar form will become clear in the the next section. In the special case when the surface is a cylinder with radius $r, r \geq 1$, and is represented in Figure 3.2.1 either by CS_Cor by CS_{CR}, whose centers coincide with that of the fixed cylinder of radius unity, the above

expressions can be written as

$$F_x = \int_S (\sigma_{rr}\cos\vartheta - \sigma_{r\vartheta}\sin\vartheta) r d\vartheta, \tag{3.2.4}$$

$$F_y = \int_S (\sigma_{\vartheta r}\cos\vartheta + \sigma_{rr}\sin\vartheta) r d\vartheta, \tag{3.2.5}$$

$$M = \int_S r\sigma_{r\vartheta} r d\vartheta. \tag{3.2.6}$$

Introducing the constitutive relations

$$\sigma_{rr} = -p + 2\mu\frac{\partial V_r}{\partial r}, \tag{3.2.7}$$

$$\sigma_{r\vartheta} = \sigma_{\vartheta r} = \mu\{r\frac{\partial}{\partial r}(\frac{V_\vartheta}{r}) + \frac{1}{r}\frac{\partial V_r}{\partial \vartheta}\}, \tag{3.2.8}$$

$$\sigma_{\vartheta\vartheta} = -p + 2\mu\{\frac{1}{r}\frac{\partial V_\vartheta}{\partial \vartheta} + \frac{V_r}{r}\}, \tag{3.2.9}$$

into expressions (3.2.4), (3.2.5) and (3.2.6) results in

$$F_x = \int_0^{2\pi} r[\frac{\partial p}{\partial \vartheta} + 2\mu\frac{1}{r}\frac{\partial}{\partial r}\{\frac{\partial^2\psi}{\partial\vartheta^2} + \psi\} - \mu\nabla^2\psi]\sin\vartheta d\vartheta, \tag{3.2.10}$$

$$F_y = -\int_0^{2\pi} r[\frac{\partial p}{\partial \vartheta} + 2\mu\frac{1}{r}\frac{\partial}{\partial r}\{\frac{\partial^2\psi}{\partial\vartheta^2} + \psi\} - \mu\nabla^2\psi]\cos\vartheta d\vartheta, \tag{3.2.11}$$

$$M = \mu\int_0^{2\pi} r^2[\frac{\partial^2\psi}{\partial r^2} - \frac{1}{r}\frac{\partial\psi}{\partial r} - \frac{1}{r^2}\frac{\partial^2\psi}{\partial\vartheta^2}]d\vartheta. \tag{3.2.12}$$

On using the equations of motion, namely Stokes Equation, and the vorticity, the equations (3.2.10) − (3.2.12 can be written in the form

$$F_x = \mu\int_0^{2\pi} r[r\frac{\partial\omega}{\partial r} - \omega + \frac{2}{r}\frac{\partial}{\partial r}(\frac{\partial^2\psi}{\partial\vartheta^2} + \psi)]\sin(\vartheta)d\vartheta, \tag{3.2.13}$$

$$F_y = -\mu \int_0^{2\pi} r[r\frac{\partial \omega}{\partial r} - \omega + \frac{2}{r}\frac{\partial}{\partial r}(\frac{\partial^2 \psi}{\partial \vartheta^2} + \psi)]\cos(\vartheta) d\vartheta, \tag{3.2.14}$$

$$M = \mu \int_0^{2\pi} r^2[\omega - \frac{2}{r}\frac{\partial \psi}{\partial r} - \frac{2}{r^2}\frac{\partial^2 \psi}{\partial \vartheta^2}]\ d\vartheta. \tag{3.2.15}$$

The above expressions are still dimensional, so expressions (3.1.5) and (3.1.15) need to be modified accordingly before they are substituted. So, if one has commenced with a rotlet of strength Γ at $(c, 0)$, which means that the circulation around the rotlet is $2\pi\Gamma$, then the coefficient values would have to be multiplied by Γ. Unfortunately, the resulting integrals are such that they need to be calculated numerically. Using Simpson's rule to undertake this evaluation results in

$$F_x = F_y = 0 \text{ and } M = 0, \text{ for } 1 \leq r < c; \tag{3.2.16}$$

$$\text{and } F_x = F_y = 0 \text{ and } M = -4\pi\mu\Gamma, \text{ for } r > c. \tag{3.2.17}$$

3.3 Method of Obtaining the Forces

Instead of using the expressions for ψ and ω from equations (3.1.5) and (3.1.15) respectively, one can view the solution of the biharmonic equation by separation of variables as

$$\psi = F_0(r) + \sum_{n=1}^{\infty}\{F_n(r)\sin(n\vartheta) + G_n(r)\cos(n\vartheta)\}, \tag{3.3.1}$$

since periodicity in ϑ is required. Due to the linearity of the terms in the integrands of equations $(3.2.13) - (3.2.15)$ it is relatively straightforward to see that contributions to the force must arise from the $F_1(r)\sin\vartheta$ and $G_1(r)\cos\vartheta$, whereas any contribution to the moment is solely due to the $F_0(r)$ term. On substituting expression (3.3.1) into equation (3.1.2) one obtains

$$F_0(r) = A_0(r^2\ln(r) - r^2) + B_0 r^2 + C_0\ln(r) + D_0, \tag{3.3.2}$$

$$F_1(r) = FA_1 r^3 + FB_1 rln(r) + FC_1 r + FD_1 r^{-1}, \tag{3.3.3}$$

$$G_1(r) = GA_1 r^3 + GB_1 r ln(r) + GC_1 r + GD_1 r^{-1}, \tag{3.3.4}$$

where $A_0, B_0, C_0, D_o, FA_1, FB_1, FC_1, FD_1, GA_1, GB_1, GC_1$ and GD_1 are constants. The forms of $F_n(r)$ and $G_n(r)$ can be derived if required as

$$F_n(r) = FA_n r^{n+2} + FB_n r^n + FC_n r^{-n+2} + FD_n r^{-n}, \tag{3.3.5}$$

$$G_n(r) = GA_n r^{n+2} + GB_n r^n + GC_n r^{-n+2} + GD_n r^{-n}. \tag{3.3.6}$$

At this stage a further digression from the original problem is undertaken. Since the usual Stokes problem is likely to involve either $(i)a$ uniform stream at infinity, so requiring the stream function to behave like $r\cos\vartheta$ or $r\sin\vartheta$ at large values of r, or $(ii)a$ rotational flow, so needing the stream function to behave as r^2 at large values of r, it seems appropriate to set A_0, FA_1, FB_1, GA_1 and GB_1 all to be zero. However, whether this restriction should be applied to FB_1 and to GB_1 is debatable since if one considers the classical problem of uniform flow past a circular cylinder such terms are present in the solution. Although it should be stressed that this solution only satisfies the biharmonic equation and the boundary conditions on the cylinder. The failure of the solution at infinity is due to the presence of the $r\ln(r)\sin\vartheta$ term which must be maintained in order for both the velocity components to vanish on the cylinder. The solution that tends to infinity most slowly as $r \to \infty$ is obtained by discarding only the $FA_1 r^3 \sin\vartheta$ and $GA_1 r^3 \cos\vartheta$ terms. The resulting solution is valid at points not too far from the cylinder but deteriorates as one moves further away. It also fails to determine the value of the constant FB_1. It should be noted that no value of GB_1 is required due to the stream function being anti-symmetric and thus one requires only terms in $\sin\vartheta$. However, the above unknown constant FB_1 can be found by treating the solution found so far as the first approximation to the inner flow past the circular cylinder as the Reynolds number tends to zero, and matching with the solution from the outer region derived from the Oseen equations. Full details regarding these expansions and matching procedure can be found in Proudman and Pearson (1957).

Returning now to the expressions (3.2.13), (3.2.14) and (3.2.15), when the $F_1(r)\sin\vartheta, G_1(r)\cos\vartheta$ and $F_0(r)$ are substituted respectively into the integrands in these expressions, the following values are produced

$$[r\frac{\partial\omega}{\partial r}-\omega+\frac{2}{r}\frac{\partial}{\partial r}\{\frac{\partial^2\psi}{\partial\vartheta^2}+\psi\}]=-\frac{4FB_1}{r}\sin\vartheta, \tag{3.3.7}$$

$$[r\frac{\partial\omega}{\partial r}-\omega+\frac{2}{r}\frac{\partial}{\partial r}\{\frac{\partial^2\psi}{\partial\vartheta^2}+\psi\}]=-\frac{4FB_1}{r}\cos\vartheta, \tag{3.3.8}$$

$$[\omega-\frac{2}{r}\frac{\partial\psi}{\partial r}-\frac{2}{r^2}\frac{\partial^2\psi}{\partial\vartheta^2}]=-\frac{2C_0}{r^2} \tag{3.3.9}$$

The evaluation of the resulting integrals result in

$$F_x=-4\pi\mu\Gamma FB_1a^{-1},\quad F_y=4\pi\mu\Gamma GB_1a^{-1}, \tag{3.3.10}$$

$$M=-4\pi\mu\Gamma C_0. \tag{3.3.11}$$

As all these quantities are independent of the radius of the surface on which the evaluation of the integrals has been undertaken, it would appear that the force components and the moment will be the same on the cylindrical body as what they are on any concentric circular region of fluid enclosing that body. This phenomenon will be discussed in greater detail in the next section where it will be generalized.

It should, however, be mentioned that for the force components and moment to remain unchanged as the radius of the cylindrical surface CS_C increases there must be no additional singularities of the flow included in the increased volume of fluid. In addition if the terms $A_0(r^2\ln(r)-r^2), FA_1r^3$and GA_1r^3had been retained in the expansions of $F_0(r), F_1(r)$ and $G_1(r)$, so allowing solutions which grow much more rapidly as $r\to\infty$, then whilst $F_x$and $F_y$would have remained unchanged the value of the moment M would have been modified to included a contribution from A_0, so

$$M=-4\pi\mu\Gamma(C_0-r^2A_0). \tag{3.3.12}$$

Initially this may appear to be a contradiction of a result to be established later, namely that the moment on a surface $CS_C$is independent of the radius, however it can be seen that the inclusion in the stream function of the term $A_0(r^2\ln(r)-r^2)$ results in

$$\omega = \nabla^2\psi = 4A_0(\ln(r) + 1), \tag{3.3.13}$$

which in turn produces a pressure distribution

$$p = 4A_0\vartheta \tag{3.3.14}$$

to within an arbitrary constant. The multivaluedness of the pressure must obviously be avoided in the present problem and hence the requirement that

$$A_0 = 0 \tag{3.3.15}$$

has to be imposed. This produces the invariance of the moment on any surface CS_C, provided that $1 \leq r <$ c.

If one now refers back to

$$\psi = \psi_1 + \psi_2, \tag{3.3.16}$$

where $\psi_1$and $\psi_2$are given by expressions (3.1.10) and (3.1.12), respectively, provided that $1 \leq r < c$, then the absence of any of the terms $\mathrm{rln}(r)\sin\vartheta$, $\mathrm{rln}(r)\cos\vartheta$ and $\ln(r)$ confirms the earlier result given by expression (3.2.16) that in the problem of flow caused by a rotlet outside a circular cylinder both the components of the force and the moment acting on the cylinder are zero.

However, the expansion in expression (3.1.10) is valid only for $1 \leq r < c$, whilst the expansion in (3.1.12) is valid for $r \geq 1$. This means that to continue the solution analytically into $r > c$ one must replace expression (3.1.10) by expression (3.1.9), but expression (3.1.12) is perfectly acceptable as the contribution for ψ_2. In the region $r > c$ expression (3.1.9) can be written as

$$\Psi_1 = \ln(r) + \frac{1}{2}\ln(1 + \frac{c^2}{r^2} - 2\frac{c}{r}\cos\vartheta), \tag{3.3.17}$$

which in turn can be expanded as

$$\psi_1 = \ln(r) - \sum_{n=1}^{\infty} \frac{c^n}{nr^n}\cos(n\vartheta) \qquad r > c. \tag{3.3.18}$$

If in the region $r > c$ one takes the stream function to consist of the sum of expressions (3.1.12) and (3.3.17), then one can see that C_0will no longer be zero. Hence, although the components of force acting on a concentric cylindrical surface $CS_{CR}$of fluid of radius $r > c$ will be zero, as they were on an identical shaped surface CS_Cbut with radius $r < c$, the moment on such surface will now be $-4\pi\mu\Gamma C_0$, where $C_0 = 1$. This change in the moment value from zero to $-4\pi\mu\Gamma$ as the radius of the surface increases above c will be discussed in detail in the next section.

3.4 Relations between the Forces

Returning to the expressions (3.2.1), (3.2.2) and (3.2.3) it is a relatively straightforward matter to show that the force and moment acting on any simply connected volume of fluid V, void of any singularities, are both zero. Since the surface integrals representing $F_x$and $F_y$can both be converted by the divergence theorem into the following volume integrals

$$F_x = \int_V [\frac{\partial \sigma_{xx}}{\partial x} + \frac{\partial \sigma_{xy}}{\partial y}]dV, \tag{3.4.1}$$

$$F_y = \int_V [\frac{\partial \sigma_{yx}}{\partial x} + \frac{\partial \sigma_{yy}}{\partial y}]dV, \tag{3.4.2}$$

and the integrands are zero from the Stokes equations, namely

$$0 = \frac{\partial \sigma_{xx}}{\partial x} + \frac{\partial \sigma_{xy}}{\partial y}, \tag{3.4.3}$$

$$0 = \frac{\partial \sigma_{yx}}{\partial x} + \frac{\partial \sigma_{yy}}{\partial y}, \tag{3.4.4}$$

and hence both components of force $F_x$and $F_y$are zero.

The evaluation of M for the same volume of fluid requires the integrand first being manipulated into the form

$$(x\sigma_{yx} - y\sigma_{xx})n_x + (x\sigma_{yy} - y\sigma_{xy})n_y, \tag{3.4.5}$$

which can be transformed into a volume integral by the divergence theorem, resulting in

$$M = \int_V [\frac{\partial}{\partial x}\{x\sigma_{yx} - y\sigma_{xx}\} + \frac{\partial}{\partial y}\{x\sigma_{yy} - y\sigma_{xy}\}]dV \tag{3.4.6}$$

$$= \int_V [\sigma_{yx} + x\frac{\partial \sigma_{yx}}{\partial x} - y\frac{\partial \sigma_{xx}}{\partial x} + x\frac{\partial \sigma_{yy}}{\partial y} - \sigma_{xy} - y\frac{\partial \sigma_{xy}}{\partial y}]dV. \tag{3.4.7}$$

The Stokes equations (3.4.3) and (3.4.4), together with the symmetry of the stress tensor, σ_{ij}, produce the moment on the region as zero. The above results mean that the force and moment on a surface S, which surrounds an object around which the fluid motion is governed by Stokes equations, are identical to the force and moment values on any other surface S_1which encloses the surface S. This can easily be seen by introducing a cut in the region between S and S_1, so that the volume between the two surfaces can be treated as a simply connected region. This enables information from the surface at infinity to predict the values of force and moment on the object. It is this information which resulted in both the force components and the moment in the earlier section being unchanged on any concentric cylindrical surface of fluid $SC_C$of radius r, where $1 < r <$ c. However, it is possible to see that the same result applies on all surfaces $GS_C$of fluid, regardless of their shape, which contain within it the circular cylinder, provided that the surface does not enclose any singularizes. The same information shows why the force components and the moment on concentric cylindrical surfaces CS_{CR}that, in addition to the cylinder, contain the rotlet singularity at $(c, 0)$ and have a radius r, where $r > c$, possess constant values. Again the values remain unchanged on any surface GS_{CR}containing the cylinder and the rotlet regardless of the shape of the surface. The surfaces $GS_C$and $GS_{CR}$are shown in Figure 3.4.1.

One can also see why there is a difference in the value of the moment of $-4\pi\mu\Gamma$ between surfaces containing the cylinder and those which in addition contain the rotlet. Yet, there is no difference in the value of the force components between surfaces containing the cylinder and those which in addition contain the rotlet. In the case of the moment on any surface $GS_{CR}$of fluid containing both the cylinder and the rotlet this value is equal to the sum of the moment on any surface $CS_C$of fluid containing only the cylinder plus the contribution

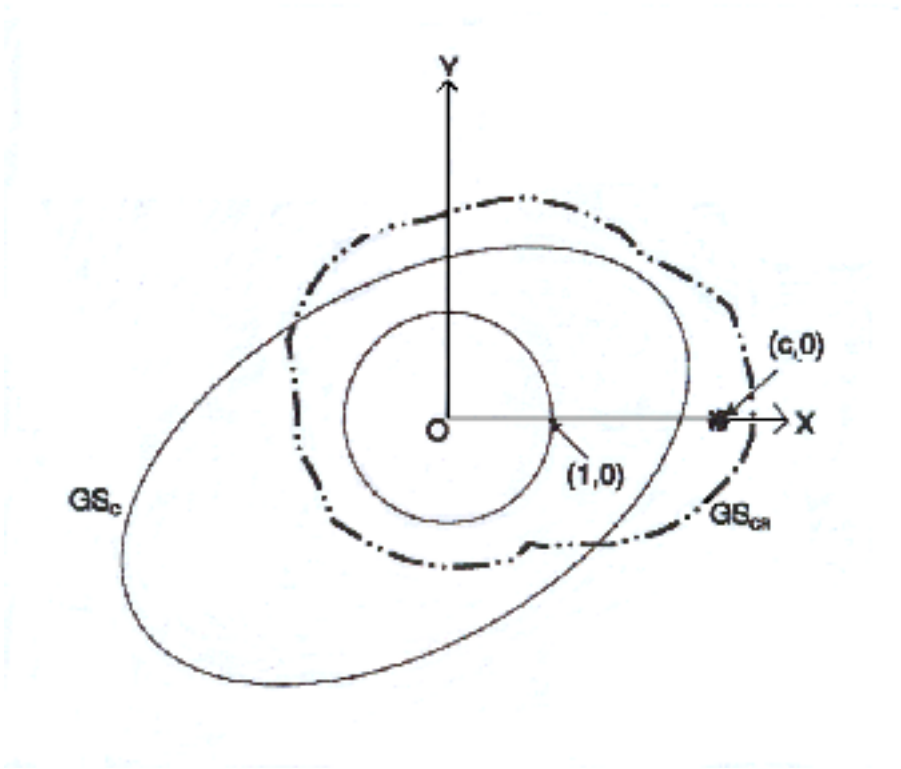

Figure 3.4.1: Generalized surfaces. GS_c and GS_{CR}represent general surfaces enclosing the circular cylinder and both the circular cylinder and the rotlet respectively.

from the moment on the rotlet. As the stream function near the rotlet can be expressed as

$$\psi \approx \ln(R_1), \tag{3.4.8}$$

which is equivalent to $a\ln(r)$ term in $F_0(r)$ in the expansion of the stream function given by expression (3.3.1), the contribution to the moment from the rotlet is $-4\pi\mu\Gamma$. Hence, the zero contribution on the inner surface GS_Ccombined with that from the rotlet produces the result for the moment established earlier on the outer surface GS_{CR}. In a similar manner the force components between the two surfaces can be related. However, the form of the stream function near the rotlet, given by expression (3.4.8), results in there being no force in either

direction on the rotlet. This results in the force components on the two surfaces $GS_C$and GS_{CR}remaining the same. Hence, since they are both zero on the inner surface, they are both zero on the outer surface. This means that provided one knows the expansion of the stream function for flow around a body at large values of r, and the expansion close to any singularity, it is possible using the coefficients of $FB_1$and $GB_1$to determine the components of force acting both on a surface of fluid containing the object at infinity and on the surface around the singularity. The difference in these quantities will produce the force on the body. In a similar manner the moment on the body can be produced from the difference between the moment on the surface of fluid at large values of r which contains the body and the moment on the singularity. In this case, the two moments are obtained directly from the values of the coefficients of C_0in the appropriate regions, and their difference produces the moment on the body itself.

3.5 Flows at Infinity

It has been establish earlier how the expansion of the stream function may be used to predict the force and the moment acting on the circular cylinder. The reverse situation will now be discussed, that is given a force and a moment acting on a circular cylinder in the presence of a rotlet, what is the stream function and how does this behave at large values of r?

In order to have a prescribed force $-4\pi\mu\Gamma(A,-B)a^{-1}$, together with a moment $-4\pi\mu\Gamma C$, acting on the circular cylinder it is necessary for the expansion at large values of r to include the $C_0\ln(r), FB_1\mathrm{rln}(r)\sin\vartheta$ and $GB_1\mathrm{rln}(r)\cos\vartheta$ terms. Obviously as these terms are solutions of the biharmonic equation and satisfy the boundary condition that the normal velocity on the cylinder is zero, the linearity of the problem allows them to be combined with the earlier result given by applying the boundary conditions in expression (3.1.3). All that remains is to combine this result with another solution of the biharmonic equation which satisfies the zero normal boundary condition but has a non zero tangential velocity. The obvious choice of this additional solution is the uniform stream potential flow solution past such a circular cylinder in order to balance the $FB_1\mathrm{rln}(r)\sin\vartheta$ and $FB_1\mathrm{rln}(r)\cos\vartheta$ terms, together with a rigid body rotation arising from an (r^2-1) term. The correct combination of the above extra solu-

tions will produce the required zero tangential velocity boundary condition on $r = 1$. Hence, the complete additional solution is

$$\begin{aligned} &C_0[ln(r) - \frac{1}{2}(r^2 - 1)] + FB_1[rln(r) - \frac{1}{2}(r - r^{-1})]\sin\vartheta \\ &+ GB_1[rln(r) - \frac{1}{2}(r - r^{-1})]\cos\vartheta \end{aligned} \tag{3.5.1}$$

and in order to produce the prescribed force it will be necessary for

$$FB_1 = A, \quad GB_1 = B, \tag{3.5.2}$$

$$\text{and} \quad C_0 = C + 1. \tag{3.5.3}$$

The moment on a surface GS_{CR} surrounding the circular cylinder and the rotlet will have a moment $-4\pi\mu\Gamma(C+1)$. When the value of the moment on the rotlet $-4\pi\mu\Gamma$ is subtracted for this value, it will produce the required value of $-4\pi\mu\Gamma C$ on the circular cylinder itself. Hence, the required stream function is

$$\begin{aligned} \psi &= \ln(R_1) - \ln(R_2 c) + \ln(r) + \frac{(r^2-1)(rc\cos\vartheta - 1)}{R_2^2 c^2} \\ &+ C[\ln(r) - \frac{1}{2}(r^2 - 1)] + A[rln(r) - \frac{1}{2}(r - r^{-1})]\sin\vartheta \\ &- B[rln(r) - \frac{1}{2}(r - r^{-1})]\cos\vartheta, \end{aligned} \tag{3.5.4}$$

together with a vorticity value given by

$$\begin{aligned} \omega = \frac{4}{c}[&\frac{r\cos\vartheta}{R_2^2} - \frac{2r(rc\cos\vartheta - 1)(rc - \cos\vartheta)}{c^2 R_2^4} + \frac{(rc\cos\vartheta - 1)}{cR_2^2}] \\ &- 2C + \frac{2(A\sin\vartheta - B\cos\vartheta)}{r}. \end{aligned} \tag{3.5.5}$$

The expression (3.5.4), with $A = B = 0$, corresponds to the result obtained by Avudainayagam and Jothiram (1987) for eccentric rotational flow around a circular cylinder in the presence of a rotlet singularity. The form of the above stream function at large values of r will be

$$\begin{aligned} \psi \approx &-\frac{1}{2}Cr^2 + Arln(r)\sin\vartheta - Brln(r)\cos\vartheta - \frac{1}{2}Arsin\vartheta \\ &+ \frac{1}{2}(\frac{2}{c} - B)rcos\vartheta + (C+1)\ln(r). \end{aligned} \tag{3.5.6}$$

In the special situation when there is no force or moment on the circular cylinder then

$$A = B = C = 0 \tag{3.5.7}$$

and at large values of r the above form of the stream function reduces to

$$\psi \approx \frac{1}{c} r cos\vartheta + \ln(r) + \frac{1}{c^2}\cos(2\vartheta) - \ln(c) + O(r^{-1}). \tag{3.5.8}$$

In fact the $O(r^{-1})$ term is $(\frac{1}{c^3}\cos(3\vartheta))$. If $\ln(R_1)$ is retained in the expansion (3.5.8) rather than $\ln(r)$ then the $O(r^{-1})$ term is $(\frac{1}{c^3}\cos(3\vartheta) + \text{ccos}(\vartheta))$. Physically expression (3.5.8) represents at large distances from the cylinder, a uniform stream of non-dimensional magnitude $\frac{1}{c}$ flowing towards the origin from the direction of the negative y axis, together with the effects of a rotlet of non-dimensional strength unity at the origin. Hence, one has the situation first established by Dorrepaal, O'Neill and Ranger (1984), namely, that provided a rotlet is added at the correct position to the problem of a uniform flow past a circular cylinder, its strength dependent on its distance from the origin and the magnitude of the uniform stream, then what originally is an ill posed Stokes problem becomes well posed. If " * " is used to denote dimensional quantities, then expression (3.5.8) for the dimensional stream function becomes

$$\psi^* \approx \Gamma[\frac{1}{c^*} r^* \cos\vartheta + \ln(r^*/a) + \frac{a^2}{c^{*2}}\cos(2\vartheta) - \ln(c^*/a) + O(r^{*^{-1}}), \tag{3.5.9}$$

where $c = c^*/a$, so the dimensional position of the rotlet is $(c^*, 0)$. The substitution of expressions (3.5.4) and (3.5.5) into expressions (3.2.13), (3.2.14) and (3.2.15), together with the evaluations of the resulting integrals using Simpson's rule, confirmed the values of A, B and C used to produce the analytical results. It possible should show the force components and moments arising by Simpsons rule corresponding to some values of A, B and C for which forces and moments are known.

Numerical values of the integrals in expressions (3.2.13), (3.2.14) and (3.2.15) were evaluated by Simpson's rule for the non-dimensional stream function and vorticity given by expressions (3.1.5) and (3.1.15) respectively. The procedure was repeated with the non-dimensional steam function and vorticity represented

by expressions (3.1.17) and (3.1.15) respectively, with the value of α equal to 1 and then 2. In each situation the contours along which the integrations were undertaken where circles, with radii of 1, 2, 4, and 5, concentric with the circular cylinder. The first two contours enclose only the cylinder, whereas the last two enclose both the cylinder and the rotlet. Due to the different contours over which the integrations were performed, different step lengths were required in order to acquire four decimal place accuracy. However, a step length of $h = 1/40$ proved sufficient to achieve this requirement on all the contours. Details of the values of F_x, F_y and M on the various contours are shown in Table 3.5.1.

TABLE (3.5.1)

The values of F_x, F_y and M on concentric circles around the circular cylinder.

Radius of concentric circle	α	$F_x/(\mu\Gamma a^{-1})$	$F_y/(\mu\Gamma a^{-1})$	$M/(\mu\Gamma)$
1	0	0.0000	0.0000	0.0000
2	0	0.0000	0.0000	0.0035
4	0	0.0000	0.0000	−12.5635
5	0	0.0000	0.0000	−12.5643
1	1	0.0000	0.0000	−12.5664
2	1	0.0000	0.0000	−12.5628
4	1	0.0000	0.0000	−25.1299
5	1	0.0000	0.0000	−25.1306
1	2	0.0000	0.0000	−25.1327
2	2	0.0000	0.0000	−25.1292
4	2	0.0000	0.0000	−37.6962
5	2	0.0000	0.0000	−37.6970

These results are as expected. Since in the case of the force components F_x and F_y are both zero due to the absence of any $rln(r)sin\vartheta$ and $rln(r)cos\vartheta$ terms from the non-dimensional stream function expression (3.1.5) and (3.1.17). The M should undertake the value $-4\pi\mu\Gamma(\alpha+1)$ on contours whose radius exceeds the value C, that is includes the rotlet as well as the circular cylinder. Whereas, on contours which exclude the rotlet the value should be $-4\pi\mu\Gamma\alpha$, due to the need to exclude the contribution to the moment from the rotlet. In addition, when the non-dimensional angular velocity of the cylinder is α, the analytical

form of the non-dimensional stream function results in the asymptotic expansion at large values of r containing an $(\alpha+1)ln(r)$ term. The above numerical values confirm the theoretical result that the moment on the circular cylinder is $-4\pi\mu\Gamma$ times the coefficient of the $ln(r)$ term in the asymptotic expansion, provided any contributions from singularities are excluded.

3.6 Conclusions

The Fourier Series Method has been used successfully to obtain an analytical solution for the solution of the biharmonic equation outside a circular cylinder with a rotelt placed in the solution domain.

Chapter 4

FLOW GENERATED BY A ROTLET

4.1 Introduction

Before embarking on the numerical scheme which has been adopted to solve the most general situation, namely when both the force and the moment on the circular cylinder are non zero, a brief discussion of an alternate approach used for the solution of the problem in the absence of any force or moment on the circular cylinder, as yet unpublished, will be given. Hence, for the present, the discussion relates to the well posed Stokes problem of a uniform stream flowing past a circular cylinder in the presence of a rotlet, but in the absence of any force or moment on the cylinder. By outlining the reason for the failure of this numerical approach to accommodate the situation when the force and moment on the cylinder are non zero leads one to understand why the later particular numerical method has been chosen.

This alternative approach follows directly the technique presented by Tang (1990) for the problem of uniform flow past a rotating circular cylinder at low Reynolds number. In their paper the stream function was expressed as that due to a uniform stream plus a perturbation affect which arises solely from the presence of the rotating cylinder. It was assumed that this removal from the stream function of the contribution due to the uniform stream would result in the stream function perturbation being $\mathbf{O}(r)$ at large values of r. Expressing

the perturbation stream function as some function of r and ϑ, namely $f(r,\vartheta)$, multiplied by r, meant that $f(r,\vartheta)$ tended to zero as $r \to \infty$. Inversion of the radial coordinate resulted in the conditions at infinity being mapped to the origin. Hence, the solution domain became $0 \leq \vartheta \leq 2\pi$ and $0 \leq \xi \leq 1$, where $\xi = r^{-1}$. In addition, the ϑ coordinate was scaled by defining $\eta = (2\vartheta)/\pi$, resulting in the final solution domain being $0 \leq \xi \leq 1$ and $0 \leq \eta \leq 4$. Although this extra scaling was mainly for convenience and not a necessary part of the method. Hence, the resulting governing partial differential equations for the function $f(\xi,\eta)$ and the vorticity ω had to be solved subject to both these quantities being (i) zero on $\xi = 0$, (ii) taking the same values on $\eta = 0$ and $\eta = 4$ in order to produce single value expressions, and (iii) on $\xi = 1$ that in the original coordinates and variables corresponded to the no slip and zero normal velocity conditions on the surface of the circular cylinder.

In applying this technique to the problem of uniform flow past a circular cylinder in the presence of a rotlet the only modification required is the removal of the singularity due to the rotlet, as well as the uniform stream, from the expression for the stream function expression. Hence, in this situation the perturbation solution was again solely due to a circular cylinder, with the basic flow being that of a uniform stream containing a rotlet. However, the difficulty experienced was having placed a rotlet at the non-dimensional position $(c,0)$, then in which direction should the uniform stream flow and what should be its magnitude? Initially it was assumed that the non-dimensional stream function for the uniform stream should have the form

$$\psi = \lambda_1 r cos\vartheta, \tag{4.1.1}$$

that is it flows along the y-axis rather than along a general direction which would have been indicated by choosing

$$\psi = \lambda_1 r cos\vartheta + \lambda_2 r sin\vartheta. \tag{4.1.2}$$

However, although expression (4.1.1) has, to a certain extent, introduced information from the asymptotic solution by the knowledge of the direction of the stream, it does no more than that since the magnitude of the stream required to produce a well posed problem is still unknown. This conveyance of information

can be readily seen if one compares expression (3.5.8) with expression (4.1.1). Obviously this unknown value of λ_1 prevents any direct solution.

An alternative approach to determining the direction of the stream could have been the physical argument. This implies that the velocity at (r, ϑ), given by $(v_r, v_\vartheta) = (a, b)$, is related to that at $(r, -\vartheta)$, where $(v_r, v_\vartheta) = (-a, b)$. Hence, the velocity components in terms of the stream function, as shown in expression (3.1.16), requires that the stream function is even in ϑ. This in turn requires that the stream function is devoid of terms containing $\sin(n\vartheta)$.

The actual approach followed to overcome the unknown magnitude of the stream was the realization that having expressed the form of the solution at large values of r as

$$\psi \approx \lambda_1 r cos\vartheta + \ln(R_1), \tag{4.1.3}$$

where the coefficient of $\ln(R_1)$ was identical to the non-dimensional strength of the rotlet at $(c, 0)$, then the force and moment on the circular cylinder would be zero. However, only when λ_1 is a particular value, in this case c^{-1}, will the problem be well posed and produce these values for the force and moment. For all other values of λ_1 one will have F_x, F_y and M dependent on this parameter. This means one can think of these three quantities as functions of λ_1, and only when λ_1 possesses the correct value will all these quantities acquire their necessary values. Hence, the technique adopted was that of a Newton Raphson iteration on $F_x(\lambda_1)$. Prior to this the governing partial differential equations were expressed in finite difference form and then solved for two values of λ_1, say $\lambda_1 = \alpha$ and $\lambda_1 = \beta$. The resulting two non zero values of $F_x(\lambda_1 = \alpha)$ and $F_x(\lambda_1 = \beta)$ being the values used in the Newton Raphson method in order to establish a new value of λ_1, say $\lambda_1 = \gamma$, at which $F_x(\lambda_1)$ is zero. The finite difference equations are resolved for this new value of λ_1, and the resulting value of $F_x(\lambda_1 = \gamma)$ used together with either $F_x(\lambda_1 = \alpha)$, or $F_x(\lambda_1 = \beta)$, whichever is closest to zero, to produce from the Newton Raphson solution a new value of λ_1. The process is continued until the value of $F_x(\lambda_1)$ reaches zero to within the required tolerance. The value of λ_1 obtained automatically resulted in the correct values for F_y and M. This procedure could equally well have been applied to setting either the value of $F_y(\lambda_1)$ or $M(\lambda_1)$ to zero.

However, what would have happened had one allowed the form of the stream

function at large values of r due to the uniform stream to be more general, namely that given by expression (4.1.3), so that neither the magnitude nor the direction of the stream is known?. Hence, the problem is only well posed for the special case of $\lambda_1 = c^{-1}$ and $\lambda_2 = 0$. This in turn means that F_x, F_y and M are functions of the parameters λ_1 and λ_2 and it is necessary to apply Newton Raphson iteration on both these quantities for the two independent parameters in order to produce $F_x(\lambda_1, \lambda_2) = F_y(\lambda_1, \lambda_2) = 0$. Again the value of M acquires its required value. It should be emphasized that the $\ln(R_1)$ term, with coefficient unity, in the stream function at large values of r also conveys a certain knowledge from the analytical solution into the numerical approach. Since this term behaves like $\ln(r)$ at large values of r, so that its coefficient is identical to the non-dimensional strength of the rotlet at $(c, 0)$, it is implied from the analytical solution that there is no moment on the cylinder.

It is possible to generalize the form of the solution at large values of r to

$$\psi \approx \lambda_1 r cos\vartheta + \lambda_2 r sin\vartheta + \lambda_3 \ln(r) + \ln(R_1), \tag{4.1.4}$$

in which case it is possible to iterate on the three expressions for F_x, F_y and M, which are now functions of the three parameters λ_1, λ_2 and λ_3, until the zero values for F_x, F_y and M are reached. In this situation the three parameters acquire the values

$$\lambda_1 = c^{-1}, \lambda_2 = 0, \lambda_3 = 0. \tag{4.1.5}$$

If, however, one wishes to introduce a non zero force on the cylinder, say $F = F_x^*$, then it is necessary to amend the expression for the stream function at large values of r to the form

$$\psi \approx \lambda_1 r cos\vartheta + \lambda_2 r sin\vartheta + \lambda_4 rlr(r) \sin\vartheta + \ln(R_1). \tag{4.1.6}$$

Similarly, for $F_y = F_y^*$, then

$$\psi \approx \lambda_1 r cos\vartheta + \lambda_2 r sin\vartheta + \lambda_5 rlr(r) \cos\vartheta + \ln(R_1). \tag{4.1.7}$$

In both these instances the $\ln(R_1)$ has continued to introduce some of the information derived from the asymptotic solution by way of the fact that its

coefficient remains unity. Since the $\ln(R_1)$ term at large values of r is identical to the $\ln(r)$ in expression (3.5.8) which implies such a choice has introduced a constraint that there is no moment on the cylinder. Again the Newton Raphson iteration procedure was applied, but this time the quantities being iterated on were $(F_x - F_x^*), F_y$ and M, or $F_x, (F_y - F_y^*)$ and M.

However, once one moves to the situation when the moment is a non zero quantity, regardless of whether the force remains so or not, then it is necessary to have an expression for the stream function of the form

$$\psi \approx \lambda_1 r cos\vartheta + \lambda_2 r sin\vartheta + \lambda_3 \ln(r) + \lambda_6 r^2 + \ln(R_1). \tag{4.1.8}$$

If in addition the components of force are also non zero, then one needs an expression

$$\psi \approx \lambda_1 r cos\vartheta + \lambda_2 r sin\vartheta + \lambda_3 \ln(r) + \lambda_4 rlr(r)\cos\vartheta + \lambda_5 rlr(r)\sin\vartheta + \lambda_6 r^2 + \ln(R_1). \tag{4.1.9}$$

For the situation given by expression (4.1.8) and by expression (4.1.9) the number of unknown parameters exceeds the three dependent variables that are to be prescribed, namely the two force components and the moment. Hence, the previous approach fails since there is no longer any obvious extra quantities, such as the value of the force and moment, that can be introduced.

The above approach has utilized the values of the force and moment, and as these are quantities that naturally arise from the values of ψ and ω, and their higher derivatives, around the circular cylinder it seems appropriate to switch to an approach where such boundary quantities play the major role in the solution. Hence, the numerical approach to be adopted in solving the general problem, as well as the more restricted situations, is that of the Boundary Element Method.

Before discussing the Boundary Element Method in detail it should be stressed that the method requires that the stream function and the vorticity be expressed as a combination of two parts, where one part contains the terms that tend to zero as $r \to \infty$. Hence, the stream function is expressed as

$$\begin{aligned}\psi = {} & \lambda_1 r cos\vartheta + \lambda_2 r sin\vartheta + \lambda_3 \ln(r) + \lambda_4 rlr(r)\cos\vartheta + \lambda_5 rlr(r)\sin\vartheta \\ & + \lambda_6 r^2 + \lambda_7 + \lambda_8 \sin(2\vartheta) + \lambda_9 \cos(2\vartheta) + \ln(R_1) + \psi^*,\end{aligned} \tag{4.1.10}$$

where $\psi^* \to 0$ as $r \to \infty$. The additional terms of $O(1)$, namely

$$\lambda_7 + \lambda_8 \sin(2\vartheta) + \lambda_9 \cos(2\vartheta), \tag{4.1.11}$$

arise from the expressions (3.3.2), (3.3.5) and (3.3.6). Hence,

$$\lambda_7 = D_0,\ \lambda_8 = FC_2 \ and\ \lambda_9 = GC_2. \tag{4.1.12}$$

It is possible to include the additional term $\lambda_8(r^2 \ln(r) - r^2)$ in expression (4.1.10) but if this is the case then the condition on the single valuedness of the pressure must be included in the numerical procedure in order to ensure that λ_8 becomes zero. This was discussed in detail in the earlier section on the analytical solution.

In the case when there is neither a force nor a moment acting upon the cylinder then it is possible from a physical argument to set

$$\lambda_2 = \lambda_5 = \lambda_8 = 0. \tag{4.1.13}$$

However, this restriction will not be imposed as the method is required to accommodate (i) non zero force and moment and in the future (ii) flows involving multi-bodies for which a physical argument will no longer be possible.

4.2 The Boundary Element Method (BEM)

The BEM has become an accepted and powerful method for the numerical solution of a range of problems such as the diffusion of heat, some types of the fluid flow motion, flows in porous media, viscous flow with the Reynolds number assumed to be zero, electrostatics and many others in which the governing equations are the classical Laplace or biharmonic equation. The BEM consists of the transformation of the partial differential equations into integral equations relating only boundary values followed by the determination of the solution of these integral equations. If the values at interior points are required, then they may be calculated from the boundary data. Since all the numerical approximations occur on the boundaries, the dimensionality of the problem is reduced by one and a smaller system of equations is obtained compared with those achieved by differential methods.

Over the past decades, numerous books and papers addressing the applications of the BEM to various problems, see for example Jaswon and Symm (1976), Banerjee and Butterfield (1981), Brebbia *et al* (1984), Manzoor (1984) and Kelmanson (1984), Brebbia and Gipson (1991), etc have been published. As such it is now unnecessary to discuss fully the basic theory of the BEM. The present section is concerned with the application of the BEM for the numerical solution of a viscous steady flow problem at zero Reynolds number (the biharmonic equation).

The crucial step in the application of the BEM is the transformation from the differential equations to the integral equations. This is achieved by using the divergence theorem

$$\int_{\partial\Omega} \underline{A} \cdot \underline{n} ds = \int_{\Omega} div \underline{A} ds, \tag{4.2.1}$$

where $\underline{A}$ is a smooth vector function, which is second-order continuously differentiable, defined within a domain Ω which is bounded by the closed contour $\partial\Omega, n$ is the outward normal to the domain, ds denotes the length element on $\partial\Omega$ and dS denote the surface element in Ω. The sense of the integration around $\partial\Omega$ is such that the domain is on the left as $\partial\Omega$ is traversed in the positive sense.

In order to be able to show how the integral identity (4.2.1) can be used to transform differential equations into integral equations consider the Laplace equation within a region Ω,

$$\nabla^2 \omega(x, y) = 0, \qquad (x, y) \in \Omega. \tag{4.2.2}$$

Applying the divergence theorem to the vector function $\underline{A} = \omega \ \mathrm{grad}\tau$, where τ is any smooth function defined within Ω, one obtains

$$\int_{\partial\Omega} (\omega grad\tau) \cdot \underline{n} ds = \int_{\Omega} div(\omega grad\tau) dS, \tag{4.2.3}$$

but $\mathrm{grad}\tau \cdot \underline{n} = \partial\tau/\partial n$, therefore

$$\int_{\partial\Omega} \omega \frac{\partial \tau}{\partial n} ds = \int_{\Omega} (grad\omega \cdot grad\tau + \omega \nabla^2 \tau) dS, \tag{4.2.4}$$

Similarly, applying the divergence theorem to the vector function τ gradω gives

$$\int_{\partial\Omega} \tau \frac{\partial \omega}{\partial n} ds = \int_{\Omega} (grad\tau \cdot grad\omega + \tau \nabla^2 \omega) dS, \tag{4.2.5}$$

Subtracting equation (4.2.5) from equation (4.2.4) one obtains

$$\int_{\partial\Omega} (\omega \frac{\partial \tau}{\partial n} - \tau \frac{\partial \omega}{\partial n}) ds = \int_{\Omega} (\omega \nabla^2 \tau - \tau \nabla^2 \omega) dS. \tag{4.2.6}$$

This identity is known as Green's Theorem and it holds for any smooth functions ω and τ defined within a plane domain Ω which is bounded by a closed contour $\partial\Omega$.

Using the fact that $\nabla^2 \omega = 0$ in Ω, equation (4.2.6) becomes

$$\int_{\partial\Omega} (\omega \frac{\partial \tau}{\partial n} - \tau \frac{\partial \omega}{\partial n}) ds = \int_{\Omega} \omega \nabla^2 \tau dS. \tag{4.2.7}$$

Furthermore, taking τ to be a particular solution of the Poisson equation

$$\nabla^2 \tau(p, q) = \delta(p - p_0), \tag{4.2.8}$$

where $p = (x, y)$ and $p_0 = (x_0, y_0)$ are in Ω and δ is the Dirac delta function. Then equation (4.2.7) becomes

$$\eta(\underline{p})\omega(\underline{p}) = \int_{\partial\Omega} \omega(\underline{q}) \frac{\partial \tau(\underline{p}, \underline{q})}{\partial n} ds - \int_{\partial\Omega} \frac{\partial \omega(\underline{q})}{\partial n} \tau(\underline{p}, \underline{q}) dS, \tag{4.2.9}$$

where $p \in \Omega \cup \partial\Omega, q \in \partial\Omega$ and $\eta(p)$ is a constant dependent upon the location of the point p and is given by

$$\eta(p) = \eta(\underline{p}) = \begin{cases} 2\pi \ \text{ when } \underline{p} \in \Omega \\ \theta \quad \text{when } \underline{p} \in \partial\Omega, \ \theta \ \text{ is the angle between} \\ \quad \text{the tangents to } \partial\Omega \text{ on either side of } \underline{p} \\ 0 \quad \text{when } \underline{p} \notin \Omega \cup \partial\Omega. \end{cases} \tag{4.2.10}$$

This boundary integral equation is usually refer

$$| \, p - p_0 \, | = \{(x - x_0)^2 + (y - y_0)^2\}^{1/2}. \tag{4.2.11}$$

Taking the prime ($'$) to denote the derivative in the direction of the outward normal to $\partial\Omega$, and the boundary value of $\omega(p)$ as $\phi(p)$, then the integral equation (4.2.9) becomes

$$\int_{\partial\Omega} \phi(\underline{q}) \ln' \mid \underline{p} - \underline{q} \mid d\underline{q} - \int_{\partial\Omega} \phi'(\underline{q}) \ln \mid \underline{p} - \underline{q} \mid d\underline{q} = \eta(\underline{p})\omega(\underline{p}). \tag{4.2.12}$$

Using the equation (4.2.12), the ω can be determined at any point $\Omega \cup \partial\Omega$ provided ϕ and $\partial\phi/\partial n$ are known at all points on the boundary $\partial\Omega$. Unfortunately, in most of the physical problems ϕ and $\partial\phi/\partial n$ are not simultaneously prescribed at all such points. However, it is still possible to apply Green's Integral Formula. In equation (4.2.12) taking $p, q \in \partial\Omega$ one has

$$\int_{\partial\Omega} \phi(\underline{q}) \ln' \mid \underline{p} - \underline{q} \mid d\underline{q} - \int_{\partial\Omega} \phi'(\underline{q}) \ln \mid \underline{p} - \underline{q} \mid d\underline{q} = \eta(\underline{p})\phi(\underline{p}). \tag{4.2.13}$$

If one knows either $\phi(p)$ or $\phi'(p)$ on $\partial\Omega$ one can obtain the other function by using equation (4.2.13). Then substitution of both these values into equation (4.2.12) gives the solution of the Laplace equation in Ω.

In practice analytical solutions of the integral equations (4.2.12) and (4.2.13) are usually impossible and thus some form of numerical approximation is necessary. This is achieved by first subdividing the boundary $\partial\Omega$ into N segments $\partial\Omega_j, j = 1, 2, \ldots,$N. On each segment ϕ and ϕ' are approximated by constants ϕ_j, and ϕ'_j , where ϕ_j and ϕ'_j take the values of ϕ and ϕ' at the midpoint of the segment $\partial\Omega_j$, respectively. Then the integral formula (4.2.12) and (4.2.13) become

$$\sum_{j=1}^{N} \phi_j \int_{\partial\Omega_j} \ln' \mid \underline{p} - \underline{q} \mid d\underline{q} - \sum_{j=1}^{N} \phi'_j \int_{\partial\Omega_j} \ln \mid \underline{p} - \underline{q} \mid d\underline{q} = \eta(\underline{p})\omega(\underline{p}), \tag{4.2.14}$$

$$\sum_{j=1}^{N} \phi_j \int_{\partial\Omega_j} \ln' \mid \underline{p}_i - \underline{q} \mid d\underline{q} - \eta_i\phi_i - \sum_{j=1}^{N} \phi'_j \int_{\partial\Omega_j} \ln \mid \underline{p}_i - \underline{q} \mid d\underline{q} = 0, \tag{4.2.15}$$

$i = 1, 2, \ldots N.$

where p_i is the midpoint of the segment $\partial\Omega_i$ and $\eta_i = \eta(\underline{p}_i)$.

Using the expression (4.2.15) one obtains

$$\sum_{j=1}^{N} \phi_j \left(\int_{\partial\Omega_j} \ln' \mid \underline{p}_i - \underline{q} \mid d\underline{q} - \eta_i \delta_{ij} \right) - \sum_{j=1}^{N} \phi'_j \int_{\partial\Omega_j} \ln \mid \underline{p}_i - \underline{q} \mid d\underline{q} = 0, \tag{4.2.16}$$

$i = 1, 2, \ldots N.$

If one writes

$$G_{ij} = \int_{\partial\Omega_j} \ln \mid \underline{p}_i - \underline{q} \mid d\underline{q}, \tag{4.2.17}$$

and

$$E_{ij} = \int_{\partial\Omega_j} \ln' \mid \underline{p}_i - \underline{q} \mid d\underline{q} - \eta(\underline{p}_i)\delta_{ij}, \tag{4.2.18}$$

where δ_{ij} is Kronecker's delta function. Then the equation (4.2.16) may be written as follow

$$\sum_{j=1}^{N} E_{ij}\phi_j - \sum_{j=1}^{N} G_{ij}\phi'_j = 0. \qquad i = 1, 2, \ldots, N. \tag{4.2.19}$$

A more accurate approximation of the solution of the Laplace equation using the BEM can be obtained by using a linear function to approximate ϕ and ϕ' on each boundary segment. In this case one lets

$$\phi_j = (1 - \xi)\phi(\underline{q}_{j-1}) + \xi\phi(\underline{q}_j), \tag{4.2.20}$$

$$\phi'_j = (1 - \xi)\phi'(\underline{q}_{j-1}) + \xi\phi'(\underline{q}_j), \tag{4.2.21}$$

where q_{j-1} and q_j are the end points of $\partial\Omega_j, \xi$ is a linear function which increases from zero at $\underline{q}_{j-1}$ to unity at $\underline{q}_j$. Inserting these functions ϕ_j and ϕ'_j into equations (4.2.12) and (4.2.13) one obtains

$$\begin{aligned} &\sum_{j=1}^{N} \{\phi_{j-1} \int_{\partial\Omega_j} (1 - \xi) \ln' \mid \underline{p} - \underline{q} \mid d\underline{q} + \phi_j \int_{\partial\Omega_j} \xi \ln' \mid \underline{p} - \underline{q} \mid d\underline{q}\} \\ &- \sum_{j=1}^{N} \{\phi'_{j-1} \int_{\partial\Omega_j} (1 - \xi) \ln \mid \underline{p} - \underline{q} \mid d\underline{q} + \phi'_j \int_{\partial\Omega_j} \xi \ln \mid \underline{p} - \underline{q} \mid d\underline{q}\} \\ &= \eta(\underline{p})\omega(\underline{p}) \qquad \underline{p} \in \bar{\Omega} \qquad \underline{q} \in \partial\Omega \end{aligned} \tag{4.2.22}$$

$$\begin{aligned}
&\sum_{j=1}^{N}\{\phi_{j-1}\int_{\partial\Omega_j}(1-\xi)\ln'\mid \underline{p}_i-\underline{q}\mid d\underline{q}+\phi_j\int_{\partial\Omega_j}\xi\ln'\mid \underline{p}_i-\underline{q}\mid d\underline{q}\}\\
&-\sum_{j=1}^{N}\{\phi'_{j-1}\int_{\partial\Omega_j}(1-\xi)\ln\mid \underline{p}_i-\underline{q}\mid d\underline{q}+\phi'_j\int_{\partial\Omega_j}\xi\ln\mid \underline{p}_i-\underline{q}\mid d\underline{q}\}\\
&=\eta(\underline{p}_i)\phi_i, \qquad i=1,2,\ldots,N \qquad \underline{p}_i,\underline{q}\in\partial\Omega
\end{aligned} \tag{4.2.23}$$

where ϕ_j and ϕ'_j denote $\phi(\underline{p}_j)$ and $\phi'(\underline{p}_j)$, and $\phi_0=\phi_N$ and $\phi'_0=\phi'_N$ respectively. As with the classical BEM (4.2.19), the expression (4.2.23) reduces to a linear system of algebraic equations of the form

$$\sum_{j=1}^{N}E^*_{ij}\phi_j-\sum_{j=1}^{N}G^*_{ij}\phi'_j=0, i=1,2,\ldots,N \tag{4.2.24}$$

where

$$E^*_{ij}=\int_{\partial\Omega_{j+1}}(1-\xi)\ln'\mid \underline{p}_i-\underline{q}\mid d\underline{q}+\int_{\partial\Omega_j}\xi\ln'\mid \underline{p}_i-\underline{q}\mid d\underline{q}-\eta_i\delta_{ij}, \tag{4.2.25}$$

$$G^*_{ij}=\int_{\partial\Omega_{j+1}}(1-\xi)\ln\mid \underline{p}_i-\underline{q}\mid d\underline{q}+\int_{\partial\Omega_j}\xi\ln\mid \underline{p}_i-\underline{q}\mid d\underline{q}, \tag{4.2.26}$$

$\partial\Omega_{N+1}=\partial\Omega_1$ and p_i is the common point of the segments $\partial\Omega_i$ and $\partial\Omega_{i+1}$.

If the segment $\partial\Omega_j$ is a straight line, then the integrals occurring in the equations (4.2.12), (4.2.13), (4.2.22) and (4.2.23) may be evaluated exactly to obtain

$$\int_{\partial\Omega_j}\ln'\mid \underline{p}-\underline{q}\mid d\underline{q}=I_1, \tag{4.2.27}$$

$$\int_{\partial\Omega_j}\ln\mid \underline{p}-\underline{q}\mid d\underline{q}=J_1, \tag{4.2.28}$$

$$\int_{\partial\Omega_j}\xi\ln'\mid \underline{p}-\underline{q}\mid d\underline{q}=\frac{1}{h}(a\cos\beta I_1+I_2), \tag{4.2.29}$$

$$\int_{\partial\Omega_j}\xi\ln\mid \underline{p}-\underline{q}\mid d\underline{q}=\frac{1}{h}(a\cos\beta J_1+J_2), \tag{4.2.30}$$

with, see Manzoor (1984),

$$I_1 = \gamma, \tag{4.2.31}$$

$$I_2 = asin\beta(lnb - lna), \tag{4.2.32}$$

$$J_1 = acos\beta(lna - lnb) + h(lnb - 1) + a\gamma \sin\beta, \tag{4.2.33}$$

$$J_2 = \frac{1}{2}(b^2 lnb - a^2 lna) - \frac{1}{4}(b^2 - a^2), \tag{4.2.34}$$

where q_{j-1} and q_j are the endpoints of $\partial\Omega_j$, see figure 4.2.1, and a, b and h are the lengths of the lines joining p to q_{j-1}, p to q_j and q_{j-1} to q_j, respectively, and β and γ are the angles $q_j q_{j-1} p$ and $q_{j-1} p q_j$, respectively.

For steady two-dimensional flow of an incompressible Newtonian fluid the Navier-Stokes and continuity equations reduce to

$$\nabla p = \nabla^2 u, \tag{4.2.35}$$

$$\nabla \cdot u = 0, \tag{4.2.36}$$

when the Reynolds number is assumed to be very small. On introducing the stream function, ψ say, such that $\partial\psi/\partial x = -v_y$ and $\partial\psi/\partial y = v_x$, then ψ satisfies the biharmonic equation, see Batchelor (1967),

$$\nabla^4 \psi = 0. \tag{4.2.37}$$

On introducing the vorticity, ω, equation (4.2.37) may be written in the form

$$\nabla^2 \psi = \omega, \tag{4.2.38}$$

$$\nabla^2 \omega = 0. \tag{4.2.39}$$

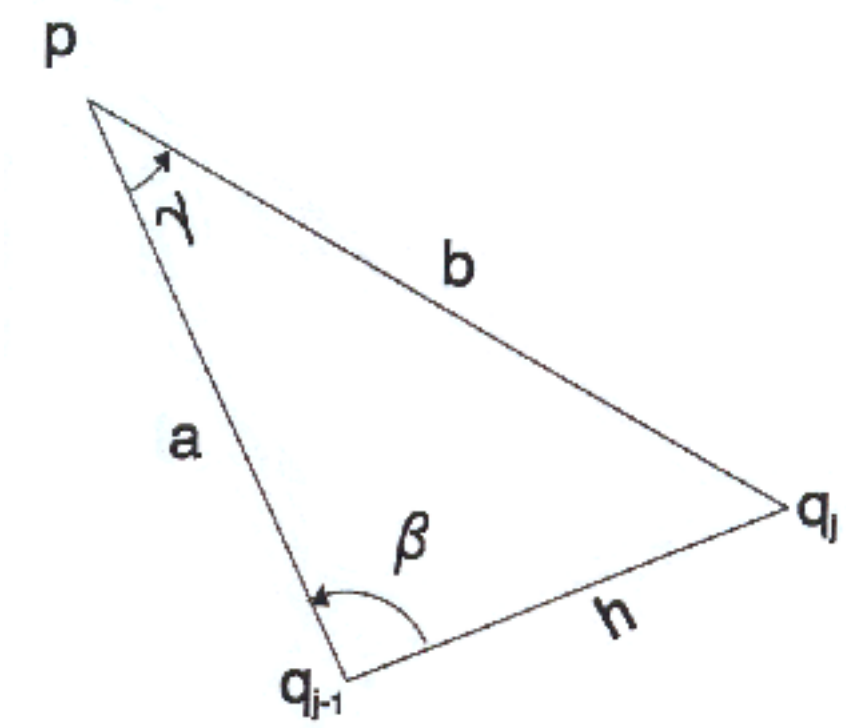

Figure 4.2.1: The notation for the analytic evaluation of integrals on straight line segment geometry.

In order to solve the equations (4.2.38) and (4.2.39) in the domain Ω one uses the BEM. For any $\underline{p} = (x, y) \in \Omega \cup \partial\Omega$ and $\underline{q} = (x_0, y_0) \in \partial\Omega$, let

$$F_1(\underline{p}, \underline{q}) = \ln \mid \underline{p} - \underline{q} \mid, \tag{4.2.40}$$

$$F_2(\underline{p}, \underline{q}) = \mid \underline{p} - \underline{q} \mid^2 (\ln \mid \underline{p} - \underline{q} \mid -1), \tag{4.2.41}$$

where $\mid \underline{p} - \underline{q} \mid = \{(x - x_0)^2 + (y - y_0)^2\}^{1/2}$. Applying Green's second identity one has

$$\begin{aligned}\eta(\underline{p})\psi(\underline{p}) = &\int_{\partial\Omega} \psi(\underline{q})F_1'(\underline{p},\underline{q})d\underline{q} - \int_{\partial\Omega} \psi'(\underline{q})F_1(\underline{p},\underline{q})d\underline{q} \\ &\frac{1}{4}\int_{\partial\Omega} \omega(\underline{q})F_2'(\underline{p},\underline{q})d\underline{q} - \frac{1}{4}\int_{\partial\Omega} \omega'(\underline{q})F_2(\underline{p},\underline{q})d\underline{q},\end{aligned} \tag{4.2.42}$$

$$\eta(\underline{p})\omega(\underline{p}) = \int_{\partial\Omega} \omega(\underline{q})F_1'(\underline{p},\underline{q})d\underline{q} - \int_{\partial\Omega} \omega'(\underline{q})F_1(\underline{p},\underline{q})d\underline{q}. \tag{4.2.43}$$

A similar strategy is now followed to that employed above when solving the Laplace equation in order to produce a solution from the integral equations (4.2.42) and (4.2.43). That is, the boundary is first subdivided into N segments, $\partial\Omega_j$, and the stream function, ψ, its derivative, ψ', the vorticity, ω, and its derivative, ω', are approximated by piecewise constant functions. This results in equation (4.2.42) producing the system of algebraic equations

$$\sum_{j=1}^{N}\{E_{ij}\psi_j - G_{ij}\psi_j' + L_{ij}\omega_j - M_{ij}\omega_j'\} = 0, i = 1, \ldots, N \tag{4.2.44}$$

where G_{ij} and E_{ij} are as given in equations (4.2.17) and (4.2.18) respectively, and L_{ij} and M_{ij} are given by

$$L_{ij} = \frac{1}{4}\int_{\partial\Omega} \omega(\underline{q})F_2'(\underline{p},\underline{q})d\underline{q}, \tag{4.2.45}$$

$$M_{ij} = \frac{1}{4}\int_{\partial\Omega} \omega(\underline{q})F_2(\underline{p},\underline{q})d\underline{q}, \tag{4.2.46}$$

Equation (4.2.44) represents N equations in $4N$ unknowns and a further N equations are derived from equation (4.2.19). This produces the system of algebraic equations

$$\left.\begin{aligned}\textstyle\sum_{j=1}^{N} E_{ij}\psi_j - G_{ij}\psi_j' + L_{ij}\omega_j - M_{ij}\omega_j' &= 0 \\ \textstyle\sum_{j=1}^{N} E_{ij}\omega_j - G_{ij}\omega_j' &= 0\end{aligned}\right\} i = 1, \ldots, N \tag{4.2.47}$$

With the application of the appropriate boundary conditions the system of equations (4.2.47) can be solved and equations (4.2.42) and (4.2.43) used to find the value of the stream function, ψ, and the vorticity, ω, at any point within the solution domain, Ω.

In order to obtain a more accurate numerical solution linear elements may be used. In this case the unknown functions ψ, ψ', ω and ω' are approximated by linear functions on each boundary segment such that

$$\psi_j = (1-\xi)\psi(\underline{q}_{j-1}) + \xi\psi(\underline{q}_j), \tag{4.2.48}$$

$$\psi'_j = (1-\xi)\psi'(\underline{q}_{j-1}) + \xi\psi'(\underline{q}_j), \tag{4.2.49}$$

$$\omega_j = (1-\xi)\omega(\underline{q}_{j-1}) + \xi\omega(\underline{q}_j), \tag{4.2.50}$$

$$\omega'_j = (1-\xi)\omega'(\underline{q}_{j-1}) + \xi\omega'(\underline{q}_j), \tag{4.2.51}$$

where ξ is as defined in equations (4.2.19) and (4.2.20). Inserting these approximations into the integral equations (4.2.42) and (4.2.43) and rearranging the resulting equations produces the following system of algebraic equations

$$\left.\begin{array}{rl} \sum_{j=1}^{N} E^*_{ij}\psi_j - G^*_{ij}\psi'_j + L^*_{ij}\omega_j - M^*_{ij}\omega'_j & = 0 \\ \sum_{j=1}^{N} E^*_{ij}\omega_j - G^*_{ij}\omega'_j & = 0 \end{array}\right\} i = 1, \ldots, N \tag{4.2.52}$$

where E^*_{ij} and G^*_{ij} are given in equations (4.2.25) and (4.2.26) respectively and L^*_{ij} and M^*_{ij} are given by

$$L^*_{ij} = \frac{1}{4}\sum_{j=1}^{N}\{\int_{\partial\Omega_{j+1}} (1-\xi)F'_2(\underline{p},\underline{q})d\underline{q} + \int_{\partial\Omega_j} \xi F'_2(\underline{p},\underline{q})d\underline{q}\}, \tag{4.2.53}$$

$$M^*_{ij} = \frac{1}{4}\sum_{j=1}^{N}\{\int_{\partial\Omega_{j+1}} (1-\xi)F_2(\underline{p},\underline{q})d\underline{q} + \int_{\partial\Omega_j} \xi F_2(\underline{p},\underline{q})d\underline{q}\}. \tag{4.2.54}$$

Similarly, if the segment $\partial\Omega_j$ is a straight line, then the integrals occurring in the equations (4.2.45), (4.2.46), (4.2.53) and (4.2.54) may be evaluated exactly using the notation shown in figure 4.2.1, namely

$$\int_{\partial\Omega_j} F'_2(\underline{p},\underline{q})d\underline{q} = a(2J_1 - h)\sin\beta, \tag{4.2.55}$$

$$\int_{\partial\Omega_j} F_2(\underline{p},\underline{q})d\underline{q} = \frac{1}{3}(h-a\cos\beta)^3(lnb-\frac{4}{3}) + \frac{1}{3}(a\cos\beta)^3(lna-\frac{4}{3}) + (a\sin\beta)^2(J_1-\frac{2}{3}h-\frac{1}{3}a\gamma\sin\beta), \tag{4.2.56}$$

$$\int_{\partial\Omega_j} \xi F_2'(\underline{p},\underline{q})d\underline{q} = \frac{2}{h}a\sin\beta(a\cos\beta J_1+J_2) - \frac{1}{2}ah\sin\beta, \tag{4.2.57}$$

$$\int_{\partial\Omega_j} \xi F_2(\underline{p},\underline{q})d\underline{q} = \frac{1}{h}a\cos\beta\int_{\partial\Omega_j} F_2(\underline{p},\underline{q})d\underline{q} + \frac{1}{4h}(b^4lnb-a^4lna) - \frac{5}{16h}(b^4-a^4) \tag{4.2.58}$$

It should be stressed that throughout the present work the emphasis when applying the Boundary Element Method has been on constant elements rather linear elements.

4.3 The Numerical Solution

In applying the above method to the flow past a circular cylinder in the presence of a rotlet the fluid domain Ω is the area outside the cylinder and the $\partial\Omega$ is the contour of the cylinder. However, prior to using the method it is necessary to accommodate the infinity boundary conditions. Since the BEM requires that the non-dimensional stream function and vorticity used in equations (4.2.47) are both $O(r^{-1})$ at large values of r, it is necessary that these quantities are expressed as perturbation values about their asymptotic expansions at large values of r and the perturbation parts used in these equations. The number of terms in the expansions being sufficient to ensure that both perturbation quantities decay to zero to satisfy the above infinity conditions. Hence,

$$\psi = \psi_A + \psi^*, \ and\ \omega = \omega_A + \omega^*, \tag{4.3.1}$$

where ψ_A and ω_A are the asymptotic expansions of ψ and ω as $r\to\infty$, and ψ^* and ω^* are the perturbations values about these expansions that tend to zero as $r\to\infty$, where

$$\nabla^2\psi_A = \omega_A \; and \; \nabla^2\omega_A = 0. \tag{4.3.2}$$

So the biharmonic equation for the stream function can be written as

$$\nabla^2\psi^* = (\omega_A - \nabla^2\psi_A) + \omega^*, \tag{4.3.3}$$

$$\nabla^2\omega^* = -\nabla^2\omega_A. \tag{4.3.4}$$

Using the equations in (4.3.2) reduces equations (4.3.3) and (4.3.4) to

$$\nabla^2\psi^* = \omega^*, \tag{4.3.5}$$

$$\nabla^2\omega^* = 0. \tag{4.3.6}$$

This results in the stream function and vorticity expressions in the above Boundary Element Method being replaced by ψ^* and ω^*. The original boundary conditions on the cylinder, provided the cylinder is not rotating, are as given in expression (3.1.3). However, the boundary conditions on ψ^* and ω^* will be as follows,

$$\psi^* = -\psi_A \; and \; \frac{\partial\psi^*}{\partial r} = -\frac{\partial\psi_A}{\partial r}, \ldots \; on \; r = 1. \tag{4.3.7}$$

Hence, in equations (4.2.47)ψ_j^* and ${\psi'_j}^*$, which have been replaced ψ_j and ψ'_j, will now take the values $-\psi_{Aj}$ and $-\psi'_{Aj}$.

In expression (4.2.47) there are $2n$ equations in $4n$ unknowns. However, if the values of ψ_j^* and ${\psi'_j}^*$ are free of any unknowns then these will provide another $2n$ conditions, so after their substitution one has a closed system of $2n$ equations in $2n$ unknowns. Unfortunately, the expressions for ψ_j^* and ${\psi'_j}^*$ will, from expression (4.1.10), be given by

$$\psi_j^* = -\lambda_1\cos(\theta_j) - \lambda_2\sin(\theta_j) - \lambda_6 - \lambda_7 - \lambda_8\sin(2\theta_j) - \lambda_9\cos(2\theta_j) - ln(R_1(1)), \tag{4.3.8}$$

$$\begin{aligned}\psi_j'^{*} = &-\lambda_1\cos(\theta_j) - \lambda_2\sin(\theta_j) - \lambda_3 - \lambda_4\cos(\theta_j)\\ &-\lambda_5\sin(\theta_j) - 2\lambda_6 - \frac{(1-c\cos(\theta_j))}{R_1^2(1)},\ j=1,\ldots,N,\end{aligned} \tag{4.3.9}$$

where $R_1^2(1) = (1 + c^2 - 2c\cos(\vartheta_j))$.

Case (a) uniform stream at infinity, so general situation has $\lambda_3 = \lambda_4 = \lambda_5 = \lambda_6 = 0$.

Obviously the extra unknowns λ_j, where $j = 1, \ldots, 9$, in the most general situation of non-zero force and moment on the cylinder, will require extra conditions. For the present the unknowns related to the non zero force and moment on the cylinder, namely $\lambda_3, \lambda_4, \lambda_5$ and λ_6, will be set to zero. In addition, if the direction of the stream is introduced by way of prescribing λ_2 also to be zero, then this results in there being an extra 4 unknowns, which require an extra 4 conditions. However, this extra restriction will not be imposed. It is proposed to introduce the conditions that there should be no force or moment on the cylinder, so expressions (3.2.13), (3.2.14) and (3.2.15) have ψ and ω replaced by $\psi^* + \psi_A$ and $\omega^* + \omega_A$, respectively. The parts of the integrals involving ψ_A and ω_A are evaluated analytically, producing linear expressions in the unknowns λ_j.The other parts involving ψ^* and ω^* are expressed after numerical integration by Simpson's method as linear expressions of $\psi_j, \psi_j'^{*}$, ω_j^* and $\omega_j'^{*}$. Hence, the resulting expressions for the force and moment on the cylinder may be written as

$$\left.\begin{aligned}F_x = 0 \quad &= +\textstyle\sum_{j=1}^{(N-1)/2}[(\omega_{2j-1}'^{*} + 4\omega_{2j}'^{*} + \omega_{2j+1}'^{*})\\ &-(\omega_{2j-1}^{*} + 4\omega_{2j}^{*} + \omega_{2j+1}^{*})](\sin(\theta_j)(2\pi/(3N)),\end{aligned}\right\} \tag{4.3.10}$$

$$\left.\begin{aligned}F_y = 0 \quad &= -\textstyle\sum_{j=1}^{(N-1)/2}[(\omega_{2j-1}'^{*} + 4\omega_{2j}'^{*} + \omega_{2j+1}'^{*})\\ &-(\omega_{2j-1}^{*} + 4\omega_{2j}^{*} + \omega_{2j+1}^{*})](\cos(\theta_j)(2\pi/(3N)),\end{aligned}\right\} \tag{4.3.11}$$

$$M = 0 = -\sum_{j=1}^{(N-1)/2}[(\omega_{2j-1}'^{*} + 4\omega_{2j}'^{*} + \omega_{2j+1}'^{*})](2\pi/(3N)), \tag{4.3.12}$$

where $\omega_1^* = \omega_N^*,\ \omega_1'^{*} = \omega_N'^{*}$ and $\psi_1^* = \psi_N^*,\ \psi_1'^{*} = \psi_N'^{*}$.

Hence, equations (4.2.47), together with equations (4.3.10), (4.3.11) and (4.3.12), and the expressions (4.3.8) and (4.3.9) result in $(2N + 3)$ equations in terms of the $(2N + 5)$ unknowns, namely $\omega_j^*,\ \omega_j'^{*},\ j = 1, \ldots .., N, \lambda_1, \lambda_2, \lambda_7, \lambda_8$

and λ_9. Obviously, two further equations are required to close the above system. One of these arises from the fact that the pressure distribution must be single valued. Hence, from the component of the Stokes equation in the ϑ direction, namely

$$0 = -\frac{1}{r}\frac{\partial p}{\partial \theta} + \frac{\partial \omega}{\partial \theta}, \tag{4.3.13}$$

one obtains that

$$0 = \int_0^{2\pi} \frac{\partial \omega}{\partial \theta} d\theta. \tag{4.3.14}$$

On applying Simpson's rule to evaluate the integral one obtains

$$0 = -\sum_{j=1}^{(N-1)/2} [(\omega'^*_{2j-1} + 4\omega'^*_{2j} + \omega'^*_{2j+1})]. \tag{4.3.15}$$

This results in equations (4.3.10), (4.3.11), (4.3.12) and (4.3.15) providing 4 of the necessary 5 extra equations that are required. In order to obtain the other equation it is necessary to appeal to the form of ψ^* at large values of r. If in equation (4.2.42) $\underline{p}$ is taken as $\underline{p}(r_1, \vartheta_1)$, where r_1 is some large value of r, then $\psi^*(\underline{p}(r_1, \vartheta_1)$ is approximately zero. Unfortunately, from the expansion in expression (4.1.10) and expression (4.3.1) this means that one has introduced an error of $O(r_1^{-1})$ into the solution. Hence, extremely large values of r_1 are required to generate accurate results, but this difficulty can be overcome to some extent by adding the next term in the expansion into expression (4.1.10), namely

$$(\lambda_{10} \sin\vartheta + \lambda_{11} \cos\vartheta + \lambda_{12} \sin(3\vartheta) + \lambda_{13} \cos(3\vartheta))\frac{1}{r}. \tag{4.3.16}$$

By introducing these extra terms into the expansion, the approximation of $\psi^*(\underline{p}(r_1, \vartheta_1)$ by zero results in an error of only $O(r_1^{-2})$, and therefore a higher degree of accuracy can be achieved without the need for such a large value of r_1. However, before one can obtain this solution it is necessary to find further equations to balance the additional unknowns $\lambda_{10}, \lambda_{11}, \lambda_{12}$ and λ_{13} that have been introduced. The obvious means of achieving these is to take another 4

values of $\underline{p}$ at large values of r, namely $\underline{p}(r_j, \vartheta_j)$ with $r_j > 10$ for $j = 2, 3, 4, 5$ and apply equation (4.2.42) with $\psi^*(\underline{p}(r_j, \vartheta_j) = 0$ for $j = 2, 3, 4, 5$.

Even with the extra terms in the equations the error that has been introduced by setting $\psi^*(\underline{p})$ in equation (4.2.42) to be zero is $O(r^{-2})$, or $O(r^{-1})$ without the additional terms, where r is the smallest of the values of $r_j, j = 1, 2, 3, 4, 5$. The necessity for these extra terms can be avoided if instead of choosing point $\underline{p}$ in expression (4.2.42) to be at some large value of r one takes it to be inside the cylinder, namely $\underline{p}(r_{I1}, \vartheta_1)$, where $r_{I1} < 1$. This means that $\eta(\underline{p})$ vanishes and there is no need to approximate $\psi^*(\underline{p})$.

Case (b) Unbounded flow at infinity corresponding to a stokeslet at the origin, so general situation has $\lambda_3 = \lambda_6 = 0$.

In this situation one has a specified non-dimensional force $4\pi(-A, B)$, and the terms $\lambda_4 \mathrm{rln}(r)\sin\vartheta$ and $\lambda_5 \mathrm{rln}(r)\cos\vartheta$ must now be retained in the asymptotic expansion (4.1.10) of ψ. Hence, equations (4.3.10) and (4.3.11) have to be replaced by

$$\left.\begin{array}{rl} F_x = -4\pi A & = -4\pi\lambda_5 + \sum_{j=1}^{(N-1)/2}[(\omega'^*_{2j-1} + 4\omega'^*_{2j} + \omega'^*_{2j+1}) \\ & -(\omega^*_{2j-1} + 4\omega^*_{2j} + \omega^*_{2j+1})](\sin(\theta_j)(2\pi/(3N)), \end{array}\right\} \quad (4.3.17)$$

$$\left.\begin{array}{rl} F_y = 4\pi B & = 4\pi\lambda_4 - \sum_{j=1}^{(N-1)/2}[(\omega'^*_{2j-1} + 4\omega'^*_{2j} + \omega'^*_{2j+1}) \\ & -(\omega^*_{2j-1} + 4\omega^*_{2j} + \omega^*_{2j+1})](\cos(\theta_j)(2\pi/(3N)). \end{array}\right\} \quad (4.3.18)$$

However, the introduction of the extra unknowns λ_4 and λ_5 makes it necessary to apply equation (4.2.42) three times with $\underline{p}$ as $\underline{p}(r_{Ij}, \vartheta_j)$, where $r_{Ij} < 1$ for $j = 1, 2, 3$, with the corresponding $\eta(\underline{p})$ being zero as the points are all within the cylinder.

Case (c) Unbounded flow at infinity which is a combination of a uniform stream and a rotational far field, so general situation has $\lambda_4 = \lambda_5 = 0$.

In this situation one has a prescribed non-dimensional moment, $-4\pi C$, hence the need to retain the terms $\lambda_3 \ln(r)$ and $\lambda_6 r^2$ in the asymptotic expansion of ψ given by expression (4.1.10). Equations (4.3.10) and (4.3.11) replace equations (4.3.17) and (4.3.18). In addition, equation (4.3.12) is replaced by

$$M = -4\pi C = 8\pi\lambda_6 - \sum_{j=1}^{(N-1)/2}[(\omega^*_{2j-1} + 4\omega^*_{2j} + \omega^*_{2j+1})](2\pi/(3N)). \quad (4.3.19)$$

Again the introduction of two additional constants, this time λ_3 and λ_6, require the enforcement of equation (4.2.42) at three points within the cylinder.

Case (d) Combination of unbounded flows at infinity due to stokeslet at the origin together with a rotational far field, so general situation has $\lambda_j \neq 0$, for $j = 1, \ldots .., 9$.

With both the force and the moment specified it is necessary to apply the equations (4.3.17), (4.3.18) and (4.3.19). As with cases, $(a), (b)$ and (c) the single valued pressure condition, given by equation (4.3.15), remains one of the extra equations. As now all the constants $\lambda_j, j = 1, \ldots\ldots, 9$, are present it is necessary to enforce equation (4.2.42) at 5 points $(\underline{r}_{Ij}, \vartheta_j)$ within the cylinder instead of at just 3 points as in *Cases* (b) and (c).

It is possible to include the term $A_0(r^2 \ln(r) - r^2)$ from expression (3.3.2), which vanished due to the single valueness of the pressure, in the asymptotic part of expression (4.1.10). However, on doing so, in the form $\lambda_0(r^2 \ln(r) - r^2)$ to conform with the adopted notation, it would require the modification of equation (4.3.15), together with the implementation of equation (4.2.42) at another point within the circular cylinder. Hence, increasing the number of points where this equation has to be applied in the most general situation, namely *Case* (d), from 5 to 6. The actual condition that would replace equation (4.3.15) would be

$$0 = 8\pi\lambda_0 - \sum_{j=1}^{(N-1)/2} [(\omega'^*_{2j-1} + 4\omega'^*_{2j} + \omega'^*_{2j+1})](2\pi/(3N)). \tag{4.3.20}$$

The term in ψ which is just a multiple of ϑ will not be considered at any stage since it obviously violates the periodicity and has been neglected throughout.

4.4 Numerical Results

In all the numerical calculations the rotlet has been located along the x-axis at the non-dimensional distance c from the center of the cylinder and the value of c has been taken to be 3 in order to correspond with the calculations by Dorrepaal et al. (1984)

Figure 4.4.1 shows the streamlines relating to expression (3.1.5). The pattern is identically to that presented by Dorrepaal et.al. (1984). Figures 4.4.2 and 4.4.3 show the corresponding streamline patterns when the cylinder rotates with

the non-dimensional angular speeds $\alpha = 1$ and $\alpha = 2$, respectively, where $\alpha > 0$ represents counter clockwise rotation. It should be noted that once the cylinder starts to rotate the four points on the cylinder where the streamlines leave the surface in figure 4.4.1 move into the fluid. In the figures presented by Dorrepaal et.al. (1984), when $\alpha = 0.5$ then there exists two stagnation points on the x-axis, one either side of the cylinder. The point on the same side of the cylinder as the rotlet lies between the cylinder and the rotlet. Figures 4.4.2 and 4.4.3 show that increasing the strength of the rotation of the cylinder appears to

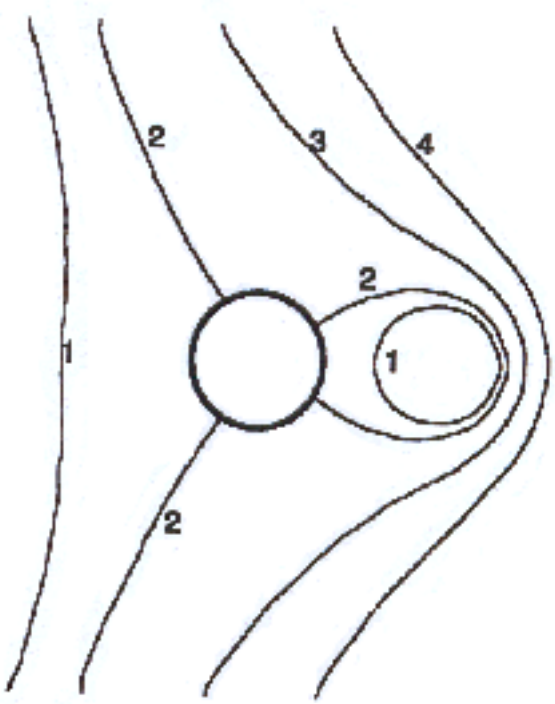

Figure 4.4.1: The streamlines obtained numerically for $Re = 0$ and $\alpha = 0$. The streamline labeled $1, \ldots, 4$ correspond to $\Psi = -0.2, 0.0, 0.4$ and 0.8 respectively. labeled $1, \ldots, 4$ correspond to $\Psi = -0.2, 0.0, 0.4$ and 0.8 respectively.

move the stagnation point which is between the rotlet and the cylinder slightly closer to the rotlet. At the same time the stagnation point on the other side of the cylinder rapidly moves away from the cylinder with increasing values of the

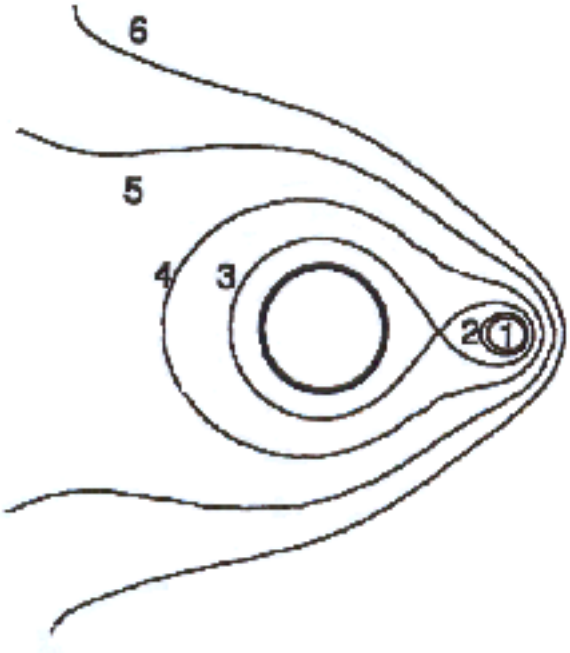

Figure 4.4.2: The streamlines obtained numerically for $Re = 0$ and $\alpha = 1$. The streamline labeled $1, \ldots$,6 correspond to Ψ = -0.2, 0.0, 0.388, 0.8, 1.2 and 1.5 respectively. labeled $1, \ldots, 6$ correspond to Ψ = -0.2, 0.0, 0.388, 0.8, 1.2 and 1.5 respectively.

parameter α. Also, as expected, with increasing α the amount of fluid rotating in closed contours, both around the cylinder and the rotlet, increases.

In figure 4.4.4 the non dimensional vorticity pattern corresponding to the streamlines for figures. 4.4.1, 4.4.2 and 4.4.3, (the analytical solution from expression (3.1.15)), is shown. These are all identical since the extra contribution to the streamline pattern in the form of the term $\alpha \ln(r)$, due to the rotation of the cylinder, produces no additional vorticity. The pattern is symmetrical about the x-axis and shows the contours of constant vorticity leaving the surface only to return within the same quadrant, where the boundaries of the quadrants are at $\vartheta \simeq (2n-1)\pi/4$, with $n = 1, 2, 3$ and 4. In addition the diagrams appear to show only a limited departure from a symmetrical pattern about the $y-$axis.

Numerical values of the integrals in expressions (3.2.13), (3.2.14) and (3.2.15)

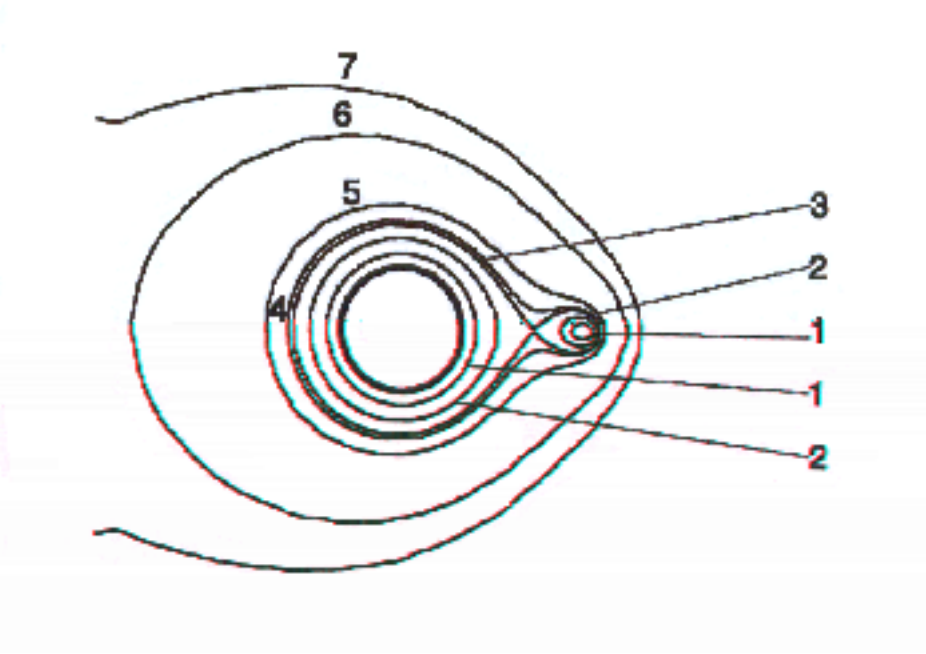

Figure 4.4.3: The streamlines obtained numerically for $Re = 0$ and $\alpha = 2$. The streamline labeled $1, \ldots, 7$ correspond to $\Psi = 0.4, 0.8, 1.105, 1.2, 1.5, 2.5$ and 3.0 respectively.

were evaluated by Simpson's rule for the non dimensional stream function and vorticity given by expressions (3.1.5) and (3.1.15) respectively. The procedure was repeated with the non dimensional stream function and vorticity represented by expressions (3.1.17) and (3.1.15) respectively, with the value of α equal to 1 and then 2. In each situation the contours along which the integrations were undertaken were circles, with radii of $1, 2, 4, 5$, concentric with the circular cylinder. The first two contours enclose only the cylinder, whereas the last two enclose both the cylinder and the rotlet. Due to the different contours over which the integrations were performed, different step lengths were required in order to acquire four decimal place accuracy. However, a step length of $h = 1/40$ proved sufficient to achieve this requirement on all the contours. Details of the values of F_x, F_y and M on the various contours are shown in Table 4.4.1.

These results are as expected. Since in the case of the force components, F_x and F_y are both zero due to the absence of any $\mathrm{rln}(r)\sin\vartheta$ and $\mathrm{rln}(r)\cos\vartheta$ terms

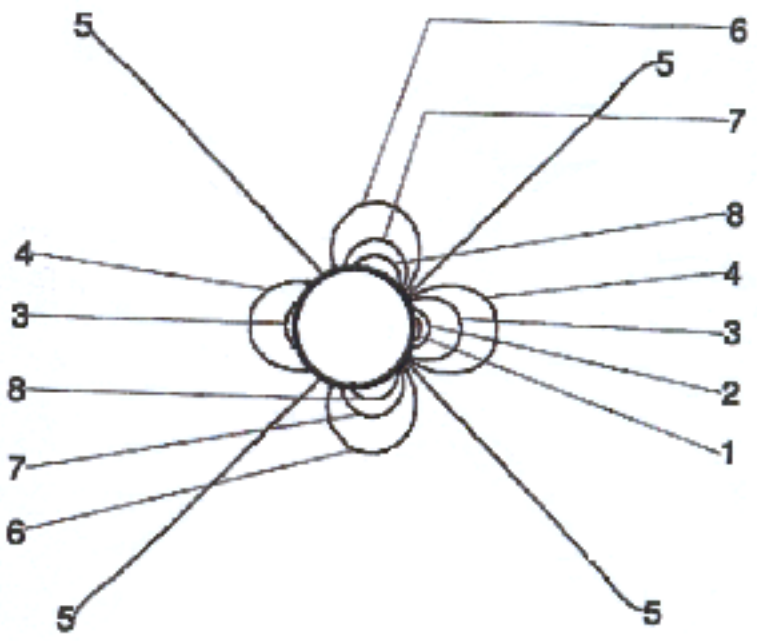

Figure 4.4.4: The vorticity corresponding to the streamlines for figures 4.4.1, 4.4.2 and 4.4.3. The labeled $1, \ldots, 8$ correspond to $\Psi = -0.7, -0.5, -0.2, -0.1, 0.0, 0.1, 0.2$ and 0.3 respectively.

from the non dimensional stream function expressions (3.1.5) and (3.1.17). The moment M should undertake the value $-4\pi\mu\Gamma(\alpha+1)$ on contours whose radius exceeds the value c, that is includes the rotlet as well as the circular cylinder. Whereas, on contours which exclude the rotlet the value should be$-4\pi\mu\Gamma\alpha$, due to the need to exclude the contribution to the moment from the rotlet. In addition, when the non-dimensional angular velocity of the cylinder is α, the analytical form of the non dimensional stream function results in the asymptotic expansion at large values of r containing an $(\alpha+1)\ln(r)$ term. The above numerical values confirm the theoretical result that the moment on the circular cylinder is $-4\pi\mu\Gamma$ times the coefficient of the $\ln(r)$ term in the asymptotic expansion, provided any contributions from singularities are excluded.

Figure 4.4.5 represents the non dimensional streamline pattern for expression

(3.5.4) with $A = 1, B = C = 0$. Physically the magnitude of the additional term $[rln(r) - \frac{1}{2}(r - r^{-1})] \sin\vartheta$ into expression (3.1.5) corresponds to a stokelet type term at the origin, pointing along the positive x-axis. Hence, it is not surprising that the pattern of the streamlines resembles that obtained by Dorrepaal et.al. (1984) when a stokelet, pointing in same direction was placed at $(c, 0)$. However, in the present case the velocity is unbounded at infinity. In both situations the fluid approaches the cylinder from the negative x-axis direction, yet whereas in the present situation there exists a stagnation point nearly exactly below

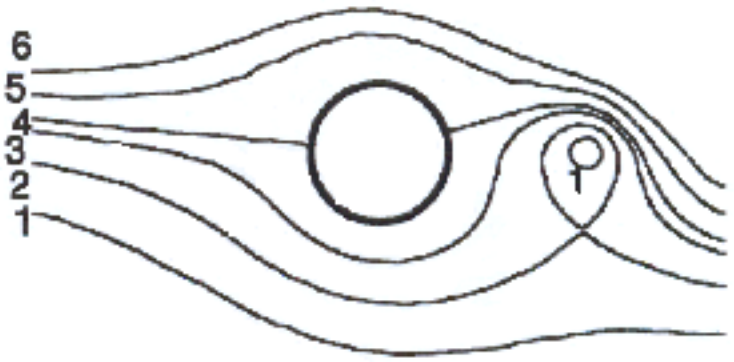

Figure 4.4.5: The streamlines corresponding to the expression (3.5.4) with $A = 1, B = C = 0$. The labeled $1, \ldots, 6$ correspond to $\Psi = -1.5, -0.7, -0.2, 0.0, 0.4$ and 0.8 respectively.

the rotlet, in the case studied by Dorrepaal et.al. the absence of any rotlet term, together with the presence of an anti-clockwise rotation of the cylinder, produced a stagnation point above the x-axis and only a small distance away from the surface of the cylinder.

Figure 4.4.6 shows the non-dimensional vorticity corresponding to the streamline pattern which occurs in figure 4.4.5. The addition to the vorticity shown in figure 4.4.4 of a term of the form $r^{-1} \sin\vartheta$ from the stokelet produces a pattern which is nearly symmetrical about the y-axis, but nearly anti symmetric about the x-axis. However, in this case the contours leave the surface of the cylinder and rejoin it either within the upper half half space or within the lower half space. Not within the four quadrants as is the situation in the absence of any

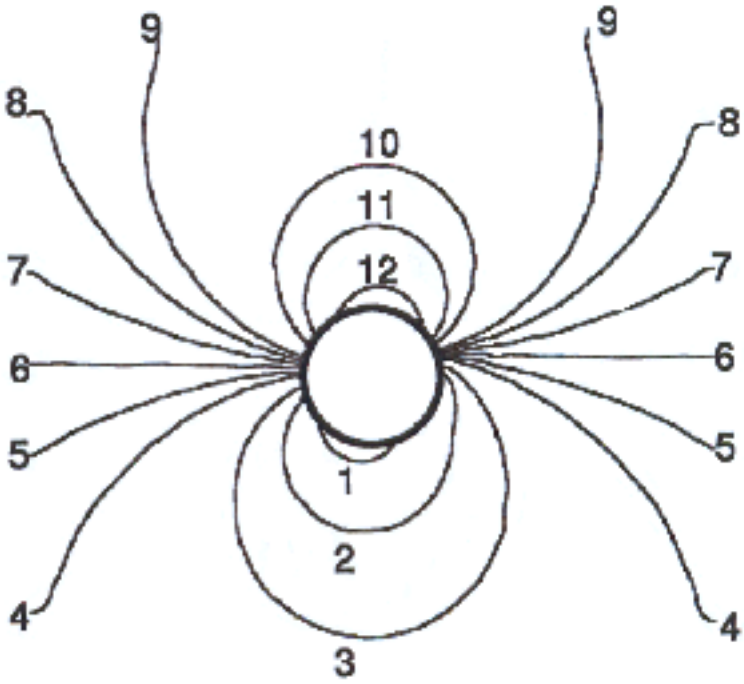

Figure 4.4.6: The vorticity corresponding to the streamlines for figure 4.4.5. The labeled $1, \ldots, 13$ correspond to $\omega = -1.4, -1.0, -0.7, -0.5, -0.2, -0.1, 0.0, 0.1, 0.2, 0.3, 0.7, 1.0$ and 1.7 respectively.

stokeslet type term which is displayed in figure 4.4.4.

Figure 4.4.7 represents the non-dimensional streamline pattern for expression (3.5.4) with $B = 1, A = C = 0$. Physically the magnitude of the additional term $[rln(r) - \frac{1}{2}(r - r^{-1})] \cos\vartheta$ into expression (3.1.5) corresponds to a stokelet type term at the origin, pointing along the positive y-axis. Hence, it is not surprising that the pattern of the streamlines resembles that obtained by Dorrepaal et.al. (1984) when a stokelet was placed at $(c, 0)$, pointing in the same direction. However, in the present case the velocity is unbounded at infinity. In both situations the fluid approaches the cylinder from the negative y-axis direction, yet whereas in the present situation there exists a stagnation point on the x-axis between the cylinder and the rotlet, in the case studied by Dorrepaal et.al. the

absence of any rotlet term, together with the presence of a clockwise rotation of the cylinder, produced two stagnation points approximately the same distance above and below the x-axis and only a small distance away from the surface of the cylinder.

Figure 4.4.8 shows the non-dimensional vorticity corresponding to the streamline pattern which occurs in figure 4.4.7. The addition to the vorticity shown in figure 4.4.4 of a term of the form $r^{-1}\cos\vartheta$ from the stokelet produces a pattern which is nearly symmetrical about the x-axis, but nearly anti symmetric about the y axes. However, in this case the contours leave the surface of the cylinder and rejoin it either within the half half space $x > 0$ or within the half space $x < 0$. Not within the four quadrants as is the situation in the absence of any stokeslet type term which is displayed in figure 4.4.4.

Figure 4.4.9 represents the non-dimensional streamline pattern for expression (3.5.4) with $C = 1, A = B = 0$. Physically the magnitude of the additional term $[\ln(r) - \frac{1}{2}(r^2 - 1)]$ into expression (3.1.5) corresponds to a far field which is rotational about the cylinder. Hence, it is not surprising that the pattern of the streamlines resembles that obtained by Avudainayagam and Jothiram (1987) when a rotlet was placed in the presence of a cylinder with a rotational flow at infinity. In both cases the streamlines form closed contours either around the cylinder or around the cylinder and the rotlet, together with a stagnation point on the x-axis. However, due to the different values of c the position of stagnation points differ. In the present case it is further along the x-axis than the rotlet, whereas in the case considered by Avudainayagam and Jothiram (1987) it lies between the rotlet and the cylinder. At infinity the form of the non-dimensional stream function from Avudainayagam and Jothiram (1987) assumes the form

$$\psi \approx (K - Lc^{-1})rcos\vartheta - L(\ln(r) - \frac{r^2}{2}) + \ln(r) \tag{4.4.1}$$

which results in their corresponding value of moment on the cylinder being

$$M = -4\pi\mu\Gamma(cK - 2L). \tag{4.4.2}$$

It should be stressed that in order for the boundary conditions to be satisfied it is necessary for $cK - L$ to be unity, which results in expression (4.4.1) becoming

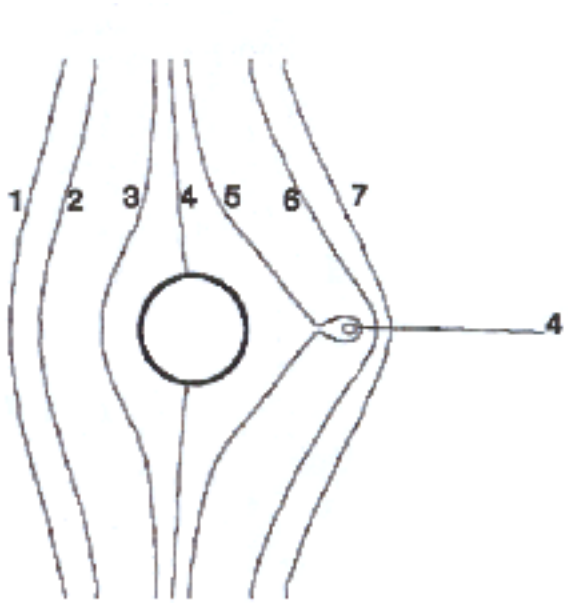

Figure 4.4.7: The streamlines corresponding to expression (3.5.4) with $B = 1, A = C = 0$. The labeled $1, \ldots, 7$ correspond to $\Psi = -3.0, -2.0, -0.425, 0.0, 0.425, 2.0$ and 3.0 respectively.

$$\psi \approx \frac{1}{c} r cos\vartheta - L(\ln(r) - \frac{r^2}{2}) + \ln(r). \tag{4.4.3}$$

Hence, for the analytical non-dimensional stream function for non zero C to correspond exactly with that of Avudainayagam and Jothiram (1987), who applied $K = L = 0.5$, it was necessary to choose $C = -0.5$. The two streamline patterns then correspond exactly. However, the moment on the cylinder in our case is $2\pi\mu\Gamma$, whereas according to expression (4.4.2) it is $-2\pi\mu\Gamma$. This discrepancy is due to the failure of Avudainayagam and Jothiram (1987) to account for the contribution within their expression of the rotlet by the subtraction of the term $4\pi\mu\Gamma$. This can be further emphasized by considering the case corresponding to that investigated by Dorrepaal et.al. (1984) when $L = 0$ and $K = c^{-1}$. For which expression (4.4.2) produces a moment on the cylinder of $-4\pi\mu\Gamma$ instead of the correct value of zero. In order to correspond to the present situation one requires $L = -1$ and $K = 0$, in which case the moment M assumes the value

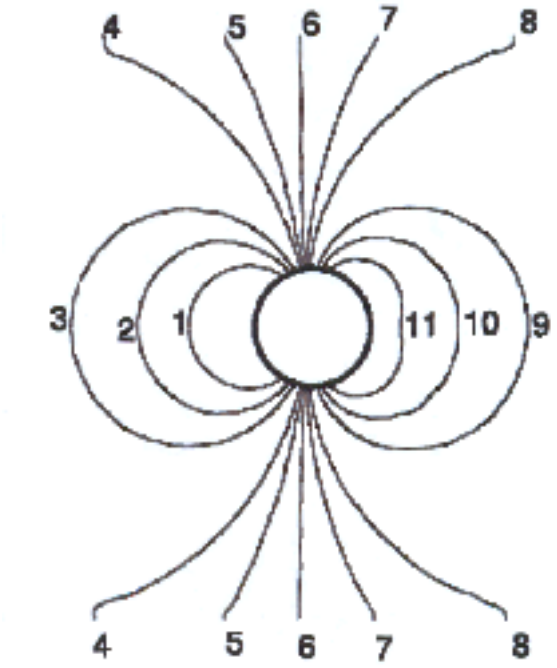

Figure 4.4.8: The vorticity corresponding to the streamlines in figure 4.4.7. The labeled $1, \ldots, 11$ correspond to $\omega = -1.0, -0.7, -0.5, -0.2, -0.1, 0.0, 0.1, 0.2, 0.5, 0.7$ and 1.0 respectively.

$-4\pi\mu\Gamma$. This value is confirmed by the results in Table 4.4.4.

In figure 4.4.11 the value of $-2C$ has been added to the non-dimensional vorticity given by expression (3.1.15) in order to produce the vorticity pattern corresponding to the streamline flow in figure 4.4.9. The contours are identical to those shown in figure 4.4.4, but for their constant change in magnitude.

The above tables clearly show that the force components and the moment on the circular cylinder from expressions (3.2.13), (3.2.14) and (3.2.15) are directly related to the coefficients of the $r\ln(r)\sin\vartheta$, $r\ln(r)\cos\vartheta$ and $\ln(r)$ terms respectively in the expansion of the stream function at large distances, as seen by expressions (3.3.10) and (3.3.11), provided that account is taken of any contributions arising from singularities with the enclosed domain.

So far the results presented have been the numerical data of analytical so-

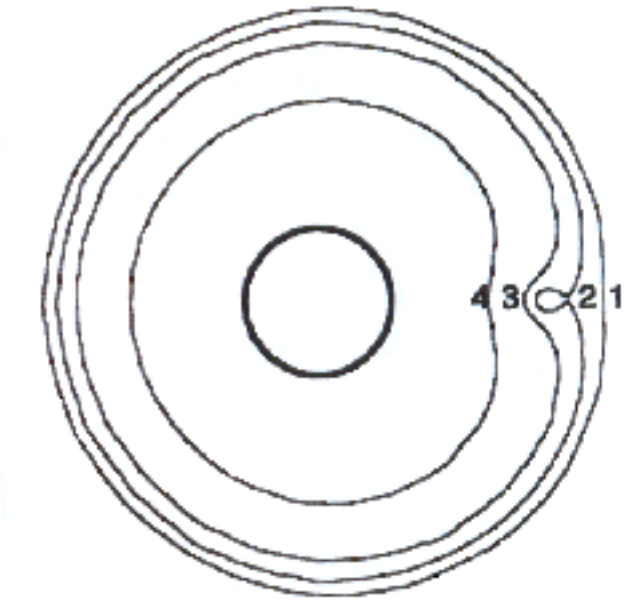

Figure 4.4.9: The streamlines corresponding to expression (3.5.4) with $C = 1$, B = A = 0. The labeled $1, \ldots, 4$ correspond to Ψ = -5.5, -4.85, -4.0 and -2.0 respectively.

lutions for the stream function and the vorticity. However, having established these it is intended to investigate how good the application of the Boundary Element Technique is in determining the solution when the force and moment on the cylinder are known. Use is made of the asymptotic form of the stream function and the vorticity in relating the coefficients of some of the terms in this expansion to the force components and the moment, as given by expressions (3.3.10) and (3.3.11), in order to validate the results.

Initially case (a), with $\lambda_2 = 0$, was investigated. This was chosen since the unknown constants $\lambda_1, \lambda_7, \lambda_8$ and λ_9 could be determined without the need to introduce extra conditions either from considering points inside the cylinder or at large values of r outside the cylinder. The conditions given by expressions $(4.3.10), (4.3.11), (4.3.12)$ and (4.3.15) produced streamline and vorticity patterns identical to those shown in figures. 4.4.1 and 4.4.4 respectively. The values of $\lambda_1, \lambda_7, \lambda_8$ and λ_9 which analytically are $c^{-1}, -\ln(c), 0$ and c^{-2} numer-

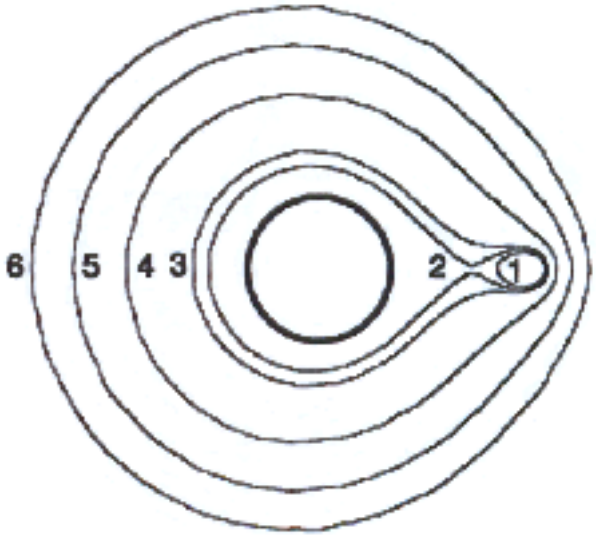

Figure 4.4.10: The streamlines corresponding to expression (3.5.4) with C = -0.5, B = A = 0. The labeled $1, \ldots, 6$ correspond to Ψ = 0.0, 0.05, 0.1, 0.2, 0.9, and 2.7 respectively.

ical are $0.3333, -1.0986, 0.0002$ and 0.1105 respectively.

Introducing an unknown λ_2 requires an extra condition, which can be achieved by assuming that the value of the perturbation stream function ψ^* from its asymptotic value at some large value of r is approximately zero. However, if this is all that was undertaken, then the error would be $O(r^{-1})$. Hence, the extra terms of $O(r^{-1})$ are taken into the asymptotic expansion resulting in a reduction in the error to $O(r^{-2})$. This means that the asymptotic expansion (4.1.10) now contains the extra 4 terms given in expression (4.3.16). As a result it was necessary to choose ψ^* to be zero at 5 large values of r. The magnitude of r for all these points was taken to be around 20. The streamline and vorticity patterns are again identical to those shown in figures. 4.4.1 and 4.4.4 respectively. The values of $\lambda_1, \lambda_7, \lambda_8$ and λ_9 which analytically are $c^{-1}, -\ln(c), 0$ and c^{-2} numerical are now $0.3333, -1.0986, 0.0002$ and 0.1112 respectively, hence showing a small change from their earlier values. The values of $\lambda_{10}, \lambda_{11}, \lambda_{12}$ and λ_{13} are all identically zero apart from λ_{13} which assumes the

value c^{-3}. Their corresponding numerical values are $-0.0005, -0.0293, 0.0000$ and 0.3705 when 40 points are taken around the cylinder, but these become $-0.0001, -0.0148, 0.0000$ and 0.3703 when the number of points is increased to 160.

The above inaccuracies arising in the coefficient λ_{11} can be overcome by choosing the extra points to be within the cylinder rather than at some large value of r. In fact since ψ^* is exactly zero there is no necessity to include the extra terms from the expression (4.3.16) within the asymptotic expansion of the stream function. Introducing an extra point within the cylinder to produce an equation to compensate for the extra unknown coefficient λ_2, results in the same values of $\lambda_1, \lambda_7, \lambda_8$ and λ_9 as given above, together with the value of λ_2 as 0.0000.

In case (b) where $\lambda_3 = \lambda_6 = 0$ the non dimensional force components F_x and F_y have non zero values - A and B respectively, which is why the coefficients λ_4 and λ_5 must be included. Setting $A = 1$ and $B = 0$ produced the streamline and vorticity patterns shown in figures 4.4.5 and 4.4.6 respectively, with the values of $\lambda_1, \lambda_7, \lambda_8$ and λ_9 unchanged from above, together with the coefficients $\lambda_2 = -0.4961$, (exact value -0.5000), $\lambda_4 = 1.0000$ and $\lambda_5 = 0.0000$. Reversing the values of A and B reverse the values of λ_4 and λ_5, together with $\lambda_2 = 0.0000, \lambda_1 = -0.1627$, (exact value $(c^{-1} - \frac{1}{2})$), λ_7, λ_8 and λ_9 remaining unchanged, and produced the streamlines and vorticity patterns shown in figures 4.4.7 and 4.4.8.

In case (c) where $\lambda_4 = \lambda_5 = 0$ the non dimensional moment M has non zero value $-C$, which is why the coefficients λ_3 and λ_6 must be included. Setting $C = 1$ produced the streamline and vorticity patterns shown in figures 4.4.9 and 4.4.11 respectively, with the values of λ_8 and λ_9 unchanged but $\lambda_1 = 0.3333, \lambda_2 = 0.0000, \lambda_3 = 0.9938$(exact value 1), $\lambda_6 = -0.5000$(exact value - $\frac{1}{2}$), $\lambda_7 = -0.5935$(exact value $-\ln(c) + \frac{1}{2}$).

In case (d) all the $\lambda_j, j = 1, \ldots\ldots, 9$ were included in the asymptotic expansion, hence requiring ψ^* to be set to zero at 5 points within the cylinder. With the parameters A, B and C set in turn to their above values the inclusion of the previous zero coefficients λ_j, for example in case (b) namely λ_3 and λ_6, were numerically calculated to be 0.0000 in all cases. Similarly, the inclusion of the $\lambda_0(r^2 \ln(r) - r^2)$ term resulted in unchanged values of the coefficients λ_j, for $j = 1, \ldots .9$, together with $\lambda_0 = 0.0000$.

Identical figures to those presented in figures 4.4.1 to 4.4.11 for the stream function and the vorticity were produced by using the results obtained from the BEM as opposed to their analytic expressions.

In all the above cases the integrals in expressions (3.2.13), (3.2.14) and (3.2.15) were evaluated numerically from the values of the stream function and vorticity on the cylinder, together with the normal derivatives of these quantities, derived during the Boundary Element Solution. In each situation the values obtained agreed within 3 decimal places to those introduced in the form of constraints by expressions (4.3.17), (4.3.18) and (4.3.19).

4.5 Conclusions

The relation of the coefficients of some of the terms in the asymptotic expansion of the stream function to the force components and the torque on a body, together with the imposition of an integral constraint, enables the Boundary Element Method (BEM), to provide a closed system of equations for the flow generated by a rotlet in the presence of a circular cylinder.

Excellent agreement is obtained between the numerical results and previous analytical expressions. The numerical scheme has been extended to solve the most general situation when both force and moment on the cylinder are non-zero, and neither the magnitude nor the direction of the stream is known.

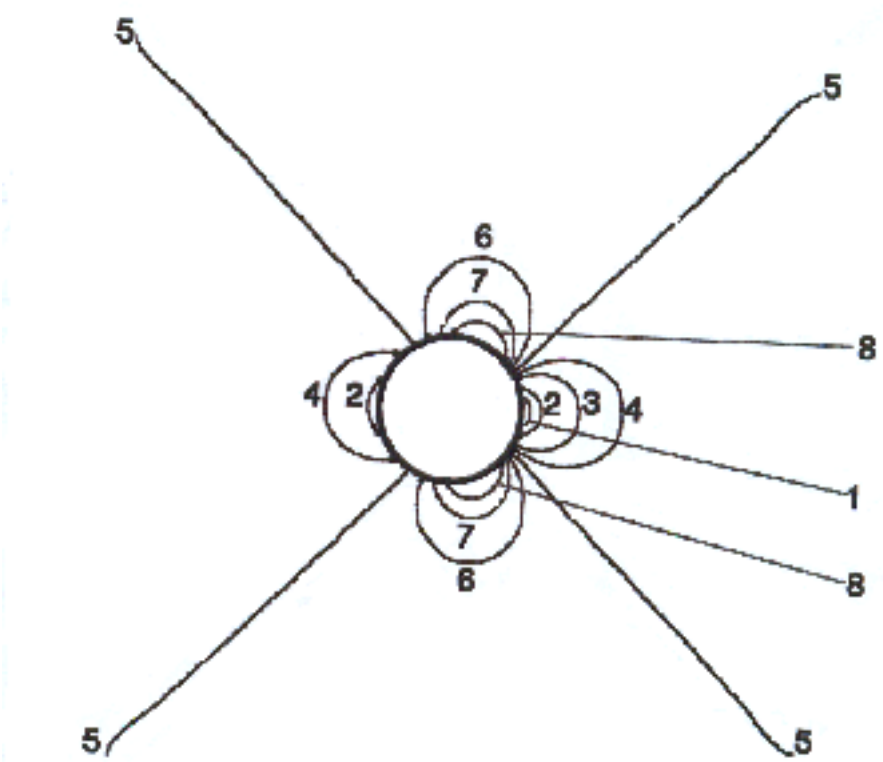

Figure 4.4.11: The vorticity pattern corresponding to the streamlines in figure 4.4.9. The labeled $1, \ldots, 8$ correspond to $\omega = -2.7, -2.5, -2.2, -2.1, -2.0, -1.9, -1.8$ and -1.7 respectively.

Chapter 5

THE ROTATION OF TWO CIRCULAR CYLINDERS

5.1 Introduction

So far our problems have been restricted to Stokes flow in the presence of a single body, although one could argue that a rotlet, in the presence of either a circular cylinder or an ellipse, may be regarded as a small rotating circular cylinder and represents a special case of a two body problem. However, such situations have been treated as single body problems. In the case of a rotlet outside an ellipse, Smith (1993) has shown that the Stokes flow at infinity is solid body rotation, except when the rotlet is placed at one particular position, or to be exact at four positions due to symmetry, whose coordinates are dependent on the strength of the rotation of the rotlet. In that special case, like that of a rotlet outside a circular cylinder, the far field corresponds to that of a uniform stream. It has been shown by Jeffery (1922) and Smith (1991) that for two body problems a similar phenomenon occurs, together with a special case.

The paradox which occurred for the above two body problem, (both cylinders of equal radii and rotating with equal speeds, but opposite senses about parallel axes), when Jeffery (1922) obtained his unusual result of the presence of a uniform stream at infinity was resolved by the work of Proudman and Pearson (1957) and Kaplun and Lagerstrom (1957), where it was shown that such a Stokes flow was only the far field of an inner solution and that an outer region

was required where the Navier-Stokes equations, or some modified approximation of them, are valid. Although at the time Jeffery's result was known to be in error due to such a flow having an infinite amount of kinetic energy, whilst supplied by torques acting on the cylinders for only a finite time so producing only a finite amount of work. It was probably this unresolved situation which caused Jeffery to present his solution for only the one particular case when the cylinders are of the same radii and rotate with equal speeds, but with opposite senses, about parallel axes, even though he had formulated the general problem for two cylinders with different radii and different angular velocities.

It was left to Smith (1992) to utilize these expressions to establish that Jeffery's result was just a special case of the more general situation where the far field solution of the Stokes flow corresponds to a rigid body rotation. In fact Smith was further able to use his solution as the inner boundary condition for the outer region, where the complete Navier-Stokes equations hold, to produce the solution in that region. Hence, producing a complete solution over the whole fluid domain to the problem of two cylinders of different radii and different angular velocities. This was achieved by means of an inner solution satisfying the Stokes equation and an outer solution which satisfies the Navier-Stokes equations. These two solutions being matched at the boundary of the far field of the inner region, or equivalently the near field of the outer region. This need for the Stokes solution before one can establish the complete solution over the whole fluid domain makes the far field form of the Stokes solution considerably more important that a mere paradox. Before embarking upon a numerical attempt to establish the Stokes flow using information from the far field of the inner region in the form of the coefficients of the stream function related to values of the lift, drag and moment generated on the two bodies, a resume of the analytical work by Jeffery (1922) and Smith (1991), inter dispersed with additional information, will be undertaken.

5.2 Co-ordinate System

Jeffery (1922) and Smith (1991) both adopted the bipolar coordinates system

$$x = \frac{A\sin(\eta)}{cosh(\xi) - \cos(\eta)}, \quad y = \frac{A\sinh(\xi)}{cosh(\xi) - \cos(\eta)}, \tag{5.2.1}$$

where (0,A) and (0,-A) are the limiting points of the two coaxial cylinders. These equations having arisen from the solution of the equation

$$\xi + i\eta = \ln[\frac{x + i(y + A)}{x + i(y - A)}], \tag{5.2.2}$$

where both sides of equation (5.2.2) represent conjugate functions. As will be seen shortly, $\xi = \xi_1$and $\xi = -\xi_2$, where $\xi_1$and $\xi_2$are both positive constants, result in two circular cylinders of radii Acosech(ξ_1) and Acosech(ξ_2) respectively, which do not enclose each other. Dorrepaal, O'Neill and Ranger (1984), who presented streamlines for the problem solved by Jeffery (1922) at different values of d/R_1, where $2d$ represents the distance between the centers of the two cylinders each of radius R_1, set A in the numerator of equations (5.2.1) to be $A = R_1 \sinh(\xi_1)$, or equivalently $R_1 \sinh(\xi_2)$, since in their work $\xi_1 = \xi_2$.

The coordinate scheme is shown in figure 5.2.1, where $0_1$and $0_2$are the points $(0, A)$ and $(0, -A)$, respectively and P is any point in the plane. If the distances 0_1P and 0_2P are $r_1$and $r_2$and 0_1P and 0_2P are inclined at angles $\vartheta_1$and $\vartheta_2$to the x-axis, respectively,

then,

$$\xi = \ln(r_2/r_1) \quad and \quad \eta = \vartheta_2 - \vartheta_1. \tag{5.2.3}$$

The curves ξ =constant are a set of co-axial circles of the limiting point kind with $0_1$and 0_2as the limiting points of the system, whereas the curves η = constant are a system of co-axial circles of the common point kind. All the circles of one system intersect all the circles of the other system orthogonally. The circles corresponding to positive values of ξ are above the x-axis, whereas those corresponding to negative values are below. The x-axis itself corresponds to $\xi = 0$. The arcs of circles corresponding to positive values of η are on the right hand side of the y-axis, whereas those corresponding to negative values are on the left hand side. On the y-axis $\eta = 0$, unless the point is between $0_1$and $0_2$when $\eta = \mp\pi$, see figure 5.2.2.

¿From equation (5.2.3) it is easily seen that as $r \to \infty$, then ξ and $\eta \to 0$. As P approaches $0_1$and 0_2, then $\xi \to \infty$ and$-\infty$, respectively. Elements measured along the normals to the curves ξ and η = constant are $h_1 d\xi$ and $h_2 d\eta$ respectively, where $h_1^2 = h_2^2 = 1/(h^2)$ and

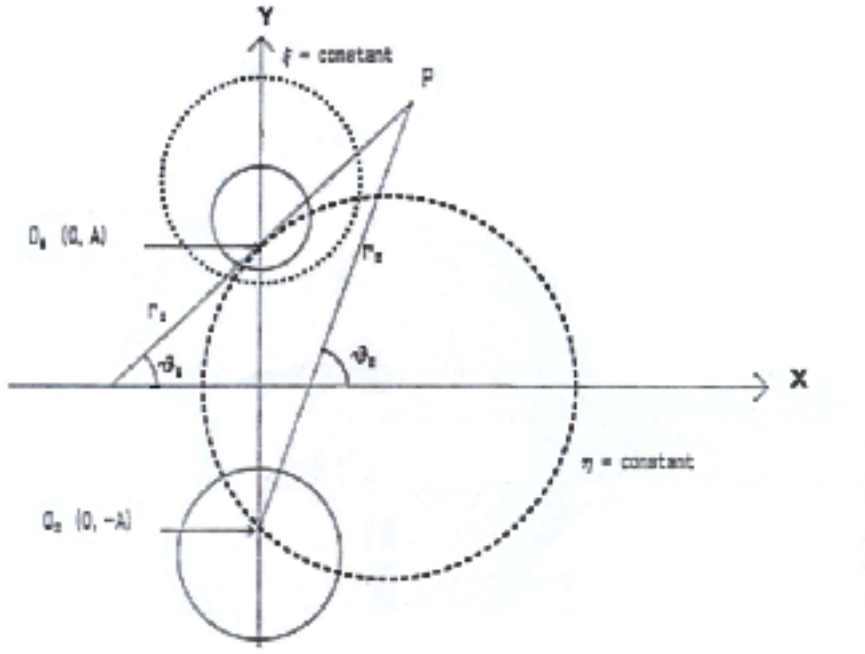

Figure 5.2.1: The geometry of the two cylinders and the coordinate scheme.

$$1/(h^2) = (\frac{\partial x}{\partial \xi})^2 + (\frac{\partial y}{\partial \xi})^2 = A^2/((cosh(\xi) - cos(\eta))^2). \tag{5.2.4}$$

The equations of the circles are

$$x^2 + (y - Acoth(\xi_1))^2 = A^2 cosech^2(\xi_1)$$

and

$$x^2 + (y + Acoth(\xi_2))^2 = A^2 cosech^2(\xi_2) \tag{5.2.5}$$

respectively, see figure 5.2.3. Obviously the modification to the transformation adopted by Dorrepaal *et al.* (1984), results in the centers of the two circles being at $(0, R_1 \cosh(\xi_1))$ and $(0, -\alpha R_1)$, where $\alpha R_1 = R_1 \sinh(\xi_1) \coth(\xi_2)$, with the radii $R_1$and $R_2 = \beta R_1 = R_1 \sinh(\xi_1)$cosech$(\xi_2)$. For the remainder of the analysis it is proposed to adopt the non-dimensional form of the transformation

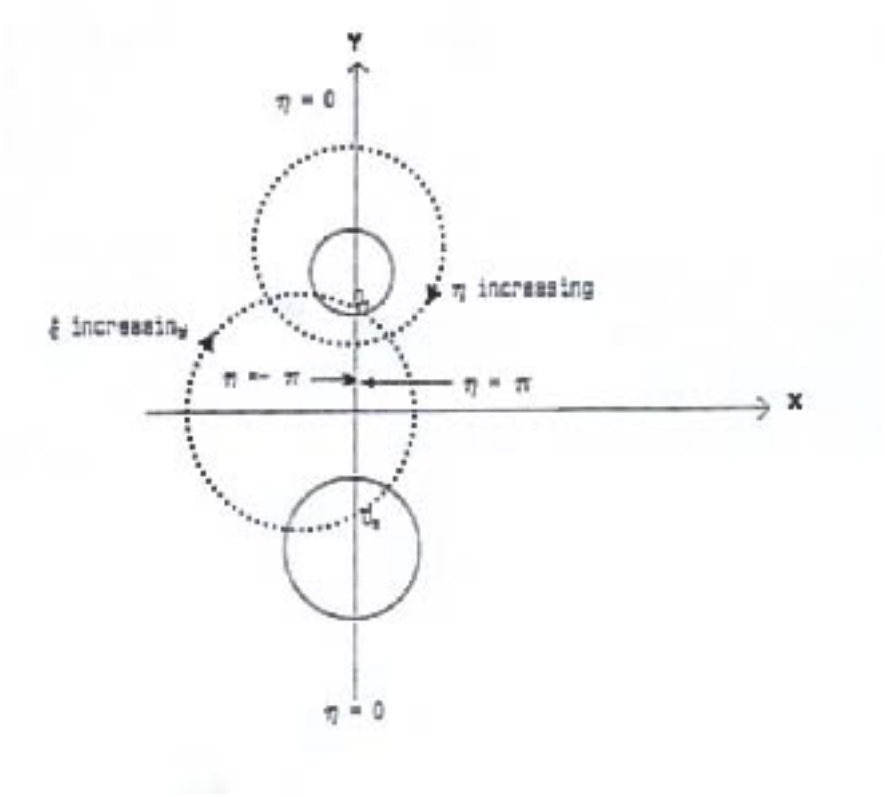

Figure 5.2.2: (ξ, η) coordinate system.

used by Dorrepaal *et al.* (1984), so the circles have radii unity and β with centers at $(0, \cosh(\xi_1))$ and $(0, -\alpha)$, respectively. Hence, the cylinders are given by $\xi = \xi_1$and $\xi = -\xi_2$and the distance between the axes of the cylinders by $(\cosh(\xi_1) + \alpha)$, with the flow region defined by $-\xi_2 < \xi < \xi_1$and $-\pi < \eta < \pi$. Instead of adopting the non-dimensional chosen by Dorrepaal *et al.* (1984), namely scaling the coordinates with respect to the radius of the upper cylinder, Smith (1991) scaled the x and y coordinates with respect to the distance A, resulting in the centers of the two cylinders having non-dimensional coordinates $(0, \coth(\xi_1))$ and $(0, -\coth(\xi_2))$, together with non-dimensional radii $\mathrm{cosech}(\xi_1)$ and $\mathrm{cosech}(\xi_2)$, respectively. However, to avoid undue confusion their non-dimensionalisation will be discussed separately later.

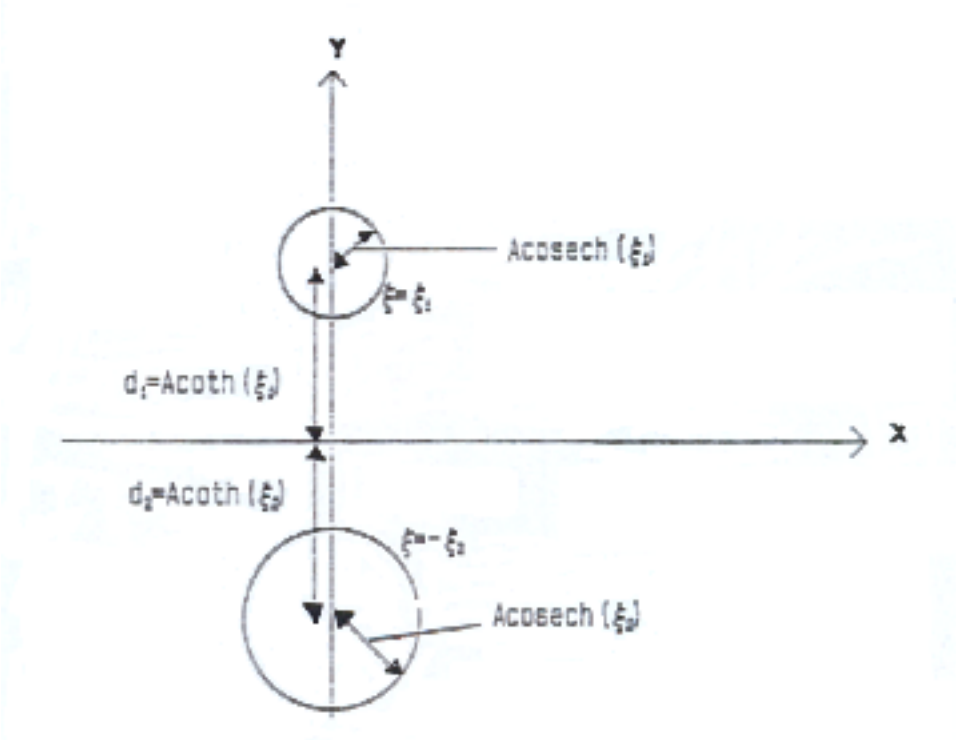

Figure 5.2.3: The radii of the two cylinders and the distances from the centers of the two cylinders to the origin.

5.3 Stream Function Expansion

In addition to the above non-dimensionalisation of the coordinates, the stream function and the vorticity are non-dimensionlised with respect to $R_1\omega_1$and ω_1, respectively, where $\omega_1$is the angular velocity of the upper cylinder. If the non-dimensional components of the velocity in the directions of increasing ξ and η are $u_\xi$and $u_\eta$respectively, see figure 5.3.4,

then the continuity equation

$$h^2(\frac{\partial}{\partial\xi}(h^{-1}u_\xi) + \frac{\partial}{\partial\eta}(h^{-1}u_\eta)) \tag{5.3.1}$$

can be satisfied by the stream function Ψ expressed by

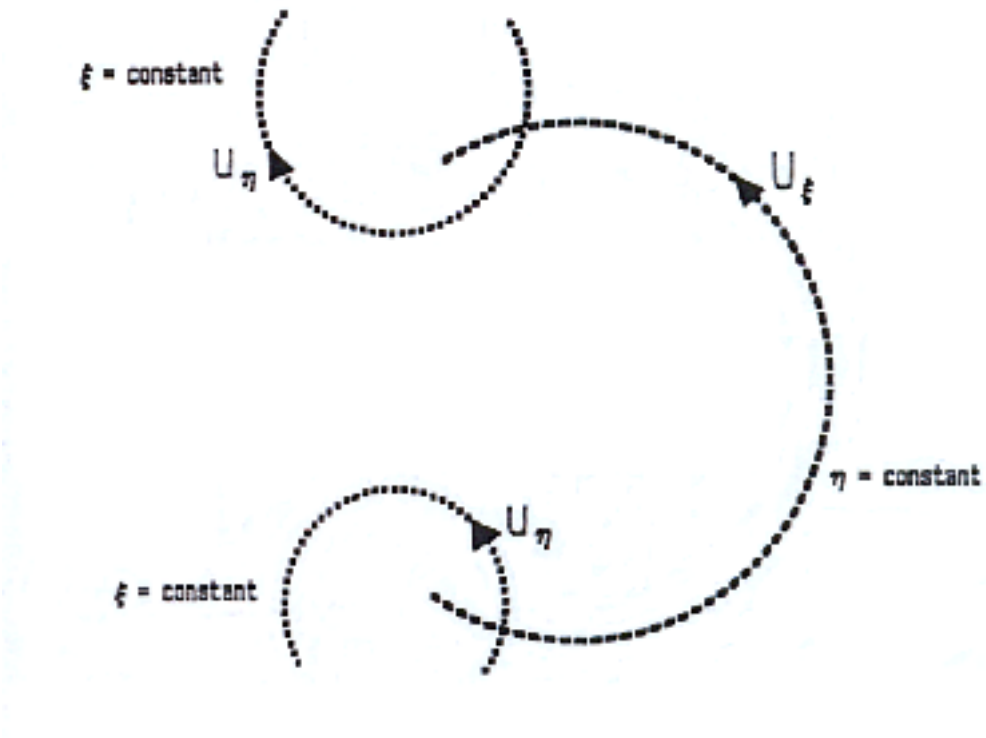

Figure 5.3.4: The direction of the non-dimensional components of the velocity $u_\xi$and u_η.

$$u_\xi = -h\frac{\partial \Psi}{\partial \xi}, \quad u_\eta = h\frac{\partial \Psi}{\partial \eta} \tag{5.3.2}$$

where in this situation h is in its non-dimensional form, namely $(\cosh(\xi) - \cos(\eta))/\sinh(\xi_1)$. In the rest of this section, when h occurs it will be assumed to be in its above non-dimensional form, as will A which adopts the form $\sinh(\xi_1)$.

Eliminating the pressure from the non-dimensional form of the two dimensional Navier-Stokes equation by operating with curl and introducing the stream function Ψ, results in the differential equation

$$\nabla^4 \Psi = \nabla^2(\nabla^2 \Psi) = 0, \tag{5.3.3}$$

where

$$\nabla^2\Psi = \nabla.(\nabla\Psi) = h^2\left(\frac{\partial^2}{\partial\xi^2} + \frac{\partial^2}{\partial\eta^2}\right) \tag{5.3.4}$$

However, on changing the dependent variable from Ψ to $h\Psi$, expression (5.3.4) becomes

$$\begin{aligned}\nabla^2\Psi = [h(\frac{\partial^2}{\partial\xi^2} + \frac{\partial^2}{\partial\eta^2}) - 2sinh(\xi)\frac{\partial}{\partial\xi} - 2sin(\eta)\frac{\partial}{\partial\eta} \\ + cosh(\xi) + cos(\eta)](h\Psi),\end{aligned} \tag{5.3.5}$$

which on repeating the operation, plus a small amount of simplification, results in equation (5.3.3) becoming a linear partial differential equation with constant coefficients, namely

$$\left[\frac{\partial^4}{\partial\xi^4} + 2\frac{\partial^4}{\partial\xi^2\partial\eta^2} + \frac{\partial^4}{\partial\eta^4} - 2\frac{\partial^2}{\partial\xi^2} + 2\frac{\partial^2}{\partial\eta^2} + 1\right](h\Psi) = 0. \tag{5.3.6}$$

Seeking a solution of equation (5.3.6) of the form $h\Psi = f(\xi)\cos(n\eta)$ or $f(\xi)\sin(n\eta)$, the periodicity, necessary from the geometry of the problem, gives rise to the ordinary differential equation

$$\left[\frac{d^4}{d\xi^4} - 2(n^2+1)\frac{d^2}{d\xi^2} + n^4 - 2n^2 + 1\right]f(\xi) = 0. \tag{5.3.7}$$

The solution of equation (5.3.7) has the form

$$\begin{aligned}f(\xi) = A_n\cosh((n+1)\xi) + B_n\cosh((n-1)\xi) + C_n\sinh((n+1)\xi) \\ + D_n\sinh((n-1)\xi), \quad \text{for} \quad n \geq 2,\end{aligned} \tag{5.3.8}$$

$$f(\xi) = A_1\cosh(2\xi) + B_1 + C_1\sinh(2\xi) + D_1\xi, \quad \text{for} \quad n = 1, \tag{5.3.9}$$

and

$$f(\xi) = A_0\cosh(\xi) + B_0\xi\cosh(\xi) + C_0\sinh(\xi) + D_0\xi\sinh(\xi), \quad \text{for} \quad n = 0, \tag{5.3.10}$$

where A_i, B_i, C_i and $D_i$for $i = 0, 1, \ldots\ldots$ are the constants of integration.

Due to the general solution of equation (5.3.6) being

$$h\Psi = \exp(\pm\xi) f(\xi \pm i\eta) \tag{5.3.11}$$

the terms $\xi\sin(\eta), \xi\cos(\eta), \xi\cosh(\xi)$ and $\xi\sinh(\eta)$ in expressions (5.3.8), (5.3.9) and (5.3.10) result in the addition solutions

$$h\Psi = \eta, \tag{5.3.12}$$

where E, F, G and H are unknown constants. However, these solutions can be rejected due to the requirement of single-valuedness of the solution. In the present problem the stream function is an even function in η, as is the function h, and therefore all the terms involving $\sin(n\eta)$ may be omitted. Thus $h\Psi$ assumes the form

$$\begin{aligned} h\Psi = {} & A_0 cosh(\xi) + B_0\xi cosh(\xi) + C_0 sinh(\xi) + D_0\xi sinh(\xi) \\ & + [A_1 cosh(2\xi) + B_1 + C_1 sinh(2\xi) + D_1\xi] cos(\eta) \\ & + \sum_{n=2}^{\infty} [A_n cosh((n+1)\xi) + B_n\xi cosh((n-1)\xi) \\ & + C_n sinh((n+1)\xi) + D_n\xi sinh((n-1)\xi)] cos(n\eta). \end{aligned} \tag{5.3.13}$$

At this point it should be observed that Jeffery (1922) noted that the above series may converge only for positive or for negative values of ξ. That is to say that different expansions of $h\Psi$ on either side of $\xi = 0$ may be required. However, as will be discussed later he was able to justify his choice of $h\Psi$ for the domain $\xi > 0$ and to establish a solution for the whole fluid space using a symmetry argument. From the component form of the Navier Stokes equation it is readily seen that both the pressure p and the expression $\nabla^2\Psi$ satisfy the Cauchy-Riemann equations, which means that the function $p+i\nabla^2\Psi$ is a regular function of $z = x + iy$, so x and y can only occur in the combination $x + iy$. However, equation (2) clearly shows that $p + i\nabla^2\Psi$ must also be a regular function of $\zeta = \xi + i\eta$. Evaluating $\nabla^2\Psi$ by substituting expression (18) into the right hand side of equation (10) results in a term $(B_0 + D_1)\xi$, which means that the pressure p must contain a term $-(B_0 + D_1)\eta$. The inclusion of such a term would violate the condition regarding the single-valuedness of the velocity and the pressure, hence it is necessary for the constraint

$$(B_0 + D_1) = 0, \tag{5.3.14}$$

to be applied.

5.4 Boundary Bonditions

Jeffery showed that a solution of the biharmonic equation $\nabla^4\Psi = 0$ in the region $-\xi_2 < \xi < \xi_1, -\pi < \eta < \pi$ which satisfies the no slip condition on $\xi = -\xi_2$and on $\xi = \xi_1$is given by

$$\begin{aligned} h\Psi = {} & A_0\cosh(\xi) + B_0\xi\cosh(\xi) + C_0\sinh(\xi) + D_0\xi\sinh(\xi) \\ & + (A_1\cosh(2\xi) + B_1 + C_1\sinh(2\xi) + D_1\xi)\cos(\eta). \end{aligned} \tag{5.4.1}$$

The zero normal velocity boundary conditions are that on

$$\xi = -\xi_2, \quad \Psi = -\Psi_2; \tag{5.4.2}$$

whilst on

$$\xi = \xi_1, \quad \Psi = \Psi_1. \tag{5.4.3}$$

This choice of $\Psi = -\Psi_2$on $\xi = -\xi_2$has been taken to coincide with that taken by Smith (1991), who followed Jeffery (1922), since the latter had employed that on $\xi = 0$ the value of Ψ was zero, so making his value of $\Psi = -\Psi_1$on $\xi = -\xi_2$by the symmetry of the particular case studied.

The components of the non-dimensional fluid velocity in terms of the non-dimensional stream function in expression (5.3.2) can be rewritten in terms of the dependent variable $h\Psi$ as follows

$$u_\xi = -h\frac{\partial\Psi}{\partial\eta} = -[\frac{\partial(h\Psi)}{\partial\eta} - \frac{\Psi}{A}\sin(\eta)], \tag{5.4.4}$$

$$u_\eta = h\frac{\partial\Psi}{\partial\xi} = -[\frac{\partial(h\Psi)}{\partial\xi} - \frac{\Psi}{A}\sinh(\xi)], \tag{5.4.5}$$

where $u_\xi$and $u_\eta$are in the directions of ξ and η increasing. This means that on $\xi = \xi_1, u_\eta = -1$, and by substituting $A = \sinh(\xi_1)$, one obtains

$$\frac{\partial}{\partial \xi}(h\Psi) = \Psi_1 - 1. \tag{5.4.6}$$

An alternative way of expressing this equation is

$$\frac{\partial \Psi}{\partial \xi} = -1/h = -\sinh(\xi_1)/[\cosh(\xi_!) - \cos(\eta)], \tag{5.4.7}$$

which agrees, but for the sign, with the condition employed by Dorrepaal *et al.* (1984). The sign difference arising due to the upper cylinder rotating in the clockwise direction in the work of Dorrepaal *et al.* (1984), but in the anti-clockwise in that of Smith (1992) and of Jeffery (1922). Also

$$\begin{aligned} \text{on } \xi = -\xi_2,\ u_\eta &= -(\omega_2/\omega_1)\sinh(\xi_1) cosech(\xi_2) = -\beta\omega_2/\omega_1, \\ &= -R_2\omega_2/(R_1\omega_1), \end{aligned} \tag{5.4.8}$$

which produces

$$\frac{\partial}{\partial \xi}(h\Psi) = \Psi_2 sinh(\xi_2)/[sinh(\xi_1) - (\omega_2/\omega_1)sinh()\xi_1 cosech(\xi_2)] \tag{5.4.9}$$

$$= \psi_2/\beta - \beta\omega_2/\omega_1. \tag{5.4.10}$$

Again this expression may be written as

$$\frac{\partial \Psi}{\partial \xi} = -\beta\omega_2/(h\omega_1), \tag{5.4.11}$$

$$= -\sinh(\xi_1) cosech(\xi_2)\omega_2/[\omega_1(cosh(\xi_2) - cos(\eta))] \tag{5.4.12}$$

which with $\xi_1 = \xi_2$, that is two identical cylinders, and $\omega_1 = \omega_2$, reduces to that adopted by Dorrepaal *et al.* (1984), but for the sign. With $\Psi_1 = \Psi_2, \omega_1 = \omega_2$and $\xi_1 = \xi_2$, then equations (5.4.6) and (5.4.9) are identical, and agree with the conditions, apart from the difference of sign, applied by Dorrepaal *et al.* (1984). The angular velocities of the two cylinders in the above have been taken as

$$\underline{\omega} = \omega_1 \underline{k} \ \text{ on } \ \xi = \xi_1 \ \text{ and } \ \underline{\omega} = -\omega_2 \underline{k} \ \text{ on } \ \xi = -\xi_2. \tag{5.4.13}$$

5.5 Linear Equation of the Boundary Conditions

The constant values of the stream function on $\xi = \xi_1$and $\xi = -\xi_2$are $\Psi_1$and $-\Psi_2$, respectively, with $\Psi_1 - (-\Psi_2) = \Psi_1 + \Psi_2$, the difference between the stream function on the two cylinders being an independent quantity. Hence, the nine unknowns are $\Psi_1 + \Psi_2, A_j, B_j, C_j, D_j$, where $j = 0$ and 1, whilst the nine equations necessary to determine these values are the constraint equation (5.3.14), plus the eight equations arising from substituting the stream function from expression (5.4.1) into the boundary conditions (5.4.2), (5.4.3), (5.4.6) and (5.4.9) and equating the coefficient of the $\cos(\eta)$ term and that of the constant term both to zero, so producing

$$\begin{aligned} &A_0\cosh(\xi_1) + B_0\xi_1\cosh(\xi_1) + C_0\sinh(\xi_1) + D_0\xi_1\sinh(\xi_1) \\ &= \Psi_1\cosh(\xi_1)/(\sinh(\xi_1)). \end{aligned} \tag{5.5.1}$$

$$A_1\cosh(2\xi_1) + B_1 + C_1\sinh(2\xi_1) + D_1\xi_1 = -\Psi_1/(\sinh(\xi_1)), \tag{5.5.2}$$

$$\begin{aligned} &A_0\sinh(\xi_1) + B_0\xi_1\sinh(\xi_1) + C_0\cosh(\xi_1) \\ &+ D_0(\xi_1\cosh(\xi_1) + \sinh(\xi_1) = \Psi_1 - 1. \end{aligned} \tag{5.5.3}$$

$$2A_1\sinh(2\xi_1) + 2C_1\cosh(2\xi_1) + D_1 = 0, \tag{5.5.4}$$

$$\begin{aligned} &A_0\cosh(\xi_2) - B_0\xi_2\cosh(\xi_2) - C_0\sinh(\xi_2) + D_0\xi_2\sinh(\xi_2) \\ &= -\Psi_2\cosh(\xi_2)/(\sinh(\xi_1)). \end{aligned} \tag{5.5.5}$$

$$A_1\cosh(2\xi_2) + B_1 - C_1\sinh(2\xi_2) - D_1\xi_2) - D_1\xi_2 = \Psi_2/(\sinh(\xi_1)), \tag{5.5.6}$$

$$\begin{aligned} A_0\cosh(\xi_2) - B_0\xi_2\cosh(\xi_2) - C_0\sinh(\xi_2) + D_0\xi_2\sinh(\xi_2) \\ = -\Psi_2\cosh(\xi_2)/(\sinh(\xi_1)). \end{aligned} \tag{5.5.7}$$

$$-2A_1\sinh(2\xi_2) + 2C_1\cosh(2\xi_2) + D_1 = 0. \tag{5.5.8}$$

Although the non-dimensionalisation in the above work has followed that of Dorrepaal *et al.* (1984), it is possible to adopt the procedure chosen by both

Jeffrey (1922) and Smith (1991). There the length non-dimensionalisation was undertaken with respect to the parameter A, where $2A$ represents the distance between the limiting points of the two cylinders in the bipolar coordinate system, instead of with respect to the radius $R_1$of the upper cylinder. With such a non-dimensionalisation the centers of the upper and lower cylinders are at $(0, \coth(\xi_1))$ and $(0, -\coth(\xi_2))$ respectively, whilst the radii are $\text{cosech}(\xi_1)$ and $\text{cosech}(\xi_2)$. In addition the non-dimensional form of the function h will be $(\cosh(\xi) - \cos(\eta))$. Application of the form for $h\Psi$ expressed in equation (5.4.1) into the boundary conditions on the two cylinders produces, in this non-dimensional system, a modified form of the equations (5.5.1) to (5.5.8), namely

$$A_0 \cosh(\xi_1) + B_0\xi_1 \cosh(\xi_1) + C_0 \sinh(\xi_1) + D_0\xi_1 \sinh(\xi_1) = \Psi_1 \cosh(\xi_1). \tag{5.5.9}$$

$$A_1 \cosh(2\xi_1) + B_1 + C_1 \sinh(2\xi_1) + D_1\xi_1 = -\Psi_1, \tag{5.5.10}$$

$$\begin{aligned} &A_0 \sinh(\xi_1) + B_0(\xi_1 \sinh(\xi_1) + \cosh(\xi_1)) + C_0 \cosh(\xi_1) \\ &+ D_0(\xi_1 \cosh(\xi_1) + \sinh(\xi_1)) = \Psi_1 \sinh(\xi_1) - \mathit{cosech}(\xi_1), \end{aligned} \tag{5.5.11}$$

$$2A_1 \sinh(2\xi_1) + 2C_1 \cosh(2\xi_1) + D_1 = 0, \tag{5.5.12}$$

$$A_0 \cosh(\xi_2) - B_0\xi_2 \cosh(\xi_2) - C_0 \sinh(\xi_2) + D_0\xi_2 \sinh(\xi_2) = -\Psi_2 \cosh(\xi_2). \tag{5.5.13}$$

$$A_1 \cosh(2\xi_2) + B_1 - C_1 \sinh(2\xi_2) - D_1\xi_2) - D_1\xi_2 = \Psi_2 \tag{5.5.14}$$

$$\begin{aligned} &A_0 \sinh(\xi_2) + B_0(\xi_2 \sinh(\xi_2) + \cosh(\xi_2)) + C_0 \cosh(\xi_2) \\ &+ D_0(\xi_2 \cosh(\xi_2) + \sinh(\xi_2)) = \Psi_2 \sinh(\xi_2) - (\frac{\omega_2}{\omega_1})\mathit{cosech}(\xi_2), \end{aligned} \tag{5.5.15}$$

$$-2A_1 \sinh(2\xi_2) + 2C_1 \cosh(2\xi_2) + D_1 = 0. \tag{5.5.16}$$

If the stream function and the coefficients $A_j, B_j, C_j$and D_j, where $j = 0$ and 1, in equations (5.5.9) to (5.5.16) are redefined as $\sinh^2(\xi_1)$ times the stream function value and $\sinh(\xi_1)$ times the coefficients, respectively, then equations

(5.5.1) to ((5.5.8) are identical with the equations (5.5.9) to (5.5.16). This means that the coefficients obtained by solving the non-dimensional set of equations in Smith (1991), namely equations (5.5.9) to (5.5.16), can be seen on multiplication by $\sinh(\xi_1)$ to give identical values to those obtained by solving equations (5.5.1) to (5.5.8). Likewise, multiplication by $\sinh^2(\xi_1)$ of the streamfunction in Smith (1991) produces the form obtained by Dorrepaal *et al.* (1984).

Returning to equations (5.5.1) to (5.5.8), then the work of Dorrepaal *et al.* (1984), with the rotation of both cylinders reversed in order to agree with the directions chosen by Jeffery (1922) and by Smith (1991), shows that there is an analytical solution when $\xi_1 = \xi_2$and $\omega_1 = \omega_2$, namely,

$$\begin{aligned}
&[\frac{\cosh(\xi) - \cos(\eta)}{\sinh(\xi)}]\Psi = h\Psi \\
&= A_0 \cosh(\xi) + B_0\xi \cosh(\xi) + C_0 \sinh(\xi) + D_0\xi \sinh(\xi) \\
&+ (A_1 \cosh(2\xi) + B_1 + C_1 \sinh(2\xi) + D_1\xi)\cos(\eta),
\end{aligned} \tag{5.5.17}$$

where

$$\begin{aligned}
&A_0 = A_1 = B_1 = D_0 = 0, B_0 = -D_1 = -(\coth(2\xi_1))/\sinh(\xi_1), \\
&C_0 = (\coth(\xi_1))/(2\sinh(\xi_1)), C_1 = -(cosech(2\xi_1))/(2\sinh(\xi_1)),
\end{aligned} \tag{5.5.18}$$

which agree, on division by $\sinh(\xi_1)$ with the coefficients presented in Jeffery (1922). These results also highlight the fact that the stream functions in the work in Jeffery (1922), or in Smith (1991), and in Dorrepaal *et al.* (1984) differ by a factor $\sinh^2(\xi_1)$.

In addition to the solutions by Jeffery (1922) and by Dorrepaal *et al.* (1984) for the case of cylinders of equal radii rotating with equal speeds but in opposite senses, Smith (1991) has solved equations (5.5.9) to (5.5.17) for the most general situation, namely different radii and different angular velocities. Unfortunately, the expressions for the various coefficients in the function $h\Psi$ are rather lengthy and as a result only those combinations necessary for the evaluations of the form of the stream function at large distances from the cylinders and the torques on the two cylinders are presented. Rather than produce algebraic expressions for the coefficients, the two sets of equations (5.5.1) to (5.5.8) and equations (5.5.9) to (5.5.16) have been solved numerically for various cylinder radii and angular velocities, and the values for the combinations of the constants, presented in Smith (1991), checked. Streamlines have been drawn for some of these radii and

angular velocities and are shown in figures 5.5.5 and 5.5.6. These cases included the special situation when the value of $(A_0 + A_1 + B_1)$ is zero, since, as will be seen later, the solution for this special value should at large distances from the cylinders correspond to a uniform stream rather than solid body rotation as occurs for all non zero values of this parameter. Corresponding to each streamline pattern, the vorticity distribution, resulting from the substitution of the expression for $h\Psi$, given by equation (5.4.1), into equation (5.3.5), producing the non-dimensional vorticity

$$\begin{aligned}\omega = \nabla^2\psi = &(\cosh(\xi) - \cos(\eta))\,(p_2 + (q_2 - q_0)\cos(\eta)) \\ &- 2\sinh(\xi)(p_1 + q_1\cos(\eta)) + q_0\sin^2(\eta) \\ &+ (\cosh(\xi) + \cos(\eta))(p_0 + q_0\cos(\eta)),\end{aligned} \tag{5.5.19}$$

where

$$\left.\begin{aligned}
&p_0 = A_0 cosh(\xi) + B_0\xi cosh(\xi) + C_0 sinh(\xi) + D_0\xi sinh(\xi), \\
&q_0 = A_1 cosh(2\xi) + B_1 + C_1 sinh(2\xi) + D_1\xi, \\
&p_1 = A_0 sinh(\xi) + B_0(cosh(\xi) + \xi sinh(\xi)) + C_0 cosh(\xi) \\
&+D_0(sinh(\xi) + \xi cosh(\xi)), \\
&q_1 = 2A_1 sinh(2\xi) + 2C_1 cosh(2\xi) + D_1, \\
&p_2 = A_0 cosh(\xi) + B_0(2sinh(\xi) + \xi cosh(\xi)) + C_0 sinh(\xi) \\
&+D_0(2cosh(\xi) + \xi sinh(\xi), \\
&q_2 = 4A_1 cosh(2\xi) + 4C_1 sinh(2\xi).
\end{aligned}\right\} \tag{5.5.20}$$

has been presented in Figures 5.5.6.

5.6 Asymptotic Form of the Stream Function

It seems that now is the appropriate time to investigate the behavior of the streamfunction at large distances from the cylinder, as documented by Smith (1991). It has already been mentioned that the condition of $x, y \to \infty$ requires $\xi, \eta \to 0$, which results in

$$\begin{aligned}&(\xi^2 + \eta^2)\Psi/\sinh(\xi_1) \simeq 2(A_0 + A_1 + B_1) + 2(C_0 + 2C_1)\xi \\ &+ (A_0 + 2D_0 + 4A_1)\xi^2/2 - (A_1 + B_1)\eta^2/2 + O(((\xi^2 + \eta^2)^{3/2}),\end{aligned} \tag{5.6.1}$$

where

$$\Delta(A_0+A_1+B_1) = (\xi_1+\xi_2)(\omega_1 sinh^2(\xi_2) - \omega_1 \sinh^2(\xi_1))\sinh(\xi_1), \tag{5.6.2}$$

$$\begin{aligned}\Delta(C_0+2C_1) &= \omega_1 sinh(\xi_1)sinh(\xi_2)[(\xi_1+\xi_2)sinh(\xi_1)cosech(\xi_1+\xi_2)\\ &+ sinh(\xi_2) + (\xi_1+\xi_2)cosh(\xi_2) - \xi_2 sinh(\xi_1+\xi_2)cosech(\xi_1)]\\ &+ \omega_2 sinh^2(\xi_1)[(\xi_1+\xi_2)sinh(\xi_2)cosech(\xi_1+\xi_2) + sinh(\xi_1)\\ &+ (\xi_1+\xi_2)cosech(\xi_1) - \xi_1 sinh(\xi_1+\xi_2)cosech(\xi_2)]\end{aligned} \tag{5.6.3}$$

with

$$\begin{aligned}\Delta &= (\xi_1+\xi_2)\{sinh^2(\xi_1) + sinh^2(\xi_2)\}\\ &+ 2sinh(\xi_1)sinh(\xi_2)sinh(\xi_1+\xi_2).\end{aligned} \tag{5.6.4}$$

As at small values of ξ and η, the non-dimensional values x and y take the form

$$x \simeq 2\eta \sinh(\xi_1)/(\xi^2+\eta^2), \tag{5.6.5}$$

and

$$y \simeq 2\xi \sinh(\xi_1)/(\xi^2+\eta^2), \tag{5.6.6}$$

it follows that

$$\begin{aligned}\Psi &\simeq (A_0+A_1+B_1)(x^2+y^2)/(2\sinh(\xi_1)) + (C_0+2C_1)y\\ &+ \sinh(\xi_1)\left\{-(A_0+2D_0+5A_1+B_1)cos(2\vartheta)\right\}/2\\ &+ \sinh(\xi_1)\left\{(A_0+2D_0+3A_1-B_1)\right\}/2\end{aligned} \tag{5.6.7}$$

as x and $y \to \infty$. Expression (5.6.7) can easily be changed to its form presented in Smith (1992). However, care must be taken to apply not only the modification necessary between the stream functions and the coefficients A_0, etc. in the two different non-dimensionalised systems but also to note that x and y are non-dimensional. The non-dimensionalisation being with respect to R_1in the present work, and in that by Dorrepaal *et al.* (1984), whereas in Smith (1991) it is with respect to A, where $A = R_1 \sinh(\xi_1)$. The $O(1)$ term in the asymptotic series of the stream function at large distances from the cylinder was not presented by Smith (1991), and under normal circumstances would be unnecessary since

it neither conveys the strength of the solid body rotation, if present, nor the magnitude of the uniform stream. However, in later work it will provide a useful check of the accuracy of the results since then the stream function is considered as the sum of its value at infinity plus a perturbation. The perturbation term being finite in the vicinity of the cylinders but tending to zero at infinity. A non-zero value of the leading order term in expression (5.6.7), $(A_0 + A_1 + B_1)r^2$, clearly indicates that, based on the Stokes equation, there is solid body rotation far from the cylinders. This fact appeared to have been overlooked by all workers on this problem prior to Smith (1992) and probably arose due to the physical situations being studied being restricted to cylinders of equal radii, with angular velocities of equal magnitude but opposite senses. If one views equation (5.6.2), excluding the situation that either $\xi_1$or $\xi_2$are zero, which means that neither of the cylinders is a plane and hence in reality possess zero angular velocity, then it is only possible to have zero rotation at infinity when

$$\omega_1 \sinh^2(\xi_2) = \omega_2 \sinh^2(\xi_1). \tag{5.6.8}$$

Multiplication of equation (5.6.8) by the dimensional A^2, namely $R_1^2 \sinh^2(\xi_1)$, results in the more physically recognizable relationship, namely

$$\omega_1 R_1^2 = \omega_2 R_2^2. \tag{5.6.9}$$

This requires that the angular momenta of the two cylinders must exactly balance, and in such a situation there is just a uniform stream at infinity in the direction perpendicular to the line of centers of the cylinders. The actual direction corresponding to that of the direction the surfaces of the cylinders when they meet the line connecting their centers. Hence, in the present case when $\omega_1$and $\omega_2$in expressions (5.4.13) are both positive the stream will be directed parallel to the x-axis and in the direction of x increasing. Since Dorrepaal *et al.* (1984) reversed both these directions of rotation, it follows that their stream should have been directed in the direction of x decreasing. However, the opposite direction appears to have been their choice.

5.7 Validation of the Expansions for $h\Psi$

Before embarking into a detailed discussion regarding the forces and the torques acting on the cylinders it seems an appropriate place to refer back to the point mentioned earlier, and discussed by Jeffery (1922), relating to whether different expansions are required in the separate domains $\xi > 0$ and $\xi < 0$ when one of the two cylinders fails to enclose the other. However, Jeffery (1922) rather than pursue the different expansions on opposite sides of the plane $\xi = 0$ opted for cylinders of equal radii, rotating with equal speeds but in opposite senses. This meant that by using a symmetry argument, together with the stream function being a constant and the shearing stress vanishing on the plane $\xi = 0$, it was possible to obtain a solution in the whole fluid domain from an expansion for the region $\xi > 0$ only. Jeffery (1922) found that the most general form of expression (5.3.13) which satisfied the boundary conditions on the upper cylinder and the boundary conditions on the plate $\xi = 0$ was that presented in expression (5.4.1). The question as to whether the expansion (5.3.13) is valid on the plane $\xi = 0$, in other words "Is it absolutely and uniformly convergent", was simply assumed for the matter of obtaining the solution, with a full physical argument presented as to its validity. Jeffery (1922) concluded that since it was possible to solve uniquely the problem of a cylinder rotating in a viscous fluid contained within a non-concentric vessel whose inner surface was smooth and so unable to exert any tangential stress on the fluid, then by allowing the radius of the outer vessel to then become infinitely large that solution should correspond to his result, found with the help of symmetry, in the upper half plane. As the flow in the contained vessel was **unique** and **did** tend at large distances from the rotating cylinder to that already found by using expansion (5.4.1) for the region $\xi > 0$, then the use of the more general form of expansion (5.3.13), namely expansion (5.4.1), on the boundary $\xi = 0$, must, regarding its convergence, be valid. Both Dorrepaal *et al.* (1984) and Smith (1991) assumed that an expansion of the form in expression (5.4.1), rather than that in expression (5.3.13), was acceptable and that there was no need for different expansions in the regions $\xi > 0$ and $\xi < 0$. However, it could be argued that Dorrepaal *et al.* (1984) had the stronger grounds for this assumption, based upon the fact that Jeffery (1922) had already found such a solution for the region $\xi \geq 0$ and could extend, by symmetry, that solution to the region $\xi < 0$. For Smith (1991), this argument was no

longer possible due to the complete lack of symmetry in the physical situations being investigated. However, Jeffery (1920), in a paper entitled, "Plane stress and plane strain in bipolar coordinates", outlined the restrictions under which a single expansion like expression (5.3.13), and hence like expression (5.4.1), might be valid throughout the whole region. If the plate was such that it contained two circular holes, neither of which enclosed the other, then it was possible to establish that provided the forces and torque acting over the two circular boundaries were in equilibrium when considered together, then a single expansion would suffice. However, if situations were studied where this was not so, then hX, where X represents the stress function, requires a term of the form

$$hX = (\cosh(\xi) - \cos(\eta)) \ln(\cosh(\xi) - \cos(\eta)), \tag{5.7.1}$$

since this allows the most general force and torque conditions to be applied at the circular boundaries. When the function (5.7.1) is expanded by Fourier Series, like expression (5.3.13), then different forms are needed on opposite sides of the plane $\xi = 0$ and hence the requirement of different expansions on the two sides of $\xi = 0$. The expansions must diverge as one tends to infinity as it will be necessary for forces and torques to be applied there in order to maintain the overall equilibrium of the plate. This appears to imply that provided one looks for a solution to the flow outside two rotating cylinders, neither of which encloses the other, by means of a single expansion valid throughout the whole fluid domain then the combination of the forces and the torques on the two cylinders must produce a system in equilibrium when the two cylinders are considered together. In Smith (1991) the expressions for the torques on the two cylinders were

$$T_1 = -4\pi\mu\omega_1 R_1^2 (B_0 \sinh(\xi_1) + D_0 \cosh(\xi_1)), \tag{5.7.2}$$

and

$$T_2 = 4\pi\mu\omega_1 R_1^2 (B_0 \sinh(\xi_1) - D_0 \coth(\xi_2) \sinh(\xi_1)), \tag{5.7.3}$$

on the upper and lower cylinders, respectively, where the constants $B_0$and D_0have been modified to the form related to the non-dimensionalisation of the problem with respect to R_1, i.e. here they correspond to $\sinh(\xi_1)$ times the

value used by Smith (1991). The expression (5.7.3) differs from that given by Smith (1991) in the sign of the $D_0 \coth(\xi_2) \sinh(\xi_1)$ term, with his error probably resulting from $\xi_2$being assumed negative when in reality it had earlier been set positive, with the negative value of ξ on the lower cylinder achieved by considering $\xi = -\xi_2$there. This correction of sign will be validated later, both in detail and in an argument based upon the conditions necessary to maintain the equilibrium of the forces and the torques on the two cylinders. In fact the expressions (5.7.2) and (5.7.3) in Smith (1991) corrected those in Jeffery (1922) where the dimensions were in error with the omission of $aR_1 \sinh(\xi_1)$ factor. In the case of cylinders of equal radii, with equal magnitudes but opposite senses of rotational velocities, then the values of the coefficients A_0, etc., are those expressed in equation (5.5.18), and their substitution into expressions (5.7.2) and (5.7.3) produces

$$T_1 = 4\pi\mu\omega_1 R_1^2 \coth(2\xi_1) = -T_2. \tag{5.7.4}$$

The expressions for the torques are identical to the values obtained by Dorrepaal *et al.* (1984), apart from the previously mentioned sign modification to account for the opposite senses of rotation. This further supports the omission of the factor $R_1 \sinh(\xi_1)$ from the values of $T_1$and T_2in Jeffery (1922). It should be stressed that since in the above situation $T_1$and T_2on the two cylinders are equal in magnitude but opposite in sign, then in order to maintain the combined equilibrium of the two cylinders, no force in the x direction can be present on either cylinder, a fact which again will be confirmed later. In addition, for all the situations where the total angular momenta of the two cylinders balance, which is that the condition in expression (5.6.9) is applied, then the coefficient $D_0$is always zero. This results in the combination of $T_1$from expression (5.7.2) and $T_2$from expression (5.7.3) being zero. Hence to maintain an overall equilibrium state on the combined system then not only must the forces on the two cylinder be equal and opposite, but each of the components in the x direction must be zero.

In the situation when the condition given by expression (5.6.9) is violated, then in order to maintain equilibrium of the combined system non-zero forces must be present on the cylinders. Assuming the forces in the (x, y) directions on the upper and lower cylinders are (F_1, L_1) and (F_2, L_2) it is necessary for

$$F_1 = -F_2 \quad \text{and} \quad L_1 = -L_2, \tag{5.7.5}$$

and the total combined torque on the two cylinders to be zero, i.e.

$$T_1 + T_2 - F_1(R_1 \cosh(\xi_1) + R_1 \sinh(\xi_1) \coth(\xi_2)) = 0. \tag{5.7.6}$$

On substituting for $T_1$and $T_2$from expressions (5.7.3) and (5.7.4) into equation (5.7.6) one obtains

$$F_1 = -4\pi\mu\omega_1 R_1 D_0. \tag{5.7.7}$$

This result will be confirmed in detail later but it can, to some extent, be predicted from Jeffery (1920). In his work it was established that when the forces and torques on the two cylindrical holes cut in the plate are in a combined equilibrium state then the torque on the upper cylinder about its limiting point can be split into two parts, namely $2\pi R_1^2 \sinh(\xi_1) G*$ and $-2\pi R_1^2 \sinh(\xi_1) H*$, whilst that on the lower cylinder it divides into $-2\pi R_1^2 \sinh(\xi_1) G*$ and $-2\pi R_1^2 \sinh(\xi_1) H*$. This means that about their limiting points the cylinders have a pair of equal and opposite torques in the form of $2\pi R_1^2 \sinh(\xi_1) G*$, and a pair of equal torques, each of the same strength and direction, namely$-2\pi R_1^2 \sinh(\xi_1) H*$. In addition, the forces acting at the limiting points of the two cylinders are $(2\pi R_1 H*, 0)$ on the upper one and $(-2\pi R_1 H*, 0)$ on the lower one. As the distance between the limiting points is $2R_1 \sinh(\xi_1)$ it is relatively easy to see that the forces and torques on the combined system of the two cylindrical holes are in equilibrium. One would expect a similar type of structure to occur in the present problem, with a pair of torques of equal magnitude but in opposite senses, a pair of torques of equal magnitude and direction and a force system which balances with the pair of equal torques to produce a system in overall equilibrium. This alone would suggest the sign modification to one of the terms in the torque expression presented by Smith (1991). Even without any detailed analysis, since the terms in expressions (5.7.2) and (5.7.3) involving the constant B_0provide the equal and opposite torque terms, whilst those involving D_0provide the equal ones, both in magnitude and sense. In addition their combined effect provides an expression containing a factor $R_1(\cosh(\xi_1) + \coth(\xi_2) \sinh(\xi_1))$, which is the distance between the axes of the two cylinders. This leads one to expect the same structure

will occur here, as for the case of the circular holes within the plate, and that the coefficient of the above factor in the expression for the combined torques $(T_1 + T_2)$ will be the multiple of the force parallel to the x axis.

5.8 Forces and Torques on the Cylinders

As the forces and torques on the two cylinders are to play an important part in the numerical calculation a detailed analysis of them will now be undertaken. An appropriate place to commence is with a definition of the rates of strain, the stress and the vorticity. The rates of strain necessary to undertake the force and torque calculations are $e_{\xi\xi}$and $e_{\xi\eta}$, where

$$e_{\xi\xi} = h\frac{\partial(u_\xi)}{\partial\xi} - u_\eta\frac{\partial h}{\partial\eta}, \tag{5.8.1}$$

and

$$e_{\xi\eta} = \frac{1}{2}\{\frac{\partial(hu_\eta)}{\partial\xi} + \frac{\partial(hu_\xi)}{\partial\eta}\}, \tag{5.8.2}$$

and the required stress components are

$$\tau_{\xi\xi} = -p + 2\mu e_{\xi\xi} \quad \text{and} \quad \tau_{\xi\eta} = 2\mu e_{\xi\eta}, \tag{5.8.3}$$

in which $h, u_\xi$and $u_\eta$are taken in their dimensional form.

Substitution of expressions (5.8.1) and (5.8.2), together with the dimensional form of expressions (5.3.2), into the stress components in equations (5.8.3) produce, after some algebra and the use of the fact that

$$\frac{\partial^2 h}{\partial\xi\partial\eta} = 0 \tag{5.8.4}$$

and on the cylinders

$$\frac{\partial\Psi}{\partial\eta} = \frac{\partial^2\Psi}{\partial\eta^2} = 0, \tag{5.8.5}$$

$$\tau_{\xi\xi} = -p - 2\mu h \frac{\partial}{\partial \eta} \left\{ \frac{\partial (h\Psi)}{\partial \xi} \right\}, \tag{5.8.6}$$

and

$$\tau_{\xi\eta} = \mu \left\{ h \frac{\partial^2 (h\Psi)}{\partial \xi^2} - h\Psi \frac{\partial^2 (h)}{\partial \xi^2} \right\}, \tag{5.8.7}$$

in terms of the function h1l1 and its derivatives. Substitution of the dimensional form of (5.4.1) expression into equation (5.8.7) produces, after some algebra,

$$\begin{aligned} \tau_{\xi\eta} = \mu\omega_1 \{ & cosh(\xi)(B_0 sinh(\xi) + D_0 cosh(\xi)) \\ & - (A_1 cosh(2\xi) + C_1 sinh(2\xi)) - \{(B_0 sinh(\xi) + D_0 cosh(\xi)) \\ & - (2A_1 cosh(2\xi) + C_1 sinh(2\xi)) cosh(\xi) \} cos(\eta) \\ & - (A_1 cosh(2\xi) + C_1 sinh(2\xi)) cos(\eta) \} \end{aligned} \tag{5.8.8}$$

where $\xi = \xi_1$ or $\xi = -\xi_2$, according as to whether one is considering 1 2 the upper or the lower cylinder, respectively. Before looking at the expression (5.8.6) it is necessary to obtain a form for the pressure. This can be achieved by first considering the equations of motion

$$0 = -\frac{1}{h_1} \frac{\partial p}{\partial \xi} - \frac{\mu}{h_2} \frac{\partial \omega}{\partial \eta}, \tag{5.8.9}$$

$$0 = -\frac{1}{h_2} \frac{\partial p}{\partial \eta} - \frac{\mu}{h_1} \frac{\partial \omega}{\partial \xi}, \tag{5.8.10}$$

Using the dimensional form of the vorticity from equation (5.5.19), (5.8.10) followed by integration of the resulting equation (8.10), then the pressure can be expressed as

$$p = \mu\omega_1 (A^* sin(\eta) + B^* sin(2\eta)/2) \tag{5.8.11}$$

to within an arbitrary function of ξ, where

$$\begin{aligned} A^* = & (4A_1 sinh(2\xi) + 4C_1 cosh(2\xi) - 2D_1) cosh(\xi) \\ & - (4A_1 coSh(2\xi) + 4C_1 sinh(2\xi)) sinh(\xi) - 2(B_0 cosh(\xi) + D_0 Sinh(\xi)), \end{aligned} \tag{5.8.12}$$

and

$$B^* = -(4A_1 sinh(2\xi) + 4C_1 cosh(2\xi)). \tag{5.8.13}$$

It should be emphasised that in obtaining this result it is necessary to apply the condition in expression (5.3.14) to $\partial p/\partial \eta$ in order to maintain the single valuedness of the pressure. The arbitrary function of be ignored from the resulting can calculations since it will neither effect the forces or the torques on the cylinders. Substitution of expressions (5.4.1) and (5.8.11) into expression (5.8.6) for $\tau_{\xi\xi}$ produces

$$\begin{aligned}\tau_{\xi\xi} &= \mu\omega_1 \{4(A_1 cosh(2\xi) + C_1 sinh(2\xi))sinh(\xi) \\ &+ 2(B_0 cosh(\xi) + D_0 sinh(2\xi) + 4D_1 cosh(\xi)\ \}\ sin(\eta) - \mu\omega_1 D_1 sin(2\eta).\end{aligned} \tag{5.8.14}$$

Following Jeffery (1920). Fourier expansions are assumed for the normal and tangential stresses over the surface $\xi = \xi_1$, namely

$$R_1 sinh(\xi_1)\tau_{\xi\eta} = a_0 + \sum_{n=1}^{\infty}(a_n cos(n\eta) + b_n sin(n\eta)), \tag{5.8.15}$$

$$R_1 sinh(\xi_1)\tau_{\xi\xi} = C_0 + \sum_{n=1}^{\infty}(c_n cos(n\eta) + d_n sin(n\eta)), \tag{5.8.16}$$

where

$$\begin{aligned}a_0 &= \mu\omega_1 R_1 sinh(\xi_1)\{2cosh(\xi)(B_0 sinh(\xi) + D_0 cosh(\xi)) \\ &\quad - 2(A_1 cosh(2\xi) + C_1 sinh(2\xi))\}, \\ a_1 &= -\mu\omega_1 R_1 sinh(\xi_1)\{2(B_0 sinh(\xi) + D_0 cosh(\xi)) \\ &\quad - 4(A_1 cosh(2\xi) + C_1 sinh(2\xi))cosh(\xi)\}, \\ a_2 &= -\mu\omega_1 R_1 sinh(\xi_1)\{2(A_1 cosh(2\xi) + C_1 sinh(2\xi))\} \\ d_1 &= \mu\omega_1 R_1 sinh(\xi_1)\{4(A_1 cosh(2\xi) + C_1 sinh(2\xi))sinh(\xi) \\ &\quad + 2(B_0 cosh(\xi) + D_0 sinh(\xi)) + 4D_1 cosh(\xi)\}, \\ d_2 &= -\mu\omega_1 R_1 sinh(\xi_1)D_1,\end{aligned} \tag{5.8.17}$$

with b_1 , b_2 , c_0 , c_1 , c_2 and a_n , b_n , c_n and d_n zero for $n \geq 3$. If the 12012 n n n n surface stresses over the upper cylinder are equivalent to forces (F_1, L_1)

on its axis and a torque T_1 (these being the values necessary to maintain the motion of the cylinder), then

$$F_1 = \int_0^{2\pi} \left(\tau_{\xi\xi} \frac{\partial x}{\partial \xi} - \tau_{\xi\eta} \frac{\partial y}{\partial \xi} \right) d\eta, \tag{5.8.18}$$

$$L_1 = \int_0^{2\pi} \left(\tau_{\xi\xi} \frac{\partial y}{\partial \xi} + \tau_{\xi\eta} \frac{\partial x}{\partial \xi} \right) d\eta, \tag{5.8.19}$$

$$T_1 = -R_1^2 \int_0^{2\pi} (\tau_{\xi\eta} sinh(\xi_1)/(cosh(\xi) - cos(\eta)))\, d\eta, \tag{5.8.20}$$

The functions $\tau_{\xi\xi}$ and $\tau_{\xi\eta}$ have already been expanded in terms of Fourier Series, and the other expressions in equations (5.8.18), (5.8.19) and (5.8.20), namely $\partial x/\partial \xi$, $\partial y/\partial \xi$ and $sinh(\xi_1)/(cosh(\xi) - cos(\eta))$, may be similarly expanded on the may surface $\xi = \xi_1$, resulting in

$$\frac{\partial x}{\partial \xi} = -R_1 sinh(\xi_1) \frac{sinh(\xi) sin(\eta)}{(cosh(\xi) - cos(\eta))^2} \tag{5.8.21}$$

$$= -2R_1 sinh(\xi_1) \sum_{n=1}^{\infty} \{ n e^{-n\xi_1} sin(n\eta) \} \tag{5.8.22}$$

$$\frac{\partial y}{\partial \xi} = -R_1 sinh(\xi_1) \frac{(cosh(\xi) cos(\eta) - 1)}{(cosh(\xi) - cos(\eta))^2} \tag{5.8.23}$$

$$= -2R_1 sinh(\xi_1) \sum_{n=1}^{\infty} \{ n e^{-n\xi_1} cos(n\eta) sinh(\xi_1)/(cosh(\xi) - cos(\eta)) \} \tag{5.8.24}$$

$$= 1 + 2 \sum_{n=1}^{\infty} \{ n e^{-n\xi_1} cos(n\eta) \} \tag{5.8.25}$$

Substituting these, and the expansions for $T_{\xi\xi}$ and $T_{\xi\eta}$), into the expressions (5.8.18), (5.8.19) and (5.8.20) for F_1, L_1 and T_1, one obtains

$$F_1 = 2\pi \sum_{n=1}^{\infty} \{ (a_n - d_n) n e^{-n\xi_1} \} \tag{5.8.26}$$

$$L_1 = -2\pi \sum_{n=1}^{\infty} \{(b_n + c_n) n e^{-n\xi_1}\} \tag{5.8.27}$$

$$T_1 = -2\pi R_1 cosech(\xi_1) \sum_{n=1}^{\infty} \{a_n e^{-n\xi_1}\} \tag{5.8.28}$$

Due to the number of non-zero terms in these series being limited to at most three it is a relatively easy task to sum them, producing

$$F_1 = -4\pi\mu\omega_1 R_1 D_0, \tag{5.8.29}$$

$$L_1 = 0 \tag{5.8.30}$$

$$\begin{aligned} T_1 &= -4\pi\mu\omega_1 R_1^2 sinh(\xi_1)(B_0 + D_0 coth(\xi_1)), \\ &= -4\pi\mu\omega_1 R_1^2 (B_0 sinh(\xi_1) + D_0 cosh(\xi_1)). \end{aligned} \tag{5.8.31}$$

When investigating the forces and the torque necessary to maintain the motion of the lower cylinder it must be remember that unlike the upper cylinder where the forces are applied from $\xi \succ \xi_1$ (these forces balancing those exerted by the fluid from the region $\xi \prec \xi_1$, the forces must be applied from the region $\xi \prec -\xi_2$, these balancing those exerted from the fluid in the region $\xi \succ -\xi_2$. Also, there is not an overall sign change in going from T_1 to T_2 , unlike F_2 and L_2, when compared with F_1 and L_1. This arises due to the torque T_2 being about an axis in the lower half plane, whereas T_1 is about an axis in the upper half plane. However, rather than simply cause a sign change to expressions (5.8.26) and (5.8.27) care must be taken due to the fact that in the region $\xi \prec 0$ the direction cosine in expression (5.8.22) changes sign, unlike the direction cosine in expression (5.8.24). This is easily seen since $\partial x/\partial\xi$ is an odd function, whereas $\partial y/\partial\eta$ is an even function, with respect to the independent variable ξ. The result of this is that a sign change is required to the terms involving b_n and d_n when one moves from the $\xi = \xi_1$ surface to the surface $\xi = -\xi_2$. There is no change in the expression for the torque when one moves onto the lower cylinder resulting from the sign change in the direction cosines since T 2 contains neither the term $\partial x/\partial\xi$ nor $\partial y/\partial\eta$, but only the term $sinh(\xi)/(cosh(\xi) - cos(\eta))$ which is an even function in ξ. For the reasons mentioned earlier, the expansion for $h\Psi$

is assumed to be valid throughout the whole fluid domain and then the resulting forces and torque on the lower cylinder become

$$F_2 = -2\pi \sum_{n=1}^{\infty} \{(a_n + d_n) n e^{-n\xi_1}\} \tag{5.8.32}$$

$$L_2 = 2\pi \sum_{n=1}^{\infty} \{(-b_n + c_n) n e^{-n\xi_1}\} \tag{5.8.33}$$

$$T_2 = -2\pi R_1 cosech(\xi_1) \sum_{n=1}^{\infty} \{a_n e^{-n\xi_1}\} \tag{5.8.34}$$

The quantities a_1 and a_2 , in expressions (5.8.17) have the functions multiplying the parameters A_1 and D_0 even with respect to the independent variable ξ, whilst the functions multiplying the parameters B_0 and C_1 are odd functions. Similarly, the quantities d_l and d_2 have the functions multiplying the parameters A_1 and D_0 odd functions with respect to that independent variable, whilst the functions multiplying the parameters B_0 and C_1 are even functions. The consequence of this is that the summations in expression (5.8.32) are identical to those in the summation (5.8.26), resulting in

$$F_2 = 4\pi\mu\omega_1 R_1 D_0. \tag{5.8.35}$$

Obviously, since all the constants b_n and c_n are zero, the force L_2 in expression (5.8.33) will be

$$L = 0. \tag{5.8.36}$$

As the torque term contains only the a_n quantities, then the same cancellation of terms will occur in expression (5.8.34) as happened in expression (5.8.28). The fact that the functions multiplying the parameters which remained in expression (5.8.28), namely B_0 and D_0 are odd and even functions, respectively, with respect to the variable ξ, means that compared with expression (5.8.31) the sign of the quantity multiplying B_0 in expression (5.8.34) will be reversed, whilst that multiplying D_0 will remain unchanged. This results in expression (5.8.34) becoming

$$\begin{aligned} T_2 &= -4\pi\mu\omega_1 R_1^2 sinh(\xi_1)(-B_0 + D_0 coth(\xi_2)), \\ &= 4\pi\mu\omega_1 R_1^2 (B_0 sinh(\xi_1) - D_0 sinh(\xi_1) cosh(\xi_2)). \end{aligned} \tag{5.8.37}$$

This confirms the discussion following equation (5.7.3) regarding the requirement that T_2 in Smith (1991) needs a sign correction, together with the statement relating to the forces and the torques on the whole system, namely, that the two combined cylinders are in an equilibrium state with both zero total force and zero total torque. This fact has not hitherto been available since none of the earlier workers investigated the forces on the cylinders.

5.9 Alternative Expressions for the Forces

Later in this work it is proposed to introduce the Boundary Element Method (BEM) in order to determine a numerical solution of this in particular problem. technique the Validation of the situation of two rotating cylinders of different radii will enable it to be applied with confidence to other multiple body problems, for which no analytical solution is possible. In such problems the cross-sections of the bodies can differ, even within a particular problem, and the limitation to the number of such bodies present will be due only to the computing restriction relating to the number of required elements. As increasing the number of bodies present will have to be met by a corresponding increase in the number of elements in order to maintain the required accuracy. However, in order to apply the BEM it is necessary for the solution the that is being derived, in the present case streamfunction, to tend to zero at infinity. This can be achieved in the standard manner, see Tang (1990), by redefining the streamfunction to be its asymptotic value at infinity, plus a perturbation, with the BEM so modified so that it is applied to the perturbation part of the streamfunction. This means that those terms forming the non-zero part of the streamfunction at infinity will occur in values on the the governing with their equations cylindrical boundaries. Since it is known from the analytical 2 solution that terms of $O(r^2)$ may be present at infinity the non-zero streamfunction part must include all solutions of the biharmonic equation whose magnitude are greater or equal to 0(1). This requires the presence of r^2, $rsin(\vartheta)ln(r)$, $rcos(\vartheta)ln(r)$, $rsin(\vartheta)$, $rcos(\vartheta)$, $ln(r)$, $cos(2\vartheta)$, $sin(2\vartheta)$ and constant terms.

Perturbing the streamfunction about its infinity value will introduce into the equations to be solved the nine unknown coefficients of the above terms. A further unknown in the problem is the difference between the streamfunction values on the two cylinders, namely $\Psi_1 + \Psi_2$, so increasing the overall number of unknowns to ten. The same number of conditions are required to be found in order for the number of unknowns in the equations to match the number of equations present.

As the forces and torques on the cylinders are related to the various coefficients of the above terms in the asymptotic form of the streamfunction at large distances, it is proposed to utilize this information to provide some of the extra conditions required. It has been establish in the work on the flow created by a rotlet in the presence of a circular cylinder that the forces on the cylinder in the (x, y) directions are (F_x, F_y), whilst the torque is $M\underline{k}$, with the values

$$F_x = -4\pi\mu\Gamma F B_1/a, \tag{5.9.1}$$

$$F_y = 4\pi\mu\Gamma G B_1/a, \tag{5.9.2}$$

$$M = -4\pi\mu\Gamma F C_0^*, \tag{5.9.3}$$

where a is the radius of the cylinder, Γ the strength of the rotlet, C_0^* the coefficient of the ln(r) term, FB_1 the coefficient of the $r\sin\vartheta\ln r$ term and GB_1 the coefficient of the $r\cos\vartheta\ln r$ term; these coefficients being those occurring in the Fourier Series for the streamfunction solution of the biharmonic equation. It was also shown that the forces (F_x, F_y) and the torque M could be written in the form

$$F_x = \mu\int_0^{2\pi} r\left(r\frac{\partial\omega}{\partial r} - \omega + \frac{2}{r}\frac{\partial}{\partial r}\left[\frac{\partial^2\Psi}{\partial\vartheta^2} + \Psi\right]\right) sin(\vartheta)d\vartheta, \tag{5.9.4}$$

$$F_y = -\mu\int_0^{2\pi} r\left(r\frac{\partial\omega}{\partial r} - \omega + \frac{2}{r}\frac{\partial}{\partial r}\left[\frac{\partial^2\Psi}{\partial\vartheta^2} + \Psi\right]\right) cos(\vartheta)d\vartheta, \tag{5.9.5}$$

$$M = \mu\int_0^{2\pi} r^2\left(\omega - \frac{2}{r}\frac{\partial\Psi}{\partial r} - \frac{2}{r^2}\frac{\partial^2\Psi}{\partial\vartheta^2}\right) d\vartheta, \tag{5.9.6}$$

If one now introduces the notation of the present problem, together with the fact that it is the forces and the torques on the cylinders that are required to maintain the motion which are being considered, rather being exerted the than the forces and the torques on cylinders by the fluid, then one obtains

$$F_1 + F_2 = 4\pi\mu\omega_1 R_1 F B_1, \tag{5.9.7}$$

$$L_1 + L_2 = -4\pi\mu\omega_1 R_1 G B_1, \tag{5.9.8}$$

$$T_1 + T_2 - R_1(cosh(\xi_1) + sinh(\xi_1)coth(\xi_2)) = 4\pi\mu\omega_1 R_1^2 C_0^*. \tag{5.9.9}$$

Similarly the forces and torques on the separate cylinders can be expressed as

$$F_1 = -\mu\omega_1 R_1 \int_0^{2\pi} \left(r^* \frac{\partial\omega}{\partial r^*} - \omega + \frac{2}{r^*}\frac{\partial}{\partial r^*}\left[\frac{\partial^2\Psi}{\partial\vartheta_1^{*2}} + \Psi\right]\right) sin(\vartheta_1^*) d\vartheta_1^*, \tag{5.9.10}$$

$$L_1 = \mu\omega_1 R_1 \int_0^{2\pi} \left(r^* \frac{\partial\omega}{\partial r^*} - \omega + \frac{2}{r^*}\frac{\partial}{\partial r^*}\left[\frac{\partial^2\Psi}{\partial\vartheta_1^{*2}} + \Psi\right]\right) cos(\vartheta_1^*) d\vartheta_1^*, \tag{5.9.11}$$

$$M = -\mu\omega_1 R_1^2 \int_0^{2\pi} \left(\omega - \frac{2}{r^*}\frac{\partial\Psi}{\partial r^*} - \frac{2}{r^{*2}}\frac{\partial^2\Psi}{\partial\vartheta_1^{*2}}\right) d\vartheta_1^*, \tag{5.9.12}$$

on the upper cylinder, where r- is the non-dimensional distance, the non-dimensionalisation being with respect to R_1, measured from the axis of the upper cylinder, $\vartheta_1^*$is the angle between a line drawn through the axis of the cylinder and a line parallel to the x-axis and Ψ and ω are in their non-dimensional form. In the integrals in expressions (5.9.10), (5.9.11) and (5.9.12), r^* is unity. Likewise, on the lower cylinder the forces and the torque are given by

$$F_2 = -\mu\omega_1\beta R_1 \int_0^{2\pi} \left(\beta\frac{\partial\omega}{\partial r^{**}} - \omega + \frac{2}{\beta}\frac{\partial}{\partial r^{**}}\left[\frac{\partial^2\Psi}{\partial\vartheta_2^{*2}} + \Psi\right]\right) sin(\vartheta_2^*) d\vartheta_2^*, \tag{5.9.13}$$

$$L_2 = \mu\omega_1\beta R_1 \int_0^{2\pi} \left(\beta\frac{\partial\omega}{\partial r^{**}} - \omega + \frac{2}{\beta}\frac{\partial}{\partial r^{**}}\left[\frac{\partial^2\Psi}{\partial\vartheta_2^{*2}} + \Psi\right]\right) sin(\vartheta_2^*) d\vartheta_2^*, \tag{5.9.14}$$

$$T_2 = -\mu\omega_1\beta^2 R_1^2 \int_0^{2\pi} \left(\omega - \frac{2}{\beta}\frac{\partial\Psi}{\partial r^{**}} - \frac{2}{\beta^2}\frac{\partial^2\Psi}{\partial\vartheta_2^{*2}}\right) d\vartheta_2^*, \tag{5.9.15}$$

where r^{**} is the non-dimensional distance, with the non-dimensionalisation again with respect to R_1, measured from the axis of the lower cylinder and ϑ_2 is the angle between a line from the axis of the cylinder to a line parallel to the x-axis. In the integrals in the expressions (5.9.13), (5.9.14) and (5.9.15) the value of r^{**} will be β. As there is no variation in either Ψ or the normal derivative of Ψ around either cylinder then some of the terms in the above integrals are zero. If use is also made of the boundary conditions on the upper cylinder. namely that on

$$r^* = 1, \quad \frac{\partial\Psi}{\partial r^*} = 1, \tag{5.9.16}$$

then one obtains that on $r^* = 1$

$$F_1 = -\mu\omega_1 R_1 \int_0^{2\pi} \left(\frac{\partial\omega}{\partial r^*} - \omega + 2\right) sin(\vartheta_1^*) d\vartheta_1^*, \tag{5.9.17}$$

$$L_1 = \mu\omega_1 R_1 \int_0^{2\pi} \left(\frac{\partial\omega}{\partial r^*} - \omega + 2\right) cos(\vartheta_1^*) d\vartheta_1^*, \tag{5.9.18}$$

$$T_1 = -\mu\omega_1 R_1^2 \int_0^{2\pi} (\omega - 2)\, d\vartheta_1^*, \tag{5.9.19}$$

Likewise, use of the boundary condition that

$$\text{on} \quad r^{**} = \beta, \quad \frac{\partial\Psi}{\partial r^{**}} = -\beta(\omega_2/\omega_1), \tag{5.9.20}$$

results in the following expressions on $r^{**} = \beta$, namely

$$F_2 = -\mu\omega_1\beta R_1 \int_0^{2\pi} \left(\beta\frac{\partial\omega}{\partial r^{**}} - \omega - 2(\omega_2/\omega_1)\right) sin(\vartheta_2^*) d\vartheta_2^*, \tag{5.9.21}$$

$$L_2 = \mu\omega_1\beta R_1 \int_0^{2\pi} \left(\beta\frac{\partial\omega}{\partial r^{**}} - \omega - 2(\omega_2/\omega_1)\right) sin(\vartheta_2^*) d\vartheta_2^*, \tag{5.9.22}$$

$$T_2 = -\mu\omega_1\beta^2 R_1^2 \int_0^{2\pi} (\omega + 2(\omega_2/\omega_1))\, d\vartheta_2^*, \tag{5.9.23}$$

If instead of using local coordinate systems with their origins on the axes of the cylinders one opts for a continuation of the bi-polar coordinate system, i.e. the substitution of expressions (5.8.21) and (5.8.23) into equations (5.8.18), (5.8.19) and (5.8.20), together with the use of equations (5.8.1), (5.8.2) and (5.8.3), then, after the removal of the pressure term by performing an integration with respect to the independent variable η, followed by use of the boundary conditions, one acquires the following expressions

$$F_1 = \mu\omega_1 R_1 sinh(\xi_1) \int_0^{2\pi} \left(-\frac{1}{h_1}\frac{\partial\omega}{\partial\xi} - \omega + 2 \right) \frac{(1 - cosh(\xi_1)cos(\eta))}{(cosh(\xi_1) - cos(\eta))^2} d\eta, \tag{5.9.24}$$

$$L_1 = \mu\omega_1 R_1 sinh(\xi_1) \int_0^{2\pi} \left(-\frac{1}{h_1}\frac{\partial\omega}{\partial\xi} - \omega + 2 \right) \frac{sinh(\xi_1)sin(\eta)}{(cosh(\xi_1) - cos(\eta))^2} d\eta, \tag{5.9.25}$$

$$T_1 = -\mu\omega_1 R_1 sinh(\xi_1) \int_0^{2\pi} (\omega - 2) \frac{1}{(cosh(\xi_1) - cos(\eta))^2} d\eta, \tag{5.9.26}$$

on $\xi = \xi_1$.

Since on $\xi = \xi_1$, or equivalently on $r^* = 1$,

$$\frac{\partial\vartheta}{\partial\eta} = -\frac{sinh(\xi_1)}{(cosh(\xi_1) - cos(\eta))}, \tag{5.9.27}$$

$$cos(\vartheta_1^*) = -\frac{sinh(\xi_1)sin(\eta)}{(cosh(\xi_1) - cos(\eta))}, \tag{5.9.28}$$

$$sin(\vartheta_1^*) = -\frac{(1 - cosh(\xi_1)cos(\eta))}{(cosh(\xi_1) - cos(\eta))}, \tag{5.9.29}$$

$$\frac{1}{h_1}\frac{\partial\omega}{\partial\xi} = -\frac{\partial\omega}{\partial r^*}, \tag{5.9.30}$$

the expressions (5.9.24), (5.9.25) and (5.9.26) are identical to the expressions (5.9.17), (5.9.18) and (5.9.19).

On the lower cylinder one has

$$F_2 = \mu\omega_1 R_1 sinh(\xi_1) \int_0^{2\pi} \left(\frac{\beta}{h_1}\frac{\partial\omega}{\partial\xi} - \omega - 2(\omega_2/\omega_1) \right) \frac{(1 - cosh(\xi_2)cos(\eta))}{(cosh(\xi_2) - cos(\eta))^2} d\eta, \tag{5.9.31}$$

$$L_2 = \mu\omega_1 R_1 sinh(\xi_1) \int_0^{2\pi} \left(\frac{\beta}{h_1} \frac{\partial \omega}{\partial \xi} - \omega - 2(\omega_2/\omega_1) \right) \frac{sinh(\xi_2) sin(\eta)}{(cosh(\xi_2) - cos(\eta))^2} d\eta, \tag{5.9.32}$$

$$T_2 = -\mu\omega_1 R_1 R_2 sinh(\xi_1) \int_0^{2\pi} (\omega + 2(\omega_2/\omega_1)) \frac{1}{(cosh(\xi_1) - cos(\eta))^2} d\eta, \tag{5.9.33}$$

and since on $\xi = -\xi_2$, or equivalently on $r = R_2$, $\frac{\partial \vartheta}{\partial \eta}$ will be positive as opposed to its negative value on $\xi = \xi_1$, or $r = R_1$, due to taking the form

$$\frac{\partial \vartheta}{\partial \eta} = -\frac{sinh(\xi_2)}{(cosh(\xi_2) - cos(\eta))}, \tag{5.9.34}$$

and

$$\frac{1}{h_1} \frac{\partial \omega}{\partial \xi} = \frac{\partial \omega}{\partial r^{**}}, \tag{5.9.35}$$

the expressions (5.9.21), (5.9.22) and (5.9.23). In equations (5.9.7) to (5.9.9) the forces on the two cylinders, namely F_1 and F_2 , and the torques, T_1 and T_2, are linked to certain coefficients of the asymptotic expansion of the stream-function at large distances from the cylinders. Likewise, expressions (5.9.17) to (5.9.19) and (5.9.21) to (5.9.23) contain the unknown values of the vorticity and its normal derivative on the two cylinders. As the BEM not only contains the above unknown coefficients, but solves for the vorticity and its normal derivative on the cylinders, the relationships (5.9.7), (5.9.8) and (5.9.9), with F_1, L_1 and T_1 from equations (5.9.17), (5.9.18) and (5.9.19), and F_2, L_2 and T_2 from equations (5.9.21), (5.9.22) and (5.9.23) can be used to form three additional equations (see section 5.11)

5.10 Additional Conditions

In addition to the above three conditions it is also necessary for the pressure to remain single valued on any contour surrounding either, or both, of the cylinders. The dimensional form of the equation of motion, in the direction, namely,

$$0 = -\frac{1}{r} \frac{\partial p}{\partial \vartheta} + \mu \frac{\partial \omega}{\partial r}, \tag{5.10.1}$$

can be expressed relative to an origin on the axis of the upper cylinder by

$$0 = -\frac{1}{r^*} \frac{\partial p}{\partial \vartheta_1^*} + \frac{\partial \omega}{\partial r^*}, \tag{5.10.2}$$

and relative to an origin on the axis of the lower cylinder by

$$0 = -\frac{1}{r^{**}}\frac{\partial p}{\partial \vartheta_2^*} + \frac{\partial \omega}{\partial r^{**}}, \tag{5.10.3}$$

where ω in equations (5.10.2) and (5.10.3) is the non-dimensional vorticity, whilst in the same equations the pressure has been non-dimensionalised with respect to $\mu\omega_1$. The single valuedness of the pressure requires that

$$\int_0^{2\pi} r^* \frac{\partial \omega}{\partial r^*} d\vartheta_1^* = 0, \tag{5.10.4}$$

$$\int_0^{2\pi} r^{**} \frac{\partial \omega}{\partial r^{**}} d\vartheta_2^* = 0. \tag{5.10.5}$$

Using expressions (5.9.27) and (5.9.30). together with h_1 on $\xi = \xi_1$ from expression (5.2.4), then

$$\text{on} \quad \xi = \xi_1, \quad \int_0^{2\pi} \frac{\partial \omega}{\partial \xi} d\eta = 0. \tag{5.10.6}$$

Similarly, expressions (5.9.34) and (5.9.35). together with h_1 on $\xi = \xi_1$ from expression (5.2.4). produces

$$\int_0^{2\pi} \frac{\partial \omega}{\partial \xi} d\eta = 0, \quad \text{on} \quad \xi = -\xi_2, \tag{5.10.7}$$

It should be noted that the expressions (5.10.6) and (5.10.7) could have been obtained directly by integration of equation (5.8.10) round the contours $\xi = \xi_1$ and $\xi = -\xi_2$, respectively.

5.11 Boundary Element Method

The solution of the biharmonic equation

$$\nabla^4 \Psi = 0, \tag{5.11.1}$$

by introducing the vorticity, ω, so enabling equation (5.11.1) to be written in the form

$$\nabla^2 \Psi = \omega, \tag{5.11.2}$$

$$\nabla^2 \omega = 0, \tag{5.11.3}$$

has already been discussed, see chapter 4 in the section entitled. the "Boundary Element Method". However, in that work the rotlet was subtracted out of the problem by including the term $ln(R_1)$ in the expression for the non-dimensional streamfunction function. where R_1 is the non-dimensional distance from the rotlet. In the present problem no such singularity occurs provided that the radius of the However, in order lower cylinder, R_2, remains non-zero. However in order to apply the BEM bounded boundary is required. Let S be the surface of a circle of radius R whose center is at the origin of the cartesian axes x and y and with R large enough such that cylinders are both the and the lower contained within the circular region, see Figure (5.11.8). As the upper

solution domain, Ω, is multiply connected, cuts are required along the y-axis from L_1 to L_2 and from L_3 to L_4 in order to produce a simply connected the domain, Ω. This domain is enclosed by boundaries S, L_2L_1, the surface of the upper cylinder, L_1L_2, L_3L_4, the surface of the lower cylinder and L_4L_3 . Application of Green's second identity to the domain Ω^*. reduces contributions to those from the surfaces of the upper and the lower cylinders, due to the integrals on L_1L_2 and L_2L_3 , and L_3L_4 and L_4L_3, being equal in magnitude but opposite in sign and the integrals on S tending to zero, see Brebbia et al. (1984), as the radius $R \rightarrow \infty$. The boundary $\partial\Omega$ in this problem consists of the two parts, that from around the upper cylinder together with that from the lower cylinder. However, prior to using the BEM it is necessary to divide both the non-dimensional streamfunction and the vorticity into two parts. In each expression one part consists of the asymptotic expansion at large distances from the cylinders, whilst the other part represents the perturbation from this expansion. The asymptotic expansions at large values of r are such that the operators remaining in equations (5.11.2) and (5.11.3) are only on the perturbation functions. The number of terms included in the asymptotic expansions for both the streamfunction and the vorticity must be sufficient to allow for the possibility of rigid body rotation at infinity, which is achieved by the presence of terms of $O(r^2)$, together with the remaining perturbation quantities tending to zero as $r \rightarrow \infty$. Following the notation in the problem of the rotlet outside

the circular cylinder the streamfunction and the vorticity are expressed as

$$\Psi = \lambda_1 r cos(\vartheta) + \lambda_2 r sin(\vartheta) + \lambda_3 ln(r) + \lambda_4 r ln(r) cos(\vartheta) + \lambda_5 r ln(r) sin(\vartheta) + \lambda_6 r^2 + \lambda_7 + \lambda_8 sin(2\vartheta) + \lambda_9 cos(2\vartheta) + \Psi^*, \tag{5.11.4}$$

$$= \psi_A + \Psi^*, \tag{5.11.5}$$

$$\omega = 4\lambda_6 + 2(\lambda_4 cos(\vartheta) + \lambda_5 sin(\vartheta)) r^{-1} - 4(\lambda_8 sin(2\vartheta) + \lambda_9 cos(2\vartheta)) r^{-2} + \omega^*, = \omega_A + \omega^*, \tag{5.11.6}$$

where

$$\nabla^2 \Psi^* = \omega^*, \tag{5.11.7}$$

and

$$\nabla^2 \omega^* = 0. \tag{5.11.8}$$

The boundary conditions on the upper cylinder, that is when

$$x = cos\vartheta_1^* \quad \text{and} \quad y = cosh(\xi) + sin\vartheta_1^*, \tag{5.11.9}$$

are

$$\Psi^* = \Psi_1 - \Psi_A, \tag{5.11.10}$$

$$\frac{\partial \Psi^*}{\partial r^*} = 1 - \frac{\partial \Psi_A}{\partial r^*}, \tag{5.11.11}$$

Whilst on the lower cylinder, when

$$x = cos\vartheta_2^* \quad \text{and} \quad y = sinh(\xi) cosech(\xi_2) + sin\vartheta_2^*, \tag{5.11.12}$$

the appropriate conditions are

$$\Psi^* = -\Psi_2 - \Psi_A, \tag{5.11.13}$$

$$\frac{\partial \Psi^*}{\partial r^{**}} = -\beta(\omega_2/\omega_1) - \frac{\partial \Psi_A}{\partial r^{**}}. \tag{5.11.14}$$

In turn the vorticity and its normal derivative can be expressed on the upper cylinder part of the boundary, as

$$\omega = \omega_A + \omega^*, \tag{5.11.15}$$

$$\frac{\partial \omega}{\partial r^*} = \frac{\partial \omega_A}{\partial r^*} + \frac{\partial \omega^*}{\partial r^*}, \tag{5.11.16}$$

whilst on the lower cylinder the conditions are

$$\omega = \omega_A + \omega^*, \tag{5.11.17}$$

$$\frac{\partial \omega}{\partial r^{**}} = \frac{\partial \omega_A}{\partial r^{**}} + \frac{\partial \omega^*}{\partial r^{**}}, \tag{5.11.18}$$

In the BEM, when the partial differential equations (5.11.7) and (5.11.8) are expressed as a system of linear algebraic equations, the values of Ψ^* and $\partial\Psi^*/\partial r^*$ on the upper cylinder can be replaced by the known expressions (5.11.10) and (5.11.11), respectively, that is they are known apart from the values of the constants λ_1, where i = 1,2,....,9. Whilst the values of Ψ^* and $\partial\Psi^*/\partial r^{**}$ on the lower cylinder can be replaced by the known expressions (5.11.13) and (5.11.14), respectively. Solution of these linear equations will produce values of ω^* and for $\partial\omega^*/\partial r^*$ and $\partial\omega^*/\partial r^{**}$, which from equations (5.11.15) to (5.11.18) will lead to the values of the vorticity and its normal derivative on the surface of both cylinders being determined.

In the above work the expressions for $\partial\Psi_A/\partial r^*$, $\partial\Psi_A/\partial r^{**}$, $\partial\omega_A/\partial r^*$, and $\partial\omega_A/\partial r^{**}$ are most easily determined by first changing Ψ_A and ω_A from cylindrical coordinates (r,ϑ) to the cartesian coordinates (x,y). Then writing

$$x = r^* cos\vartheta_1^* \quad \text{and} \quad y = cosh(\xi_1) + r^* sin\vartheta_1^*, \tag{5.11.19}$$

or

$$x = r^{**} cos\vartheta_2^* \quad \text{and} \quad y = -sinh(\xi_1) cosech(\xi_2) + r^{**} sin\vartheta_2^*, \tag{5.11.20}$$

according as to whether one requires to determine $\partial/\partial r^*$ or $\partial/\partial r^{**}$, Alternatively, one can use

$$tan\vartheta = (cosh(\xi_1)/(r^* cos\vartheta_1^*) + tan\vartheta_1^*, \tag{5.11.21}$$

$$r^2 = r^* sin^2(\vartheta_1^*)(cosh(\xi_1) + r^* sin(\vartheta_1^*))^2, \tag{5.11.22}$$

and

$$\frac{\partial}{\partial r^*} = \frac{\partial r}{\partial r^*}\frac{\partial}{\partial r} + \frac{\partial \vartheta}{\partial r^*}\frac{\partial}{\partial \vartheta}, \tag{5.11.23}$$

for conditions on the upper cylinder. With the conditions

$$tan\vartheta = (-sinh(\xi_1)cosech(\xi_2))/(r^{**}cos\vartheta_2^*) + tan\vartheta_2^*, \tag{5.11.24}$$

$$r^2 = (r^{**2}cos^2\vartheta_2^*) + (-sinh(\xi_1)cosech(\xi_2) + r^{**}Sin\vartheta_2^*)^2, \tag{5.11.25}$$

and

$$\frac{\partial}{\partial r^{**}} = \frac{\partial r}{\partial r^{**}}\frac{\partial}{\partial r} + \frac{\partial \vartheta}{\partial r^{**}}\frac{\partial}{\partial \vartheta}, \tag{5.11.26}$$

on the lower cylinder.

Use of expressions (5.11.23) and (5.11.26) are required in equations (5.11.11) and (5.11.14), respectively, in order to determine the boundary conditions $\partial\Psi^*/\partial r^*$ and $\partial\Psi^*/\partial r^{**}$. In the expressions (5.9.17) to (5.9.19), which are used in equations (5.9.7) to (5.9.9), it is necessary to introduce the relationships (5.11.15), (5.11.16) and (5.11.23). Similarly, in the expressions (5.9.21) to (5.9.23), which also occur in equations (5.9.7) to (5.9.9), the relationships (5.11.15), (5.11.16) and (5.11.26) are required. The contributions from ω_A, $\partial\omega_A/\partial r^*$ and $\partial\omega_A/\partial r^{**}$, in the various integrals are evaluated numerically and result in linear expressions of the parameters λ_i, i = 1,2,.....,9, together with integrals of ω^*, $\partial\omega^*/\partial r^*$ and $\partial\omega^*/\partial r^{**}$. The equations (5.10.4) and (5.10.5) have to be dealt with in an equivalent manner, and similarly produce linear functions of λ_i, i = 1,2,.....,9, with known numerical coefficients, plus integrals of the above unknown quantities.

5.12 Results

In all the numerical calculations presented in this thesis the distance between the two cylinders was taken along the y-axis in order to correspond with the calculations by Jeffery (1922) , Dorrepaal et al. (1984) and Smith (1991). In these results we use 2N elements on the boundary of the two cylinders and since we have 2N +10 unknowns, we use 3 points inside the lower cylinder, 2 points inside the upper cylinder, integral condition on the lower cylinder, integral

condition of the upper cylinder together with equations for the resultant of drag, the resultant of lift and the resultant of moment. In addition to checking these coefficients, the numerical integration of the forces and torques on the two cylinders, namely F_1, F_2, L_1, L_2, M_1 and M_2, using the values of the streamfunction, the vorticity and their derivatives found in the BEM solution, is undertaken and the results compared with those arising from the analytical expressions given in (5.8.29), (5.8.30), (5.8.31), (5.8.35), (5.8.36) and (5.8.37),.

Numerical details for three separate situations are presented:

- (i) zero angular momenta of the combined system, $\omega_1 = \omega_2$, $r_1 = r_2$,
- (ii) zero angular momenta, namely $\omega_1 r_1^2 = \omega_2 r_2^2$, with $r_1 \neq r_2$,
- (iii) non-zero angular momenta, $\omega_1 r_1^2 \neq \omega_2 r_2^2$.

Case (i) $r_1 = r_2 = 1$, $\omega_1 = \omega_2 = 1$. The situation in which the distance between the two cylinders was taken to be 3.0816 has been investigated in detail. The values of λ_2 and $\psi_1+\psi_2$ which are theoretically predicted to be -0.324 and -1.075, see Dorrepaal et al. (1984), numerically are -0.332 and -1.056, respectively, for N = 80, whilst for N = 120 are -0.328 and -1.067. It is concluded that as the value of N increases then the numerical solutions appear to be approaching the analytical solution. All the other values of λ_1 are found theoretically to be zero, see Dorrepaal et al. (1984), I and the numerical results with both N = 80 and 120 give results which are zero to three decimal places.. The numerical predicted values of F_1, F_2, L_1, L_2, M_1 and M_2 are 0.000, 0.000,0.000, 0.000, -1.037 and 1.038, respectively, for N = 120 and these results should be compared with the analytically predicted results, namely, 0.000, 0.000, 0.000, 0.000, -1.037 and 1.038, respectively. Figure 5.13.9 shows the non-dimensional streamline and the vorticity pattern and the results are indistinguishable from the numerical results calculated from the analytical solutions of Dorrepaal et al . (1984) and Smith (1991). This figure shows a uniform stream at infinity in the direction perpendicular to the plane containing the axes of the two cylinders. There is consequently a region of closed streamlines surrounding the cylinders, a limiting closed streamline, which divides the flow which passes the cylinders from that which is trapped in a circulatory motion about the cylinders and stagnations points on the x-axis. The streamline and the vorticity both are symmetrical about the x-axis and the y-axis, both upstream and downstream of the bodies.

Case (ii) $r_1 = 1, r_2 = 0.5, \omega_1 = 1, \omega_2 = 4$. The situation in which the distance between the two cylinders was taken to be 2.8202 has been investigated in detail. The values of λ_2 and $\psi_1 + \psi_2$ which are theoretically predicted to be -0.355 and -1. 620, see Smith (1991) numerically are -0.354 and -1.621, respectively, for N = 80, which for N = 120 are -0.355 and -1.620. It is concluded that as the value of N increases then the numerical solutions appear to be approaching the analytical solution. All the other values of λ_1 are found theoretically to be zero, see Smith (1991), and the numerical results with both N = 80 and 120 give results which are zero to three decimal places.. The numerical predicted values of F_1, F_2, L_1, L_2, M_1 and M_2 are 0.000, 0.000, 0.000, 0.000, -1.011 and 1.012, respectively, for N = 120 and these results should be compared with the analytically predicted results, namely, 0.000, 0.000, 0.000, 0.000, -1.011 and 1.012, respectively.

Figure 5.13.10 represents the non-dimensional streamline and the vorticity patterns and the results are almost indistinguishable with the results obtainable from the analytical solutions by Smith (1991) Although the combined angular momentum of the system remains unchanged both figures show a clear departure from the symmetry about the x-axis, coupled with an increase in the rotation of the fluid flow about the smaller cylinder. However, although the area of the closed contours of fluid flow about the smaller cylinder has increased there are still stagnation points on the x-axis, both upstream and downstream of the cylinders. The vorticity pattern, whilst remaining of a similar form on the larger cylinder, sees contours of constant value leaving its surface to Join onto the smaller cylinder at points no longer directly opposite but now on the far side of the upper cylinder.

Case (iii) $r_1 = 1, r_2 = 1, \omega_1 = 8, \omega_2 = 1$. The situation in which the distance between the two cylinders was taken 3.0816 has been investigated in detail. The values of λ_1, λ_9 and $\psi_+\psi_2$ which are theoretically predicted to be -1.458, -1.3856 and -4.565, see Smith (1991) numerically are -1.479, -1.3855 and -4.596, respectively, for N = 80, whilst for N = 120 are -1. 468, -1. 3856 and -4.567. It is concluded that as the value of N increases then the numerical solutions appear to be approaching the analytical solution. All the other values of λ_i are found theoretically to be zero, see Smith 1 (1991), and the numerical results with both N = 80 and 120 give results which are zero to three decimal places. The numerical predicted values of F_1, F_2, L_1, L_2, M_1 and M_2 , are -1.926, 1.925,

0.000, 0.000, 1.684 and 7.630, respectively, for N = 120 and these results should be compared with the analytically predicted results, namely, -1.925, 1.925, 0.000, 0.000, 1.683 and -7.629, respectively, see Smith (1991).

This further increase in angular momentum of the upper cylinder from 4 to 8, but such that the overall angular momentum of the combined system is no longer zero, is presented in figure 5.13.11 for the streamfunction and the vorticity patterns. The streamlines, whilst still continuing to form some closed contours around the upper cylinder, no longer do so for the lower cylinder. Hence, streamlines enclosing the lower cylinder also enclose the upper cylinder. In addition, the uniform stream at infinity, present in Figures 5.13.9 and 5.13.10, has been replaced by a flow which is consistent with that of a rigid body rotation. This combined angular momentum of the system also results in a change in the vorticity pattern, as illustrated in Figure 5.13.11, showing an increase in the area over which vortex lines leave the upper cylinder and attach to the lower cylinder.

5.13 Conclusions

The Boundary Element Method has been employed, along with certain relationships between the forces and the torque on the combined system and the coefficients in the asymptotic expansion for the streamfunction, to obtain the solution of the problem of slow fluid flow which is produced by the rotation of two circular cylinders. This solution agrees with the previously published analytical solutions in which the two cylinders are in a state of overall equilibrium. In order to produce a solution for situations in which the combined system is not in a state of overall equilibrium then it is necessary to implement the full asymptotic expansion as suggested by Jeffery (1922) together with some further conditions which have to be applied at large distances from the cylinders. Numerical results have also been obtained for this situation.

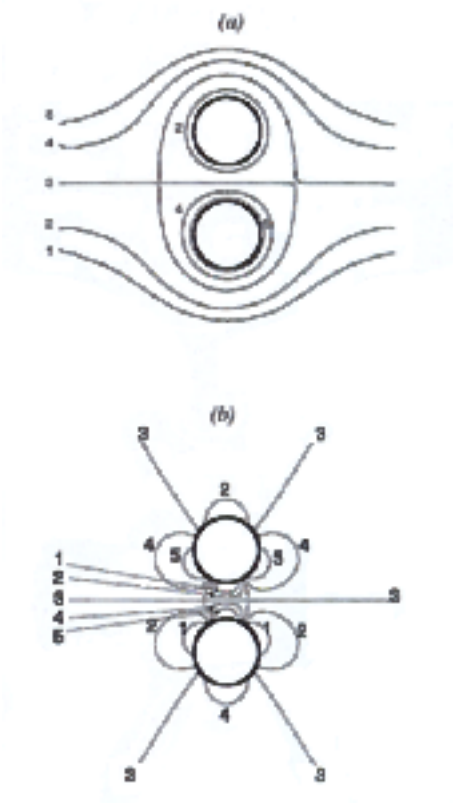

Figure 5.5.5: $r_1 = r_2 = 1$ and $\omega_1 = \omega_2 = 1(a)$ The streamlines labled $1, \ldots, 5$ corresponding to $\Psi = -1.0, -0.8, -0.53755, -0.2$ and 0.0 respectively (b) The vorticity lines labled $1, \ldots, 5$ corresponding to $\omega = -0.3, -0.1, 0.0, 0.1$ and 0.3 respectively. labeled $1, \ldots, 5$ corresponding to $\omega = -0.3, -0.1, 0.0, 0.1$ and 0.3 respectively.

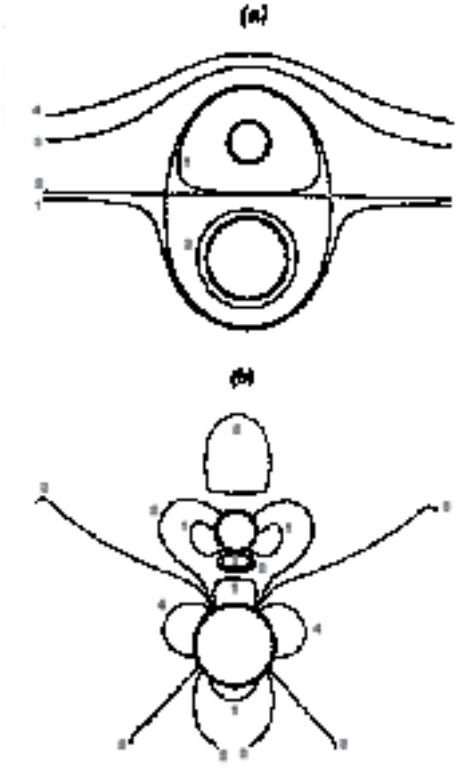

Figure 5.5.6: $r_1 = 1, r_2 = 0.5, \omega_1 = 1$ and $\omega_2 = 4(a)$ The streamlines labeled $1, \ldots, 4$ corresponding to $\Psi = -0.6, -0.55815, -0.2$ and 0.0 respectively (b) The vorticity lines labeled $1, \ldots, 9$ corresponding to $\omega = -0.6, -0.3, -0.15, -0.1, -0.025, 0.0, 0.15, 0.3$ and 0.6 respectively.

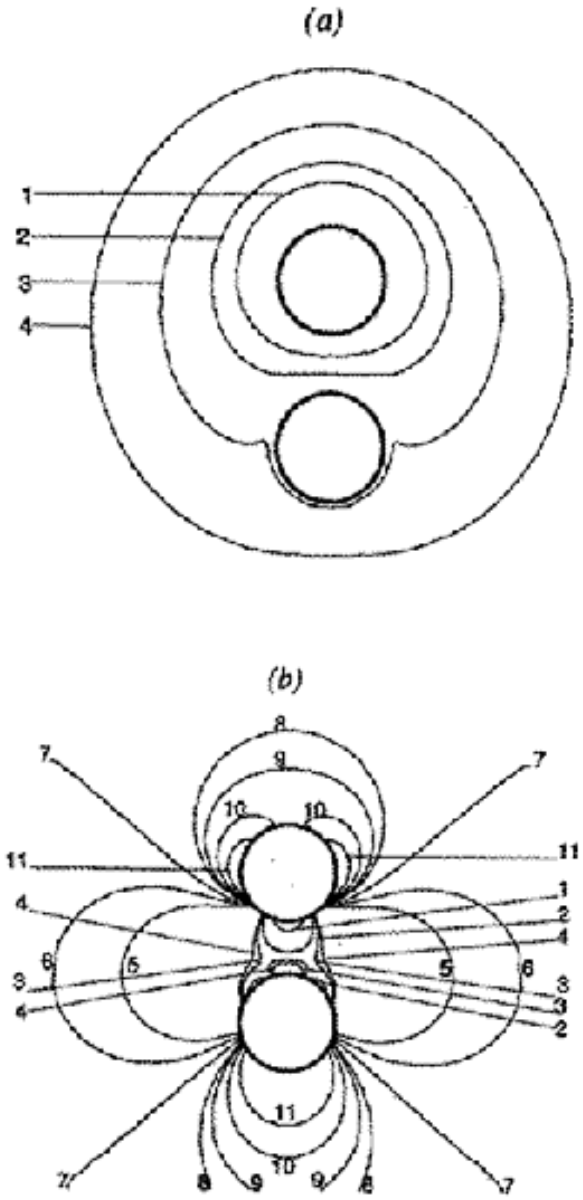

Figure 5.5.7: $r_1 = r_2 = 1, \omega_1 = 1$ and $\omega_2 = 8.(a)$ The streamlines labeled $1, \ldots, 4$ corresponding to $\Psi = -2.0, -1.0, 0.0$ and 4.0, respectively (b) The vorticity lines labeled $1, \ldots, 11$ corresponding to $\omega = -6.0, -0.3, -2.25, -1.95, 1.5, 1.8, 2.1, 2.4, 2.5, 2.7$ and 3.0, respectively.

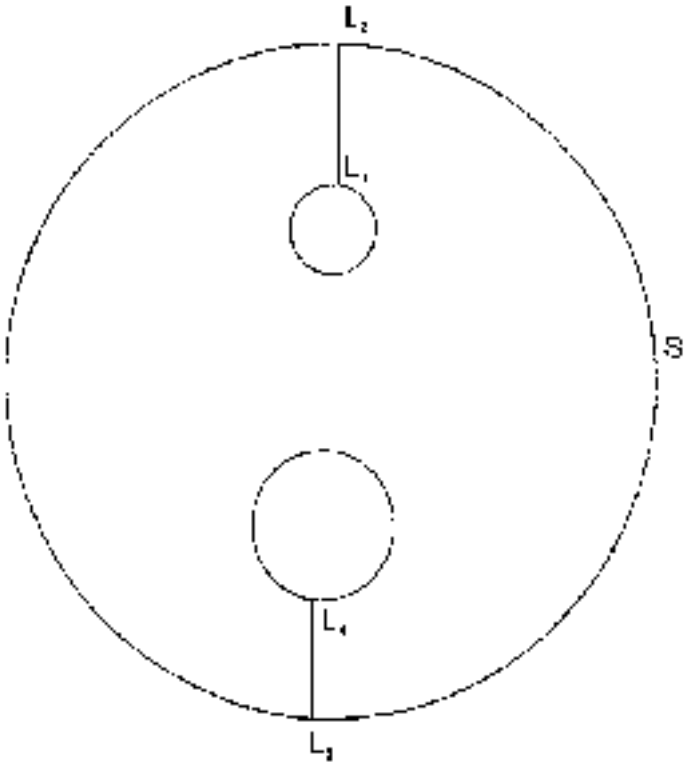

Figure 5.11.8: The geometry of the solution domain.

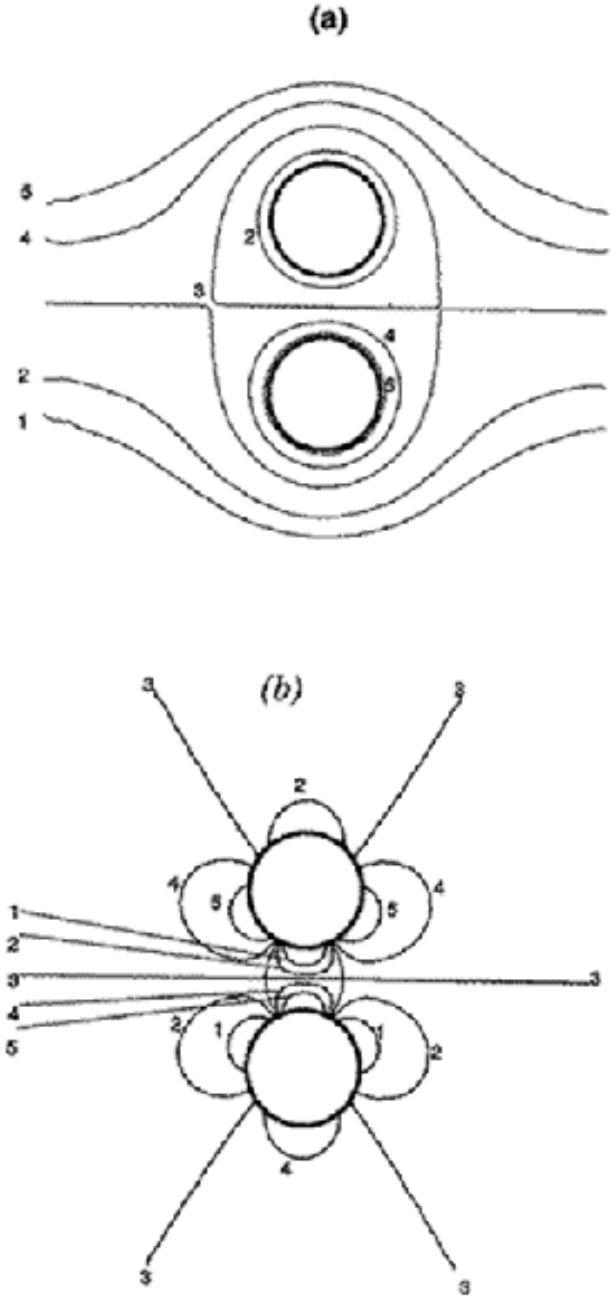

Figure 5.13.9: $r_1 = r_2 = 1$ and $\omega_1 = \omega_2 = 1$, using BEM. (a) The streamlines labeled $1, \ldots, 5$ corresponding to $\Psi = -1.0, -0.8, -0.53755, -0.2$ and 0.0 respectively (b) The vorticity lines labeled $1, \ldots, 5$ corresponding to $\omega = -0.3, -0.1, 0.0, 0.1$ and 0.3 respectively.

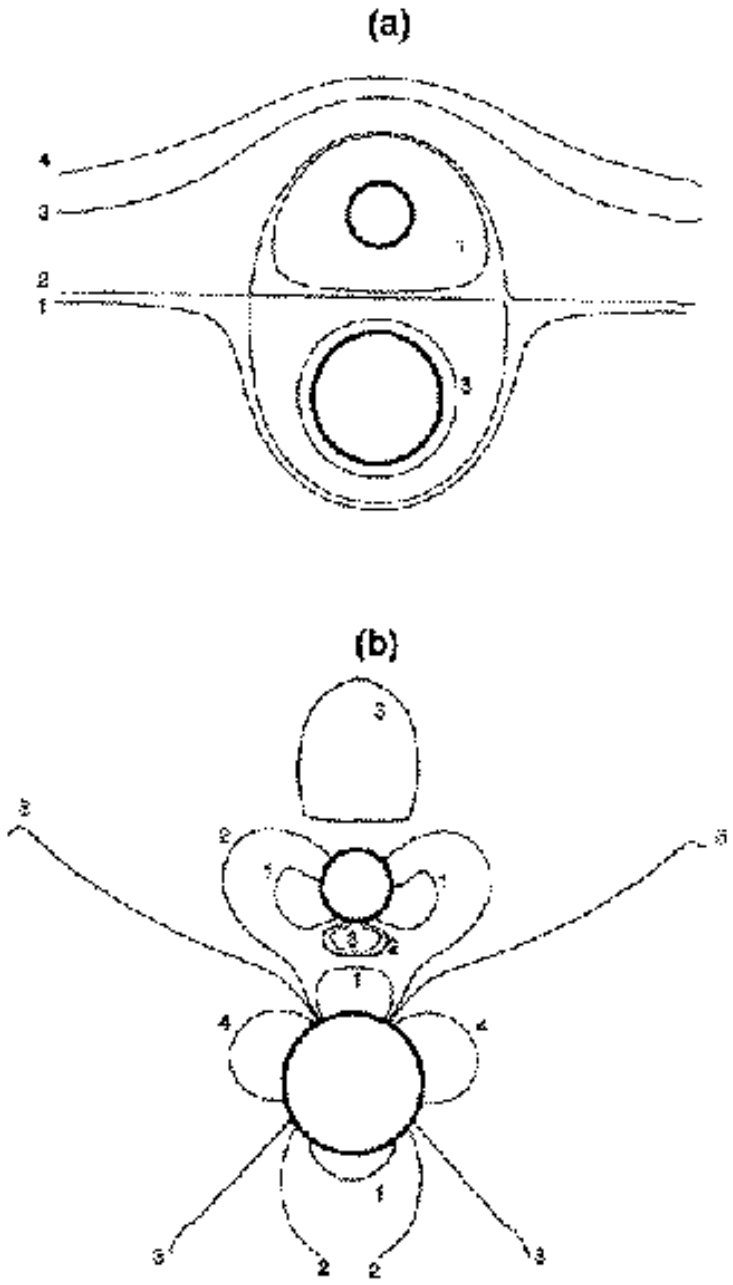

Figure 5.13.10: $r_1 = 1, r_2 = 0.5, \omega_1 = 1$ and $\omega_2 = 4$, using BEM. (a) The streamlines labeled $1, \ldots, 4$ corresponding to $\Psi = -0.6, -0.55815, -0.2$ and 0.0 respectively (b) The vorticity lines labeled $1, \ldots, 9$ corresponding to $\omega = -0.6, -0.3, -0.15, -0.1, -0.025, 0.0, 0.15, 0.3$ and 0.6 respectively.

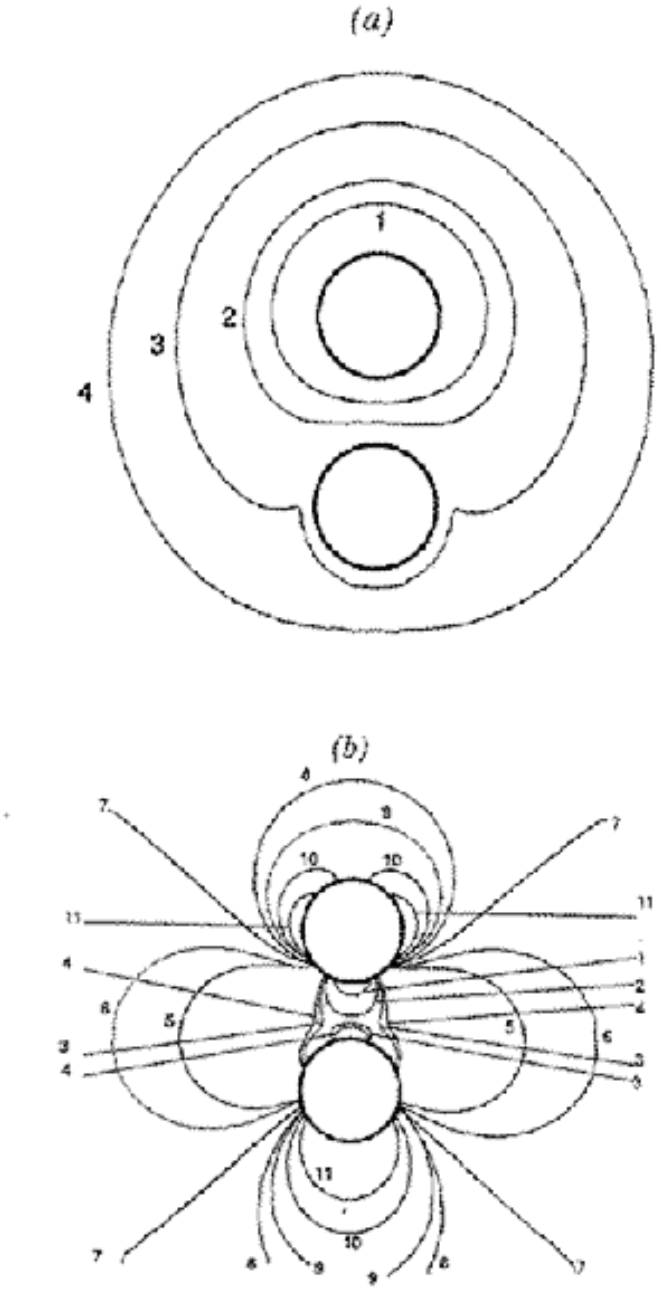

Figure 5.13.11: $r_1 = r_2 = 1, \omega_1 = 1$ and $\omega_2 = 8$, using BEM. (a) The streamlines labeled $1, \ldots, 4$ corresponding to $\Psi = -2.0, -1.0, 0.0$ and 4.0, respectively (b) The vorticity lines labeled $1, \ldots, 11$ corresponding to $\omega = -6.0, -0.3, -2.25, -1.95, 1.5, 1.8, 2.1, 2.4, 2.5, 2.7$ and 3.0, respectively.

Chapter 6

ELLIPTICAL CYLINDER AND A ROTLET

6.1 Introduction

There are a good many known solutions of problems of the two-dimensional motion of an infinite viscous fluid disturb by a moving solid body. [77] involves, in the case of the elliptic cylinder, infinite vorticity and indeterminate velocities at the ends of the axes.

In [72], first treat the problem as a limiting case of the motion of an ellipsoid through infinite viscous fluid, and his solution fulfills all the boundary conditions, in particular making the velocity zero at infinity, gives, in the limiting case of the elliptic cylinder, a solution which involves the velocity being logarithmically infinite in the direction of flow. The solution appear to be unique, subject to this condition, and has been obtained a definite value for the resistance and then treated the circular cylinder as a limiting case of the elliptic cylinder.

The problem of slow viscous flow past elliptical cylinder in the presence of rotlet has been solved analytically in [69], namely that of a rotlet of strength Γ placed at a distance C, where

$$C = a\cosh(\gamma), \qquad \gamma > \alpha \tag{6.1.1}$$

from a cylinder whose boundary is $\xi = \alpha$, the transformation from Cartesian to

elliptical coordinates is defined by

$$x = a\cosh(\xi)\cos(\eta) \tag{6.1.2}$$

$$y = a\sinh(\xi)\sin(\eta) \tag{6.1.3}$$

By introducing the dimensionless variable

$$x' = x/a, y' = y/a, c = C/a, \beta = \Gamma a/C. \tag{6.1.4}$$

For convenience the $'s$ will from now on be removed and the position of the rotlet at $(c, 0)$ and the major and minor axes of the ellipse are fixed $5/4$ and $3/4$ respectively see figure 6.1.1.

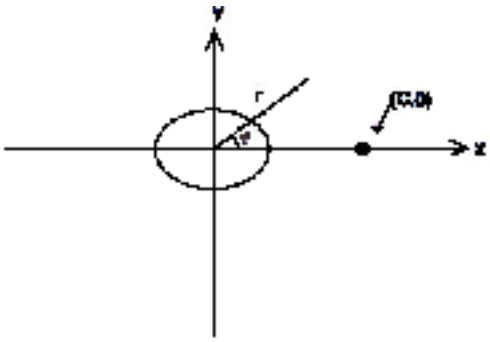

Figure 6.1.1: Diagram illustrating The geometry of the elliptical cylinder and the position of the rotlet.

In this approach it is required to solve the biharmonic equation

$$\nabla^4\psi = 0. \tag{6.1.5}$$

for the stream function $\psi(\xi, \eta)$, where $\xi \geq \alpha$ and

$$\nabla^2 = \frac{1}{h^2}(\frac{\partial^2}{\partial\xi^2} + \frac{\partial^2}{\partial\eta^2}) \tag{6.1.6}$$

where

$$h = (\cosh^2(\xi)\sin^2(\eta) + \sinh^2(\xi)\cos^2(\eta))^{1/2} \tag{6.1.7}$$

(ξ, η) are elliptic coordinates.

Before embarking on a numerical solution of this problem, it is important to discuss the analytical solution obtained by [69] who found the Fourier Series representation for the rotlet term

$$\psi_0 = \frac{1}{2}\ln((x-c)^2 + y^2) \tag{6.1.8}$$

to be given by

$$\psi_0 = -\sum_{n=1}^{\infty} \frac{e^{-n\gamma}}{n}(e^{-n\xi} + e^{n\xi})\cos(\eta) + (\xi_0 - \ln(2))for\xi < \xi_0. \tag{6.1.9}$$

He then put the complete solution as $\psi = \psi_0 + \psi_1$where $\psi_1$is the analytic outside the ellipse. Using the general solution of $\nabla^4\psi = 0$ as $\phi_0 + (x^2+y^2)\phi_1$where $\phi_0$and $\phi_1$are harmonic, we can write

$$\psi_1 = \frac{1}{2}C_0 + d_0 r^2 + \sum_{n=1}^{\infty}(C_n e^{-n\xi} + 2d_n(\sinh(2\xi) + \cos(2\eta)e^{-n\xi})\cos(n\eta) \tag{6.1.10}$$

The solution of $\nabla^4\psi = 0$ can be found by adding the general Fourier Series in term of $\cos(n\eta)$ and $\sin(n\eta)$ to $\psi_0(\xi, \eta)$, which is the solution for the rotlet in the absence of the ellipse, finding the coefficients in (6.1.10) to satisfy the no-slip conditions, and the summing the series, i.e.

$$\psi = \frac{1}{2}\ln[(\cosh(\xi)\cos\eta - \cosh(\gamma)\cos\phi)^2 + (\sinh(\xi)\sin\eta - \sinh(\gamma)\sin\phi)^2]$$
$$- \frac{1}{2}\ln[(\cosh(\alpha)\cos\eta - \cosh(\xi+\gamma-\alpha)\cos\phi)^2 + (\sinh(\alpha)\sin\eta$$
$$- \sinh(\xi+\gamma-\alpha)\sin\phi)^2] + (\xi-\alpha)$$
$$+ \sinh(\xi-\alpha)\sin(\eta) I_m[\frac{sinh(\xi+\delta-\gamma)}{sinh(\delta)(cosh(\xi+\delta-2\gamma)-cos(\eta)}$$
$$+ \sinh(\xi-\alpha) R_e[\frac{cosh(\xi+\alpha)e^{-\delta}}{sinh(\delta)cosh(2\alpha)} - \frac{cosh(\alpha)-cosh(\xi+\delta-\alpha)cos(\eta)}{sinh(\delta)(cosh(\xi+\delta-2\gamma)-cos(\eta)}] \tag{6.1.11}$$

where

$\delta = \alpha - i\phi, i = \sqrt{-1}, I_m$and $R_e$are the imaginary and real parts in (6.1.11) respectively. At large distances from the ellipse (6.1.11) can be written in the form

$$\psi \simeq Ar^2 \tag{6.1.12}$$

where

$$A = \frac{cos(2\phi) - e^{-2\gamma}}{cosh(2\alpha)[cosh(2\gamma) - cos(2\phi)]} \tag{6.1.13}$$

Hence a solid body rotation is induced at large distances from the ellipse except at $\phi = \arccos(e^{-2\gamma})/2$ which give a uniform flow when a rotlet at this point see figure 6.1.2. In fact, it is possible to obtain uniform flow at large distances of the rotlet is placed at any one of four points due to symmetry of the problem. To simplify the analytical solution in order to compare with the numerical solution we put the analytical solution in the form

$$\Psi = \psi_B + \psi^* \tag{6.1.14}$$

where

$$\begin{aligned}\psi_B &= b_1 r\cos(\vartheta) + b_2 r\sin(\vartheta) + b_3 + b_4\sin(2\vartheta) + b_5\cos(2\vartheta)\\ &+ b_6\ln(r) + b_7 r^2 + b_8 r\ln(r)\cos(\vartheta) + b_9 r\ln(r)\sin(\vartheta)\\ &+ \ln(r^2 + c^2 - 2rc\cos(\vartheta)) + b_{10}\cos(\vartheta)/r + b_{11}\sin(\vartheta)/r\\ &+ b_{12}\cos(3\vartheta)/r + b_{13}\sin(3\vartheta)/r\end{aligned} \tag{6.1.15}$$

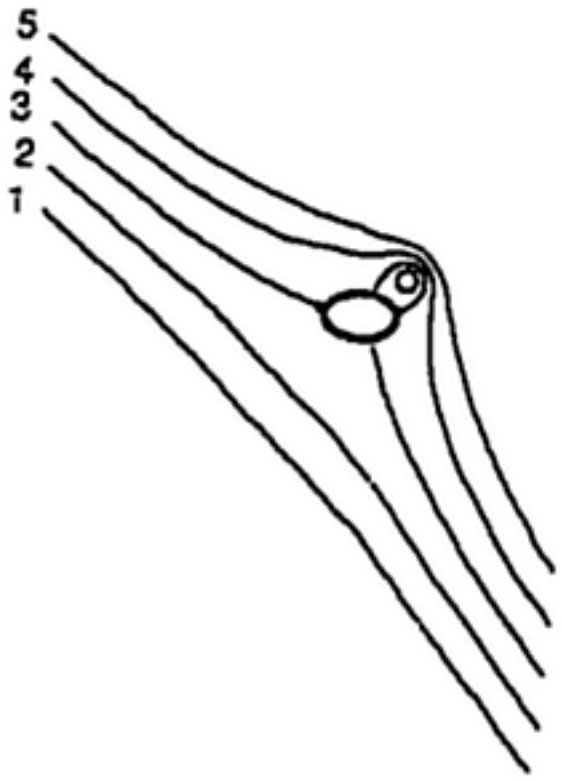

Figure 6.1.2: The uniform flow obtained when a rotlet at the position (2.236,0.758).
The streamlines labeled 1, 2, 3, 4 and 5, correspond to
$\Psi = -1.0,\ -0.5,\ 0.0,\ 0.5$ and 1.0, respectively.

and ψ_B is the asymptotic expansion of ψ and ψ^* is the perturbation value about this expansion that tend to zero as $r \to \infty$, if then we use sufficient large r, say, $r \geq 30$ and we use (6.1.11) to find the value of ψ and we repeat this 13

times we can get 13 equations and 13 unknowns $b_j, j = 1, 2, \ldots, 13$ and we use the Gauss required elimination method we can find the values of b_j as

$$\begin{aligned} &b_1 = 0.500, b_2 = 0.000, b_3 = -1.092, b_4 = 0.000, b_5 = 0.208, \\ &b_6 = 0.000, b_7 = 0.056, b_8 = 0.000, b_9 = 0.000, b_{10} = -0.015, \\ &b_{11} = -2.585, b_{12} = 0.105, b_{13} = -0.002. \end{aligned} \tag{6.1.16}$$

Equation (6.1.11) can be transform to the solution obtained by [16] by change the variables by writing $\xi + \alpha$ in place of ξ, then the ellipse itself is given by $\xi = 0$ and making $\alpha \to \infty, a \to 0$, so that acosh$\alpha \to A$, asinh$\alpha \to A$, where A is the radius of the cylinder see [72].

6.2 Forces and Moment on the Ellipse

The components of the force (F_x, F_y) and the moment M acting on a volume V of fluid which is enclosed by the surface S can be expressed as

$$F_x = \int_S (\sigma_{\xi\xi}\partial x/\partial\xi - \sigma_{\xi\eta}\partial y/\partial\xi)dS/h \tag{6.2.1}$$

$$F_y = \int_S (\sigma_{\xi\xi}\partial y/\partial\xi + \sigma_{\xi\eta}\partial x/\partial\xi)dS/h \tag{6.2.2}$$

$$M = \int_S [(\sigma_{\xi\xi}\partial x/\partial\xi - \sigma_{\xi\eta}\partial y/\partial\xi)y - (\sigma_{\xi\xi}\partial y/\partial\xi + \sigma_{\xi\eta}\partial x/\partial\xi)x]dS/h, \tag{6.2.3}$$

where x and y in elliptic co-ordinates defined in (6.1.2) and (6.1.3) respectively, and

$$\sigma_{\xi\xi} = -p + 2\mu(\frac{\partial V_\xi}{\partial\xi}/h - V_\eta\frac{\partial(1/h)}{\partial\eta}) \tag{6.2.4}$$

$$\sigma_{\xi\eta} = \sigma_{\eta\xi} = \mu(\frac{\partial}{\partial\xi}\left[\frac{V_\eta}{h}\right] + \frac{\partial}{\partial\eta}\left[\frac{V_\xi}{h}\right]) \tag{6.2.5}$$

$$h = \left(\cosh^2(\xi)\sin^2(\eta) + \sinh^2(\xi)\cos^2(\eta)\right)^{1/2} \tag{6.2.6}$$

Inserting these values of $\sigma_{\xi\xi}, \sigma_{\xi\eta}$into expressions (6.2.1),(6.2.2) and (6.2.3) and using the Stokes equations of motion, we obtain, after some simplifications,

$$F_x = \int_S \left[\frac{\partial \omega}{\partial n} \sinh(\alpha) \sin(\eta) - \omega \cosh(\alpha) \sin(\eta)/h \right] ds, \tag{6.2.7}$$

$$F_y = -\int_S \left[\frac{\partial \omega}{\partial n} \cosh(\alpha) \cos(\eta) - \omega \sinh(\alpha) \cos(\eta)/h \right] ds, \tag{6.2.8}$$

$$M = \int_S \left[\frac{\partial \omega}{\partial n} \left\{ \cosh^2(\alpha) \cos^2(\eta) + \sinh^2(\alpha) \sin^2(\eta) \right\} /2 + \omega \sinh(\alpha) \cosh(\alpha)/h \right] ds \tag{6.2.9}$$

The integrals, which occur in equations (6.2.7), (6.2.8) and (6.2.9) are evaluated numerically using Simpson's rule.

6.3 The Governing Equations

For slow steady, two-dimensional flow of an incompressible Newtonian fluid the Navier-Stokes and continuity equations reduce to

$$\nabla p = \nabla^2 u, \tag{6.3.1}$$

$$\nabla \cdot u = 0, \tag{6.3.2}$$

where the Reynolds number is assumed to be so small. On introducing the stream function, ψ say, such that $\partial\psi/\partial x = -v_y$and $\partial\psi/\partial y = v_x$, then ψ satisfies the biharmonic equation, see [5],

$$\nabla^4 \psi = 0. \tag{6.3.3}$$

On introducing the vorticity, ω, equation (6.3.3) may be written in the following form

$$\nabla^2 \psi = \omega, \tag{6.3.4}$$

$$\nabla^2\omega = 0. \tag{6.3.5}$$

In order to solve the equations (6.3.4) and (6.3.5) in the domain Ω we use the BEM. For any $p = (x, y) \in \Omega \cup \partial\Omega$ and $q = (x_0, y_0) \in \partial\Omega$, let

$$f(p, q) = \ln \mid p - q \mid, \tag{6.3.6}$$

$$g(p, q) = \mid p - q \mid^2 (\ln \mid p - q \mid -1), \tag{6.3.7}$$

where $\mid p-q \mid = \{(x-x_0)^2 + (y-y_0)^2\}^{1/2}$. Applying Green's second identity we have

$$\begin{aligned} \eta(\underline{p})\psi(\underline{p}) &= \int_{\partial\Omega} \psi(\underline{q}) f'(\underline{p}, \underline{q}) d\underline{q} - \int_{\partial\Omega} \psi'(\underline{q}) f(\underline{p}, \underline{q}) d\underline{q} \\ &+ \frac{1}{4} \int_{\partial\Omega} \omega(\underline{q}) g'(\underline{p}, \underline{q}) d\underline{q} - \frac{1}{4} \int_{\partial\Omega} \omega'(\underline{q}) g(\underline{p}, \underline{q}) d\underline{q} \end{aligned} \tag{6.3.8}$$

$$\eta(\underline{p})\omega(\underline{p}) = \int_{\partial\Omega} \omega(\underline{q}) f'(\underline{p}, \underline{q}) d\underline{q} - \int_{\partial\Omega} \omega'(\underline{q}) f(\underline{p}, \underline{q}) d\underline{q} \tag{6.3.9}$$

The boundary is first calculated by using Runge Kitta method and is found 6.386 which is agree with handbook of mathematical table and then subdivided into N segments, $\partial\Omega_j$, by solving differential equation

$$d\eta/ds = 1/h \tag{6.3.10}$$

and the stream function, ψ, its derivative, ψ', the vorticity, ω, and its derivative, ω', are approximated by piecewise constant functions. This results in the following system of algebraic equations

$$\left.\begin{aligned} \textstyle\sum_{j=1}^{N} E_{ij}\psi_j - G_{ij}\psi'_j + L_{ij}\omega_j - M_{ij}\omega'_j &= 0 \\ \textstyle\sum_{j=1}^{N} E_{ij}\omega_j - G_{ij}\omega'_j &= 0 \end{aligned}\right\} i = 1, \ldots, n \tag{6.3.11}$$

where $G_{ij},\ E_{ij},\ L_{ij}$ and M_{ij} are given by

$$G_{ij} = \int_{\partial\Omega_j} f(p_i, q) dq,$$

$$E_{ij} = \int_{\partial\Omega_j} f'(p_i, q)dq - \eta(p_i)\delta_{ij},$$

$$L_{ij} = \frac{1}{4}\int_{\partial\Omega_j} g'(p_i, q)dq,$$

$$M_{ij} = \frac{1}{4}\int_{\partial\Omega_j} g(p_i, q)dq,$$

Equations (6.3.11) represents $2N$ equations in $4N$ unknowns. With the application of the appropriate conditions the system of equations (6.3.11) can be solved and equations (6.3.8) and (6.3.9) used to find the value of the stream function, ψ, at any point within the solution domain, Ω.

6.4 Numerical Solution

In the present work the fluid flow passing through an elliptical cylinder in the presence of a rotlet is investigated. In the mathematical model the fluid flow is assumed to be two-dimensional and the ellipse, with major and minor axes of lengths a and b, respectively, and the rotlet is at a distance c from the center of the ellipse as shown in figure (6.1.1).

In order to solve numerically Navier-Stokes equations in an exterior region, it is very advantageous to use the BEM because there is a simple fundamental solution, which enables one to covert the equations into integral equations, which only involves boundary integrals. Further, these integral equations are very convenient when dealing with the infinite boundary condition, see for example [41] and [9].

In this work the BEM with constant elements is used. It is convenient to separate the stream function and the vorticity into two parts, namely,

$$\Psi = \psi_A + \psi^* \tag{6.4.1}$$

$$\omega = \omega_A + \omega^* \tag{6.4.2}$$

where

$$\begin{aligned}\psi_A &= \lambda_1 r\cos(\vartheta) + \lambda_2 r\sin(\vartheta) + \lambda_3 + \lambda_4\sin(2\vartheta)\\ &+ \lambda_5\cos(2\vartheta) + \lambda_6\ln(r) + \lambda_7 r^2 + \lambda_8 r\ln(r)\cos(\vartheta)\\ &+ \lambda_9 r\ln(r)\sin(\vartheta) + (\beta/2)\ln(r^2 + c^2 - 2rc\cos(\vartheta))\end{aligned} \tag{6.4.3}$$

$$\begin{aligned}\omega_A &= -4\lambda_4\sin(2\vartheta)/r^2 - 4\lambda_5\cos(2\vartheta)/r^2 - 4_7\lambda\\ &- 2\lambda_8\cos(\vartheta)/r - 2\lambda_9\sin(\vartheta)/r\end{aligned} \tag{6.4.4}$$

Those ψ_A and ω_A are asymptotic expansions of ψ and ω as $r \to \infty$, and ψ^* and ω^* are the perturbations values about these expansions that tend to zero as $r \to \infty$,

Considering the surface of the ellipse as the streamline $\psi = 0$, then ψ^* and ω^* satisfies

$$\nabla^2\psi^* = \omega^* \tag{6.4.5}$$

$$\nabla^2\omega^* = 0. \tag{6.4.6}$$

with

$$\psi^* = -\psi_A \text{ and } \psi^{*\prime} = -\psi_A' \text{ on the boundary} \tag{6.4.7}$$

Equations (6.4.7) provides another N equations to be $2N$ and the number of unknowns $2N + 9$ which means that we need another 9 conditions to close the system

The extra unknowns λ_j, where $j = 1, \ldots, 9$, will require extra conditions:

Case (a)

Let us assume for the moment that the values of the drag, lift and moment are all zeros. Using the expressions (6.2.7), (6.2.8) and (6.2.9) where we have replaced ω by $\omega_A + \omega^*$, the parts of the integrals involving ω_A were evaluated analytically producing linear expressions in the unknowns λ_j. The other parts involving ω^* are expressed after numerical integrations using Simpson's method as linear expressions in ω_j^* and $\omega_j^{*'}$. The resulting expressions for the drag, lift and moment can be written as

$$\sum_{j=1}^{(N-1)/2} [(\omega^{*'}_{2j-1} + 4\omega^{*'}_{2j} + \omega^{*'}_{2j+1}) \sinh(\alpha) \sin(\eta_j) - (\omega^{*}_{2j-1} + 4\omega^{*}_{2j} + \omega^{*}_{2j+1}) \cosh(\alpha) \sin(\eta_j)/h_j](2\pi/3N) = 0, \tag{6.4.8}$$

$$\sum_{j=1}^{(N-1)/2} [(\omega^{*'}_{2j-1} + 4\omega^{*'}_{2j} + \omega^{*'}_{2j+1}) \cosh(\alpha) \cos(\eta_j) - (\omega^{*}_{2j-1} + 4\omega^{*}_{2j} + \omega^{*}_{2j+1}) \sinh(\alpha) \cos(\eta_j)/h_j](2\pi/3N) = 0, \tag{6.4.9}$$

$$\sum_{j=1}^{(N-1)/2} [(\omega^{*'}_{2j-1} + 4\omega^{*'}_{2j} + \omega^{*'}_{2j+1}) h_j^2/2 + (\omega^{*}_{2j-1} + 4\omega^{*}_{2j} + \omega^{*}_{2j+1}) \sinh(\alpha) coh(\alpha)/h_j](2\pi/3N) = 0, \tag{6.4.10}$$

where

$$h_j = (\cosh^2(\alpha) \sin^2(\eta_j) + \sinh^2(\alpha) \cos^2(\eta_j))^{1/2} \tag{6.4.11}$$

$$\omega^{*}_{1} = \omega^{*}_{N}, \tag{6.4.12}$$

$$\omega^{*'}_{1} = \omega^{*'}_{N}, \tag{6.4.13}$$

Equations (6.4.8), (6.4.9) and (6.4.10) gives three conditions plus one extra condition arising from the fact that the pressure distribution is single value(6.4.14).

$$-\sum_{j=1}^{(N-1)/2} [(\omega^{*'}_{2j-1} + 4\omega^{*'}_{2j} + \omega^{*'}_{2j+1})](2\pi/3N) = 0 \tag{6.4.14}$$

Hence, equations (6.4.5) and (6.4.6), together with (6.4.8), (6.4.9), (6.4.10) and (6.4.14) result in $(2N+4)$ equations in terms of the $(2N+9)$ unknowns which mean that we need five extra conditions to complete the system of equations.

In order to obtain the other equations, we make use of the fact that $\eta(p)$ vanishes outside the domain, i.e when p is inside the elliptical cylinder, namely $p(\xi_{Ij}, \eta_j)$, where $\xi_{Ij} < \alpha$ for $j = 1, 2, 3, 4$ and 5

Case (b)

In this situation we use the asymptotic expansion of ψ given in equation (6.4.3). Hence, equations (6.4.8), (6.4.9) and (6.4.10) have to be replace by

$$\begin{aligned} &-4\pi\lambda_9 + \sum_{j=1}^{(N-1)/2} [(\omega_{2j-1}^{*'} + 4\omega_{2j}^{*'} + \omega_{2j+1}^{*'})\sinh(\alpha)\sin(\eta_j) \\ &-(\omega_{2j-1}^{*} + 4\omega_{2j}^{*} + \omega_{2j+1}^{*})\cosh(\alpha)\sin(\eta_j)/h_j](2\pi/3N) = 0, \end{aligned} \tag{6.4.15}$$

$$\begin{aligned} &4\pi\lambda_8 - \sum_{j=1}^{(N-1)/2} [(\omega_{2j-1}^{*'} + 4\omega_{2j}^{*'} + \omega_{2j+1}^{*'})\cosh(\alpha)\cos(\eta_j) \\ &-(\omega_{2j-1}^{*} + 4\omega_{2j}^{*} + \omega_{2j+1}^{*})\sinh(\alpha)\cos(\eta_j)/h_j](2\pi/3N) = 0, \end{aligned} \tag{6.4.16}$$

$$\begin{aligned} &4\pi\lambda_6 - \sum_{j=1}^{(N-1)/2} [(\omega_{2j-1}^{*'} + 4\omega_{2j}^{*'} + \omega_{2j+1}^{*'})h_j^2/2 \\ &+(\omega_{2j-1}^{*} + 4\omega_{2j}^{*} + \omega_{2j+1}^{*})\sinh(\alpha)coh(\alpha)/h_j](2\pi/3N) = 0 \end{aligned} \tag{6.4.17}$$

Then we can proceed in the same way as described in case (a). However in this situation we did not assume that the forces and the moment are zero. This hover has given rise to certain computational difficulties, which we will discuss in some detail later in the results section. To overcome these difficulties we developed case (c):

Case (c)

Here we used the same methodology adapted in case (b) except that we have replaced the lift condition (6.4.16) by one point inside the ellipse. This gave us six points inside the ellipse, one integral condition (6.4.14) together with the expressions for the drag (6.4.15) and that for the moment (6.4.17).

6.5 Numerical Results

Numerical details for situations when the position of the rotlet at (2.236,0) is presented for three cases

Initially case (a) the drag, the lift and the moment are all enforce to be zero. The values of $\lambda_1,\ \lambda_2,\ \lambda_3,\ \lambda_4,\ \lambda_5,\ \lambda_6,\ \lambda_7,\ \lambda_8$ and λ_9 which are analytically are

0.500, 0.000, −1.092, 0.000, 0.208, 0.000, 0.056, 0.000 and 0.000 numerically are 0.477, 0.000, −1.091, −0.024, 0.204, 0.000, 0.056, 0.032 and 0.006 respectively. The above inaccuracies arising in the coefficients are overcome by using case (c).

In case (b) The asymptotic expansion for the drag, the lift and the moment at infinity are included. The values of $\lambda_1,\ \lambda_2,\ \lambda_3,\ \lambda_4,\ \lambda_5,\ \lambda_6,\ \lambda_7,\ \lambda_8$ and λ_9 are 0.477, 0.000, −1.091, −0.024, 0.204, 0.000, 0.056, 0.032 and 0.006 respectively which are also inaccurate as in case (a).

In case (c) six points inside the elliptical cylinder were used beside the asymptotic expansion at infinity of the drag and the moment and the integral condition, this case was chosen because the lift is appear to be inaccurate in case (b) and is very sensitive to the discretization. The values of $\lambda_1,\ \lambda_2,\ \lambda_3,\ \lambda_4,\ \lambda_5,\ \lambda_6,\ \lambda_7,\ \lambda_8$ and λ_9 for $N = 600$ are 0.501, 0.000, -1.091, 0.001, 0.207, 0.000, 0.056, 0.000 and 0.000 respectively

Figure 6.5.1 represents the non-dimensional streamline pattern and the vorticity pattern. The streamline is symmetric about the x-axis and show a rotational flow about the elliptical cylinder and form closed contours a round the cylinder and the rotlet, together with a stagnation point on the x-axis opposite to the position of the rotlet. However, due to the different values of c the position of stagnation points differ. The streamline for $-0.65,\ 0.00$ and 0.19 are presented also the non-dimensional vorticity for $-0.07,\ 0.0,\ 0.22,\ 0.3$ and 0.4 are presented in figure 6.5.1(b).

Figure 6.5.2 represents the non-dimensional streamline pattern and the vorticity pattern. The streamline is symmetric about the y-axis and show a rotational flow about the elliptical cylinder and form closed contours a round the cylinder and the rotlet, together with a stagnation point on the y-axis. However, due to the different values of c the position of stagnation points differ. The streamline for $-1.5,\ -0.75,\ 0.0,\ 0.75$ and 1.5 are presented also the non-dimensional vorticity for $-0.5,\ -0.4,\ 0.0$ and 0.2 are presented in figure 6.5.2(b).

6.6 Conclusions

The numerical technique used in chapters 4 and 5 have again been employed in order to investigate the slow viscous flow past an elliptical cylinder in the

presence of a rotlet. It is found that the numerical results are in reasonable agreement with those obtained analytically.

It is found that the determination of the lift is very sensitive to the form of the discretization. In order to overcome this problem it was found necessary to use six points inside the elliptical cylinder, instead of the expected five points, with the constraint on the lift being omitted.

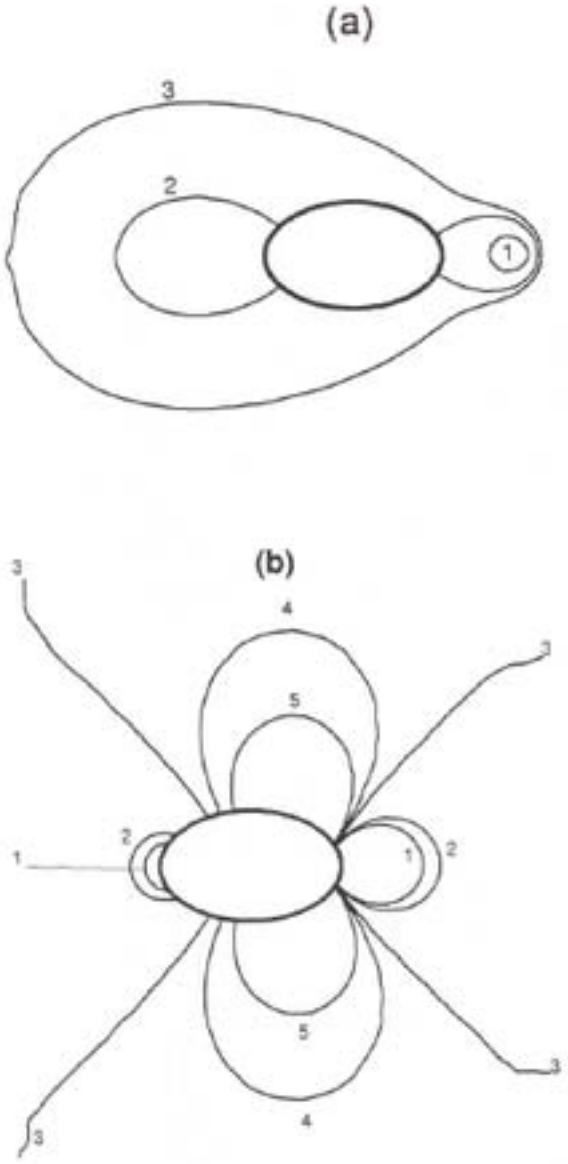

Figure 6.5.1: The numerically obtained streamlines and vorticity pattern for $c = 2.236$ with $N = 800$.
(a) the streamlines labeled 1, 2 and 3 correspond to
$\Psi = -0.65,\ 0.00$ and 0.19, respectively,
(b) the vorticity lines labeled $1,\ 2,\ 3,\ 4$ and 5 correspond to
$\omega = -0.07,\ 0.0,\ 0.22,\ 0.3$ and 0.4, respectively.

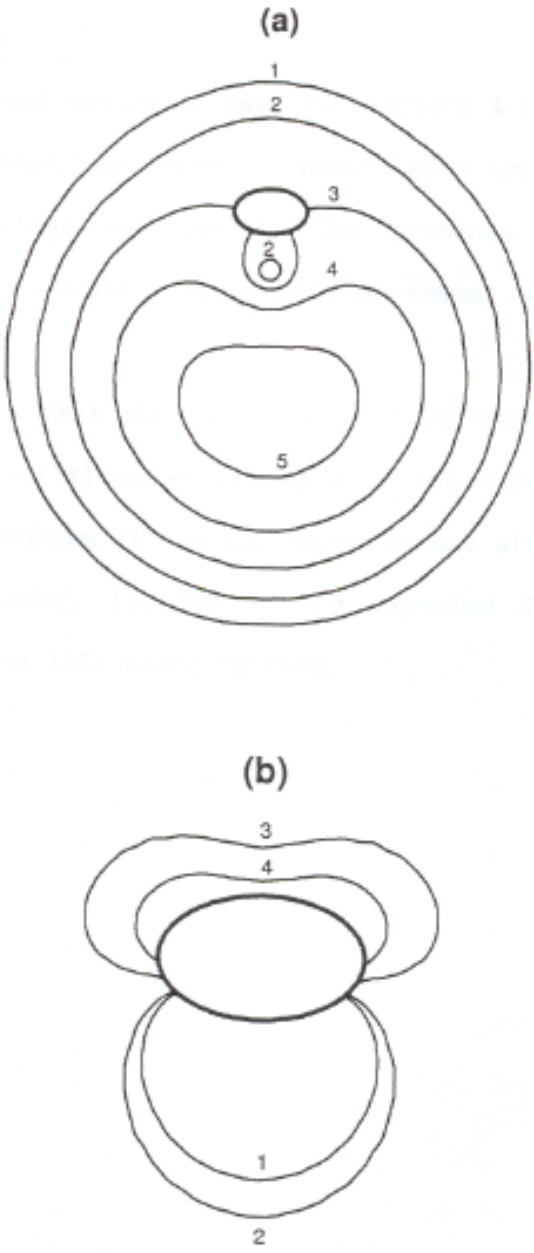

Figure 6.5.2: The numerically obtained streamlines and vorticity pattern for $c = 2.236$ with $N = 800$.
(a) the streamlines labeled 1, 2, 3, 4 and 5 correspond to
$\Psi = -1.5,\ -0.75,\ 0.0,\ 0.75$ and 0.5, respectively,
(b) the vorticity lines labeled 1, 2, 3 and 4 correspond to
$\omega = -0.5,\ -0.4,\ 0.0$ and 0.2, respectively.

Chapter 7

CONCLUSIONS

The solution of the unbounded, steady, two-dimensional, incompressible viscous fluid flows past a body, or bodies, at small values of Reynolds number is very important both mathematically and physically. It is interesting to note that some solutions of the full Navier-Stokes Equations for small values of the Reynolds number were found but from these solutions it was not clear what the solution is at zero Reynolds number. Therefore a numerical technique was developed to overcome this difficulty and a unique solution was obtained. In many situations the validity of the solution obtained by setting the Reynolds number to be zero is important. Even in situations where no solutions are possible for zero Reynolds number there will always exist a region in the vicinity of the body, or bodies, where the solution of the biharmonic equation is valid. Thus it is very important to develop robust computational techniques, which are able to solve complex, unbounded, steady, two-dimensional, incompressible viscous fluid flows past a body, or bodies. In this thesis we have demonstrated that the Boundary Element Method, combined with the appropriate asymptotic solution of the biharmonic equation, can be used to solve a large variety of fluid flow problems. In all the investigated the cases numerically obtained solution is in very good agreement with all the available analytical solutions. Hence, it may be assumed, with confidence, that the techniques developed in this thesis may be used to solve the biharmonic equation for unbounded flows in situations where no analytical solutions are possible. Examples of such flows are where the body in the fluid flow does not have a simple shape, Le. the body may not

be smooth or have a complex shape, and also where multiply bodies are present in the flow. Future extensions of this work should address such flows.

Bibliography

[1] Alarcon, E., Martin, A. and Paris, F., 1979, Boundary Element in Potential and Elasticity Theory, Comp. and Stru., **10**, 351 – 362.

[2] Badr, H.M. and Dennis, S.C.R., 1985, Time-dependent Viscous Flow Past an Impulsively Started Rotating and Translating Circular Cylinder, J. Fluid Mech. **158**, 447 – 488.

[3] Backus, G. and Gilbert, F., 1970, Uniqueness in the Inversion of Inaccurate Gross Earth Data, Phil. Trans R. Soc. London Ser. *A***266**,123 – 192.

[4] Banerjee, P.K., and Butterfield, R., 1981, Boundary Element Methods in Engineering Science, Mcgraw-Hill, New York.

[5] Batchelor, G.K. (1967) An Introduction to Fluid Dynamics, Cambridge University Press, London, New York, Melbourne.

[6] Beck, J.V., Blackwell, B. and St. Clair, C.R., 1985, Inverse Heat Conduction, Wiley-Interscience, London, Washington.

[7] Bialecki, R. and Nowak, A.J., 1981, Boundary Value Problem in Heat Conduction with Nonlinear Material and Boundary Conditions, Appl. Math. Modelling. **5**, 416 – 421.

[8] Brebbia, C.A. and Gipson, G.S. (Editor), 1991, Proc. 13th Int. Conf. on Boundary Element Methods in Enginering, Springer-Verlag, Berling, Heidelberg, New York, Tokyo.

[9] Brebbia, C.A., Telles, J.C.F. and Wrobel, L.C., 1984, Boundary Element Techniques, Springer-Verlag, Berling, Heidelberg, New York and Tokyo.

[10] Bretherton, F.P., 1961, The Motion of Long Bubbles in Tubes, J. Fluid Mech., **10**, 166 – 189.

[11] Carrera, J. and Neuman, S.P., 1986, Estimation of Aquifer Parameters Under Transient and Steady State Conditions, Parts 1, 2 and 3, Water Resources Research, **22**, 199 – 242.

[12] Chen, W.H. and Seinfeld, J.H., 1972, Estimation of Spatially Varying Parameters in Partial Differential Equations, Int. J. Control, **15**, 487 – 495.

[13] Cox, B.G., 1962, On Driving a Viscous Fluid out of a Tube, J.Fluid Mech., **14**, 81 – 96.

[14] Coyne, J.C. and Elrod, H.G., 1970, Conditions for the Rupture of a Lubricating Film, Part 1, Theoretical Model, Trans. A.S.M.E. J. of Lub. Tech., **92**, 451 – 456.

[15] Dennis, S.C.R. and Chang, G.Z., 1970, Numerical Solution for Steady Flow Past a Circular Cylinder at Reynolds Numbers up to 100, J. Fluid Mech. **42**, 471 – 489.

[16] Dorrepaal, J.M., *O'*Neill, M.E. and Ranger, K.B., 1984, Two-dimentional Stokes Flows with Cylinders and Line Singularities, Mathematika **31**, 65 – 75.

[17] Falk, R.S. and Monk, P.B., 1986, Logarithmic Convexity for Discrete Harmonic Functions and the Approximation of the Cauchy Problem for Poison*'s* Equations, Math. of Comp., **47**, 135 – 149.

[18] Filon, L.N.G., 1926 The Forces on a Cylinder in a Stream of Viscous Fluid, Proc. Roy. Soc., **A113**, 7 – 27.

[19] Fornberg, B., 1980, *A* Numerical Study of Steady Viscous Flow Past a Circular Cylinder, J. Fluid Mech. **98**, 819 – 855.

[20] Fornberg, B., 1985, Steady Viscous Flow Past a Circular Cylinder up to Reynolds number 600, J.Comput. Phys. **161**, 297 – 320.

[21] Fletcher, R., 1981, Practical Methods of Optimization, 2, Constrained Optimization, John Wiley and Sons, New York and Toronto.

[22] Flynn, M.R. and Ellenbecker, M.J., 1985, The Potential Flow Solution for Air Flow into a Flanged Circular Hood, Am. Ind. Hyg. Assoc. J., **46**, 318 – 322.

[23] Flynn, M.R. and Miller, C.T., 1991, Discrete Vortex Methods for the Simulation of Boundary Layer Separation Effects on Worker Exposure, Ann. Occup. Hyg., **35**, 35 – 50.

[24] Fredholm, I., 1903, Sur Une Classe D'equations Fonctionells, Acta Math., **27**, 365 – 439.

[25] Gilbarg, D. and Trudinger, N.S., 1983, Elliptic Partial Differential Equations of Second Order, $2ndEd.$, Springer-Verlag, Berlin, Heidelberg, New York, Tokyo.

[26] Guschchin, V.A. and Schennikov, V.V., 1974, A Numerical Method of Solving the Navier-Stokes Equations, Zh. Vychist. Mat. Mat. Fiz. **14**, 242 – 250.

[27] Gill, P.E., Murray, W. and Wright, M.H., 1981, Practical Optimization, Academic Press, London and New York.

[28] Glauert, M.B., 1957 The Flow Past a Rapidly Rotating Circular Cylinder, Proc. Roy. Soc. Lond. **A242**, 108 – 115.

[29] Glauert, M.B., 1957A Boundary Layer Theorem, with Applications to Cylinders, J. Fluid Mech. **2**, 89 – 99.

[30] Hamielec, A.E. and Raal, J.D., 1969 Numerical Studies of Viscous Flow around Circular Cylinders, Phys. Fluids **12**, 11 – 20.

[31] Han, H., 1982, The Finite Element Method in a Family of Improperly Posed Problems, Math. of Comp., **38**, 55 – 65.

[32] Homsy, G.M., 1987, Viscous Fingering in Porous Media, Annu. Rev. Fluid Mech., **19**, 271 – 311.

[33] Imai, I., 1951, On the Asympototic Behaviour of Viscous Fluid Flow at a Great Distance from a Cylinderical Body, Proc. Roy. Soc. **A208**, 487−516.

[34] Kelmanson, M.A., 1984, Boundary Integral Equation Analysis of Singular, Potential and Biharmonic Problems, 7, Lecture Notes in Engineering, Springer-Verlag, Berlin, Heidelberg, New York, Tokyo.

[35] Tang, T., 1990, *A* Numerical Investigation into the Steady Flow Past a Rotating Circular Cylinder at Low and Intermediate Reynolds Numbers, J. Comput. Phys., **87**, 91 – 107.

[36] Harrington, R.F., Pontoppidan, K., Abrahamsen, P. and Albertsen, N.C., 1969, Computation of Laplacian Potentials by an Equivalent-source Method, Proc, IEE **116**, 1715 – 1720.

[37] Hess, J.L., and Smith, A.M.O., 1967, Calculation of Potential Flow about Arbitrary Bodies, Progress in Aeronautical Sciences, 8, Pergamon Press, London.

[38] Jeffery, G.B., 1920, Plane Stress and Plane Strain in Bipolar Co-ordinates, Phil Trans., **A221**, 265 – 293.

[39] Jeffery, G.B., 1922, The Rotation of Two Circular Cylinders in a Viscous Fluid, Proc. Roy. Soc. London Ser. **A101**, 169 – 174.

[40] Jaswon, M.A., 1963, Integral Equation Methods in Potential Theory, I, Proc. Roy. Soc. Ser., **A275**, 23 – 32.

[41] Jaswon, M.A. and Symm, G.T., 1977, Integral Equation Methods in Potential Theory and Elastostatics, Academic Press, London.

[42] Jain, P.C. and Kawakuti, M., 1966 Numerical Study of a Viscous Fluid Past a Circular Cylinder, J. Phys. Soc. Japan **21**, 2055 – 2062.

[43] Jain, P.C. and Sankara, Rao, K., 1969, Numerical Solution of Unsteady Viscous Incompressible Fluid Flow Past a Circular Cylinder, Phys. Fluids Suppl. **II**, 57 – 61.

[44] Kawaguti, M., 1953, Numerical Solution of the Navier-Stokes Equations for the Flow Around a Circular Cylinder at Reynolds Number 40, J. Phys. Soc. Japan **8**, 747 – 757.

[45] Khader, M.S., 1980, Heat Conduction with Temperature Dependent Thermal Conductivity, Paper $80 - HT - 4$, National Heat Transfer Conf., ASME, Orlando, Florida.

[46] Kuiken, H.K., 1990, Deforming Surface and Viscous Sintering, Proc. Conf. on the Math. and the Comp. of Deforming Surface, Oxford Univ. Press, London and New York.

[47] Lachat, J.C. and Watson, J.O., 1976, Effective Numerical Treatment of BIE, Int. J. Num. Meth. in Eng., **10**, $991 - 1005$.

Langlois, W.E., 1964, Slow Viscous Flow, Macmillan, New York.

[48] Lavrentiev, M.M., 1956, On the Cauchy Problem for the Laplace Equation, Izv. Akad. Nauk SSSR Ser. Math., **20**, $819 - 842$(Russian).

[49] Louguet-Higgins, M.S. and Cokelet, E.D., 1976, The Deformation of Steep Surface Waves on Water, Part, 1 A Numerical Method of Computation, Proc. Roy. Soc. London, **A350**, $1 - 26$.

[50] Lyul V.A., 1970 Numerical Solution of the Problem of the Rotation of a Cylinder in a Flow of Viscous Incompressible Fluid, Zh. Vychisl. Mat. Mat. Fiz., **17**, $470 - 481$.

[51] Manzoor, M., 1982, Heat Flow Through Extended Surface Heat Exchanges, Lecture Notes in Engineering, 5, Springer-Verlag, Berlin, Heidelberg, New York, Tokyo.

[52] Moore, D.W., 1957, The Flow Past a Rapidly Rotating Circular Cylinder in an Infinite Stream, J. Fluid Mech. **2**, $541 - 550$.

[53] Nieuwstadt, F. and Keller, H.B., 1973 Viscous Flow Past Circular Cylinders, Comp. Fluids **1**, $59 - 71$.

[54] Oberhettinger, F., 1973 Fourier Expansions, Academic Press, New York.

[55] Patel, V.A., 1981, Flow Around an Impulsively Started Elliptic Cylinder at Various Angles of Attack, Comp. Fluids **9**, $435 - 462$.

[56] Payne, L.E., 1960, Bounds in the Cauchy Problem for the Laplace Equation, Arch. Rational Math. Anal., **5**, $35 - 45$.

[57] Payne, L.E., 1970, On a Priori Bounds in the Cauchy Problem for Elliptic Equations, SIAM J. Math. Anal., **1**, $82 - 89$.

[58] Payne, L.E., 1975, Improperly Posed Problems in Partial Differential Equations, Regional Conf. Ser. Appl. Math. Philagelphia, PA SIAM.

[59] Prandtl, L. and Tietjens, O.G., 1934, Applied Hydro-mechanics and Aeromechanics, McGraw-Hill, New York.

[60] Proudman, I. and Pearson, J.R.A., 1957, Expansions at Small Reynolds Numbers for the Flow Past a Sphere and a Circular Cylinder, J. Fluid Mech. **2**, 237 – 262.

[61] Saffman, P.G., 1982, Lecture Notes in Physics, **154**, Springer-Verlag, Berlin, Heidelberg, New York, Tokyo.

[62] Shail, R. and Onslow, S.H., 1988, Some Stokes Flows Exterior to a Spherical Boundary, Mathematika **35**, 233 – 246.

[63] Shen, E.I. and Udell, K.S., 1985, *A* Finite Element Study of Low Reynolds Number Two Phase Flow in Cylindrical Tubes, J. Appl. Mech., **52**, 253 – 256.

[64] Sayers, A.T., 1979, Lift Coefficient and Flow Visualization on the Leading Edge Rotating Cylinder Rudder, Int. J. Mech. Elec. Engng **7**, 75 – 87.

[65] Smith, F.T., 1979 Laminar Flow of an Incompressible Fluid Past a Bluff Body: the Separation, Reattachment, Eddy Properties and Drag, J. Fluid Mech. **92**, 171 – 205.

[66] Smith, F.T., 1985*A* Structure for Laminar Flow Past a Bluff Body at High Reynolds Number, J. Fluid Mech. **155**, 175 – 191.

[67] Smith, G.D., 1984, Numerical Solution of Partial Differential Equations: Finite Difference Methods, *3rd.Ed.*, Oxford Applied Mathematics and Computing Science Series.

[68] Smith, S.H., 1990, The Jeffery Paradox as the Limit of a Three-dimentional Stokes Flow, Phys. Fluids **A2**(**5**), 661 – 673.

[69] Smith, S.H., 1991, The Rotation of Two Circular Cylinders in a Viscos Fluid, Mathematika, **38**, 63 – 66.

[70] Symm, G.T., 1963, Integral Equation Methods in Potential Theory, II, Proc. Roy. Soc. Ser. **A275**, 33 – 46.

[71] Symm, G.T., 1973, Treatment of Singularities in the Solution of Laplace's Equation by an Integral Equation Method, NPL Report NCA31.

[72] Swain, M., 1922, The Steady Motion of a Cylinder Through Infinite Viscous fluid, Proc. Roy. Soc. Ser. **A102**, $766 - 778$.

[73] Tennant, J.S., Johnson, W.S. and Krothapalli, A., 1976, Rotating Cylinder for Circulation Control on an Aerofoil, J. Hydronautics **10**, $102 - 117$.

[74] Tuann, S.Y. and Olson, M.D., 1978, Numerical Studies of the Flow Around a Circular Cylinder by a Finite Element Method, Comp. Fluids **6**, $219 - 240$.

[75] Underwood, R.L., 1969, Calculations of Incompressible Flow Past a Circular Cylinder at Moderate Reynolds Numbers, J. Fluid Mech. **37**, $95 - 114$.

[76] Watson, E.J., 1994 The Rotational of Two Circular Cylinders in a Viscous Fluid, to be published in Mathematika.

[77] Wilton, J.R., 1915 The Solution of Certain Problem of Two-Dimensional Physics, Phil.Mag., **30**, $761 - 779$.

[78] Wood, W.W., 1957 Boundary Layers whose Streamlines are Closed, J. Fluid Mech., **2**, $77 - 87$.

Index